Control of retinal astrocyte numbers during development of the retina

Heloise West

Wolfson Institute for Biomedical Research

and Department of Biology,

University College London.

A thesis submitted to the University of London in part fulfilment of the degree of Doctor of Philosophy

January 2003

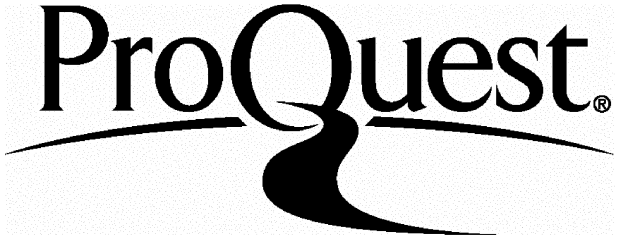

Abstract

Retinal astrocytes are associated not only with retinal neurons but also with the retinal vasculature during development. They control vascular development after birth, attracting vascular cells to invade the retina from the optic nerve head and spread out towards the periphery. It is not clear what controls growth of the astrocyte population itself.

To address this I looked at control of retinal astrocyte proliferation during development. I showed that astrocytes migrating ahead of the spreading vasculature are highly proliferative but, once caught up by the vessels, they stop proliferating. The proliferative, avascular regions are also associated with up-regulation of *VEGF* expression. Since *VEGF* is known to be upregulated under hypoxic conditions in vitro, these observations suggest that oxygen concentration might be instrumental for controlling astrocyte gene expression and proliferation in vivo.

To test this idea I manipulated oxygen levels in vivo by keeping mice in hyperoxic conditions (80% oxygen), which limits development of the retinal vasculature and gives rise to regions of both hypoxia and hyperoxia. I found a positive correlation between astrocyte proliferation and areas of hypoxia, implicating oxygen as a negative regulator of retinal astrocyte proliferation in vivo. I also showed that astrocytes proliferate at a higher rate in low oxygen in culture. Taken together, my findings suggest that oxygen, brought into the retina by the developing vasculature, is responsible for shutting down

proliferation of astrocytes, thus preventing further vascular development in a homeostatic feedback loop.

I also show a developmental phenotype in the eyes of mice lacking the *Ink4a/Arf* locus. The *Ink4a/Arf* locus encodes two proteins – p16Ink4a and p19Arf. These proteins have been shown to trigger G1 growth arrest in vitro and to act as tumour suppressor proteins in vivo. In the absence of these two proteins, excess cells accumulate in the hyaloid vasculature. A simple explanation based on these and other observations is that Arf prevents over proliferation of cells in the hyaloid vasculature during development.

Acknowledgements

I would like to thank Bill Richardson and members of his lab for their advice, friendship and encouragement during my PhD. Many thanks to those at the Wolfson Institute for Biomedical Research and MRC Laboratory for Molecular Cell Biology, who have also provided support and friendship. Special thanks to Marcus Fruttiger for his enthusiam and support during my PhD and for being a great supervisor. Outside of the lab, I am especially grateful to Paul for his love and support throughout my PhD. I am also very grateful to my family for their love and support during this time.

Chapter 2. Materials and Methods 53

List of figures

List of abbreviations

BBB	blood brain barrier
BCIP	5-bromo-4-chloro-3-inolyl-phosphate
bFGF	basic fibroblast growth factor
BrdU	bromodeoxyuridine
BSA	bovine serum albumin
cDNA	complementary deoxyribonucleic acid
CDK	cyclin-dependent kinase
CNS	central nervous system
DEPC	diethylpyrocarbonate
DIG	digoxygenin
DMEM	Dulbecco's modified Eagle's medium
DNA	deoxyribonucleic acid
E	embryonic age (days post coitum)
EBSS	Earle's balanced salt solution
EDTA	ethylene diamine tetra-acetic acid
Epo	erythropoietin
ER	endoplasmic reticulum
FCS	foetal calf serum
FITC	fluorescein isothiocyanate (green fluorophore)
GFAP	Glial fibrillary acidic protein
GGF	glial growth factor

h	hour(s)
HIF	hypoxia inducible factor
HRE	hypoxia response element
HUVEC	human umbilical vein endothelial cells
HVS	hyaloid vascular system
Ig	immunoglobulin
IGF	insulin-like-growth-factor
kb	kilobase pair
kDa	kilodalton(s)
LIF	leukaemia inhibitory factor
mRNA	messenger ribonucleic acid
NAC	N-acetyl-L-cysteine
NGF	Nerve growth factor
NSE	neuron specific enolase
OD^n	optical density at a wavelength of 'n' nm
ODD	oxygen degradation domain
OLP	oligodendrocyte progenitor
P	postnatal age (days after birth)
PBS	phosphate-buffered saline
PCD	programmed cell death
PCR	polymerase chain reaction
PDGF(R)	platelet-derived growth factor (receptor)
PDL	poly-D-lysine

PH	prolyl hydroxylase
PHTVL	persistant hyperplastic tunica vasculosa lentis
PI3K	phosphoinositol 3-kinase
Rb	retinoblastoma protein
RGC	retinal ganglion cell
RNA	ribonucleic acid
RNase	ribonuclease
s.d.	standard deviation
Shh	sonic hedgehog
SVZ	sub-ventricular zone
TG	transgenic
TUNEL	TdT-mediated dUTP nick end labeling
VEGF(R)	vascular endothelial growth factor (receptor)
VHL	von Hippel Lindau protein
VHP	vasa hyaloidea propria
WT	wild-type

Chapter 1. Introduction

1.1 Control of cell number during development

Control of cell number together with cell size determines the size of an organ or organism. The number of cells in a tissue, and the proportional representation of one cell type versus another is essential to the normal functioning of that tissue and the organ of which it is part. In the retina, for instance, the precise layered arrangement of different cell types is essential for vision. What controls proportional growth of cell populations during development? Learning about these controls might help us understand what goes wrong in diseases where cell proliferation is deregulated such as cancer and proliferative retinopathies associated with diabetes or premature birth. In this Thesis I study control of cell number in the developing retina, looking in particular at the development of retinal astrocytes.

Cellular processes such as cell death, proliferation and migration can all regulate cell number. These processes depend on intracellular pathways that are regulated by extracellular signalling molecules. Understanding the interactions between extracellular signals and intracellular responses might help explain how the growth from embryo to adult is controlled and how deregulation of these processes can cause disease.

Control of proliferation

Extracellular factors act via signal transduction molecules to regulate intracellular effectors of cell proliferation. The dependence of cell division on local signals from

neighbouring cells might help to match numbers of one cell type to another within a tissue and might also help co-ordinate the timing of development of different cell types (discussed further below). For example, insulin-like-growth-factor (IGF) is a locally produced mitogen that acts in a paracrine fashion to control cell survival in many tissues and cell proliferation in some (Raff, 1996b; Nakae et al., 2001). The role of another extracellular growth factor - Platelet-derived growth factor (PDGF) - in regulating proliferation during development of the central nervous system, will be described later in this Chapter. In addition, systemic controls on cell proliferation, such as growth hormone, might act to co-ordinate development of different organs in the body.

Cyclin dependent kinase inhibitors and the cell cycle

The core intracellular proteins that control the cell division cycle are the cyclin dependent protein kinases (Cdks), which are activated sequentially to trigger the different phases of the cell cycle (Nigg, 1995a; Nurse, 1994). Cdks themselves are regulated by a variety of intracellular proteins including cyclins that activate them, Cdk inhibitors that suppress them and kinases and phosphatases that either inhibit or activate them (Morgan, 1995; Roussel, 1998).

The mitotic cell cycle consists of four phases: one dedicated to synthesis of the genomic DNA (S phase) , one to mitosis (M), and two gap (G1 and G2) phases. G1 occurs between the end of mitosis and S phase (Fig 1.1). Here, critical decisions are made to commit to enter another round of cell division, to exit the cell cycle permanently or to exit transiently to a G0 phase. Once committeed to a new cell cycle, cells require

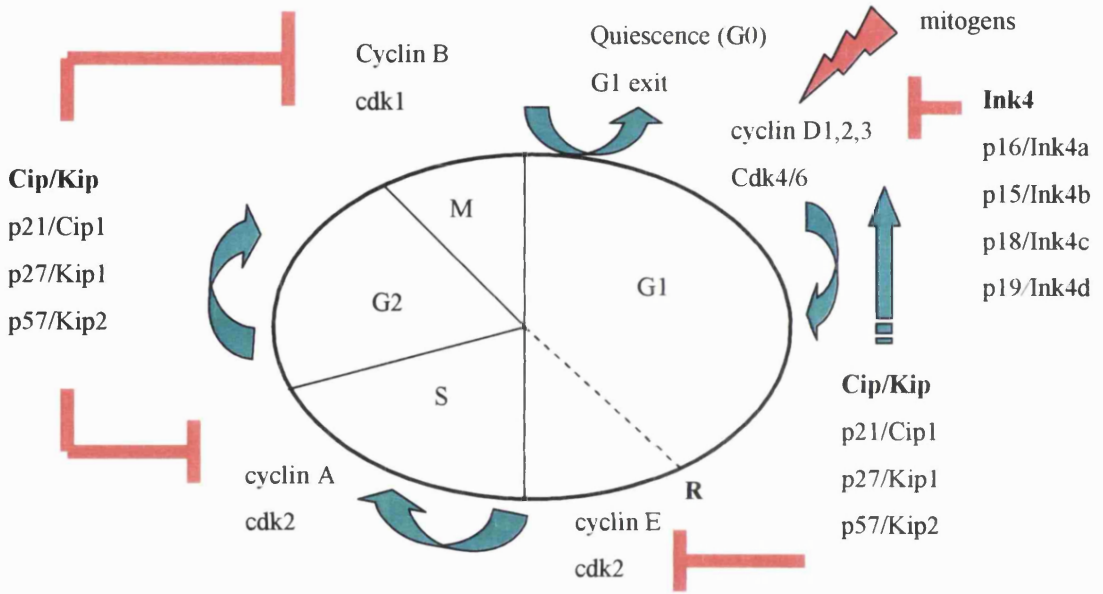

Figure 1.1 **Schematic representation of the mammalian cell cycle.** ***Adapted from Cunningham and Roussel (2001)***

Figure 1A. The mammalian cell cycle is divided into four phases, G1, S, G2 and M. Progression from one phase to the next is regulated by cdks associated with their cyclin subunits. Inhibition of the cyclin-cdk complexes is mediated by two families of cdk inhibitors, Ink4 proteins (p16/Ink4a, p15/Ink4b, p18/Ink4c and p19/Ink4d) and Cip/Kip proteins (p21/Cip1, p27/Kip1 and p57/Kip2). Whereas Ink4 proteins specifically bind to and inhibit cdk4/6, Cip/Kip family members can inhibit cyclin/cdk complexes including cyclinE-cdk2, cyclinA-cdk2, and cyclinB-cdk1 at a 1:1 stoichiometry. Cip/Kip proteins can also positively regulate cyclinD-cdk4/6 by promoting their assembly. Mitogen stimulation induces synthesis of D-type cyclins and is necessary for cells to proceed through G1 until they reach the restriction point (R), after which cells independently complete the first cell cycle. Cells can exit from the cell cycle and enter a state of quiescence, G0.

sustained stimuli to reach the 'restriction point' in G1 after which they replicate their genome and progress to the next G1 phase (Pardee, 1989). G2, between the end of S and the beginning of M phase allows cells to repair replication errors and strand breaks made during DNA synthesis and the preparations for mitosis. Progression through each phase of the cell cycle is governed by Cdks, which are activated by phosphorylation/ dephosphorylation events and binding to regulatory subunits or cyclins to form heterodimers (discussed above)(Nigg, 1995b; Cunningham and Roussel, 2001).

Mitogen stimulation induces entry and progression through G1 in part by ligand binding to receptors, activating multiple signalling pathways that converge on the transcription of immediate early genes, D type cyclins and assembly of cyclin-cdk4/6 kinase complexes (Roussel, 1998). Activated cyclinD-cdk4/6 complexes preferentially phosphorylate pRb and pRb related proteins p107 and p130 (Weinberg, 1995). The initial Rb phosphorylation is followed by additional phosphorylation of pRb by the cyclin E-cdk2 holoenzyme. Once phosphorylated, pRb and related proteins release tethered E2F transcription factors that, in complex with their heterodimeric partner proteins DRTF1-polypeptide (DP-1 or –2) either activate or repress gene transcription essential for the G1 to S phase transition and commitment to mitosis. Cyclin-cdk complexes are negatively regulated by cyclin dependent kinase inhibitors (Cdkis). In mammals, Cdkis are divided into two families, the Cip/Kip family comprising p21Ink/Cip1, p27/Kip1 and p57Kip2, and the Ink4 family (so named because they inhibit cdk4/6) which includes p16/Ink4a, p15/Ink4b, p18/Ink4c and p19/Ink4d (Fig 1.1).

Control of cell number by an intracellular cell division counter

Control of oligodendrocyte numbers during development has been well studied and it provides an interesting comparison to other studies on mammalian cell number control. In culture, there is evidence for a "clock" mechanism that controls the timing of oligodendrocyte differentiation and withdrawal from the cell cycle. It has been proposed that the timer has two components, one that counts time per se and another that stops the cell cycle and initiates differentiation when the time is right (Barres and Raff, 1994). These mechanisms involve the combined action of extracellular factors and the intracellular cell cycle machinery. Some of these components have been identified and are discussed below.

The progeny of individual oligodendrocyte precursors (OLPs) tend to stop dividing and differentiate at approximately the same time in culture (Temple and Raff, 1986). The observation that two sister OLPs cultured in different microwells divide the same number of times before leaving the cell cycle and differentiating, suggested that an intrinsic mechanism operates in precursor cells to limit their proliferation lifetime and trigger differentiation after a certain time or number of cell divisions (Temple and Raff; 1985). However, precursors cultured at 33°C stop dividing earlier and differentiate earlier than cells maintained at 37°C even though they divide more slowly at 33°C, suggesting that the intrinsic mechanism measures time, not cell divisions (Gao and Raff, 1997). In principle, therefore, the timer might stop cell division after some time interval, resulting in a fairly constant number of cell divisions (assuming a roughly constant cell cycle time) and ultimately a fairly reproducible number of cells (Gomer, 2001).

However, more recent data suggest that cell-intrinsic mechanisms are not solely responsible for limiting progenitor cell number during development. Experiments by Van Heyningen et al (2001), suggest that progenitor cell number is limited by environmental factors rather than a cell-intrinsic mechanism in vivo.

Control of cell division by limiting amounts of mitogen supply

Mitogenic growth factors are probably produced in limiting amounts in vivo. For example, Van Heyningen et al (van Heyningen et al., 2001) showed that the number of oligodendrocyte progenitor cells (OLPs) is limited by the supply of extracellular PDGF-A. PDGF-A is made by neurons, mainly, and acts on OLPs via the PDGF alpha-receptor (PDGFRα). Increasing the expression of *PDGF-A* in neurons in transgenic mice by introduction of *PDGF-A* transgenes led to an increase in the number of progenitors. Different lines of transgenic mice that expressed different numbers of *NSE-PDGF-A* transgenes were inter-bred. This created a battery of mouse embryos that expressed different amounts of *PDGF-A* in neurons [under the neuron-specific enolase, *(NSE)* promoter]. The level of *PDGF-A* expression and the number of OLPs was analysed in these different lines and a direct linear relationship between the levels of *PDGF-A* mRNA (presumably reflecting rate of production of PDGF-A protein) and final numbers of OLPs was apparent. Despite a more than 10-fold increase in the number of OLPs, there was no evidence of a cell-intrinsic limit on proliferation that could kick in to halt cell division. Van Heyningen et al (2002) also showed that, as numbers of oligodendrocyte progenitors increase in vivo, the cell cycle time increases (from ~20hr to ~100hr between E14 and E17). However, if progenitors are removed from the animal

and cultured in saturating levels of PDGF-A, the cell cycle accelerates, independently of their previous rate of division in vivo. This demonstrates that PDGF is limiting in vivo and suggests strongly that cells limit their own proliferation in vivo by consuming the available PDGF. Alternatively, OLPs might produce an autocrine, antiproliferative factor, that slows the cell cycle progressively. Such autocrine anti-proliferative factors do exist; for example the myostatin family of growth factors, members of which inhibit proliferation of myoblasts during muscle development (Lee and McPherron; 1999). Nevertheless, regardless of whether OLPs consume mitogens, produce autocrine anti-mitogens, or both, the van Heyningen experiments clearly demonstrate that OLP number in vivo is controlled by the environment in vivo, not by a cell-intrinsic mechanism.

One prediction of the "mitogen-depletion" model is that, if the proliferating cells should provide their own mitogen supply - i.e if an autocrine mitogenic loop is set in place – then the mitogen supply will be unrestricted and cell proliferation unlimited. This could be tested by arranging to express *PDGF-A* in OLPs in transgenic mice. This experiment cannot be done at present because no OLP-specific transcriptional regulatory elements have yet been identified. However, it might be possible to test the general principle of "mitogen-depletion" in another cellular system. We know, for example, that retinal astrocytes express PDGFRα and depend partly on PDGF-A for their proliferation (Fruttiger et al 1996). *A GFAP-PDGF-A* transgene (GFAP = Glial Fibrillary Acidic Protein, an astrocyte-specific intermediate filament protein) should therefore drive an autocrine PDGF mitogenic loop in retinal astrocytes. These mice have been generated in the Richardson lab and indeed cause massive overgrowth, but not unlimited proliferation

of retinal astrocytes. Why this should be, and how intracellular and extracellular controls on cell number are interrelated, has been the major question addressed in this Thesis.

PDGF signalling

PDGF was originally identified in platelets and in serum as a mitogen for fibroblasts, smooth muscle cells and glia in culture. A family of PDGFs have been identified which consists of four members: PDGF-A, -B, -C and -D (Li et al., 2000; Bergsten et al., 2001). These family members assemble in the endoplasmic reticulum and are secreted as hetero- or homodimers (PDGF-AA, -BB, -CC, -DD or -AB). Their action is mediated via two cell-surface receptor tyrosine kinases PDGFRα and PDGFRβ (Heldin et al., 1998; Heldin and Westermark, 1999). The receptors dimerise into PDGFR-αα, PDGF-ββ or PDGF-αβ depending on which ligands are available. PDGFR-α binds PDGF-A, -B and -C, whereas PDGFR-β binds PDGF-B and -D. Once these receptors dimerise upon ligand binding, a trans-phosphorylation occurs between the receptor partners. SH2 domain containing proteins (e.g the adaptor protein Grb2) then recognise and bind to newly phosphorylated tyrosine residues. In the case of Grb2, this protein then recruits the nucleotide exchange factor Sos1 to allow activation of the Ras pathway as well as directly binding enzymes such as the Src tyrosine kinase and phopholipase C-γ. These activate separate signalling pathways, which appear to converge on a set of immediate early genes that become transcriptionally active.

Gene knockout experiments in mice have revealed the importance of *PDGF* and *PDGFR*s during development (Fruttiger et al., 1999; Betsholtz et al., 2001a; Orr-Urtreger

et al., 1992; Soriano, 1997). The two receptors have different developmental roles in vivo by virtue of their different expression patterns. However, intracellular domain swopping experiments demonstrate that signalling downstream of the two receptors can largely compensate for each other (Klinghoffer et al., 2001).

PDGF-A is expressed even in the preimplantation embryo and is co-expressed with *PDGFR-α* in the blastocyst inner cell mass. Later, signalling becomes paracrine (Palmieri et al., 1992) and *PDGF-A* becomes widely expressed in epithelia, muscle and nervous tissue. In contrast, *PDGFR-α* is expressed by most mesenchymal cells i.e expression is non-overlapping but adjacent to its ligand PDGF-A (Orr-Urtreger and Lonai, 1992). In general, it appears that PDGF acts on specific populations of progenitor cells in a variety of different developmental processes (Schatteman et al., 1992). The most well documented function of PDGFs in vitro is control of cell proliferation, for example in retinal astrocytes and oligodendrocyte progenitors as I discuss here. Other roles include control of cell migration, actin reorganization and membrane ruffling (Betsholtz et al., 2001b).

Control of cell survival

Control of cell survival and cell death is also used to control cell number. It has been proposed that cells are constantly dependent on survival signals, in the absence of which they die by programmed cell death (PCD). This ensures that cells survive only when and where they are needed (Raff, 1996a). During development of the nervous system many types of neurons are overproduced and then compete with one another for limiting

amounts of survival signal secreted by the target cells that they innervate. This serves to match the number of neurons to the number of target cells. In the retina itself, it appears that naturally occurring cell death contributes to controlling the number of retinal ganglion cells (RGC) that develop. The last retinal ganglion cells develop by E18 in mice. RGC death then begins at or just before birth, peaks at around P4-P6 and is almost complete by P12 (Strom and Williams 1998). In a transgenic mouse overexpressing Bcl-2, an inhibitor of apoptosis, the RGC layer has 40-50% more neurons than normal (Martinou et al 1994).

PCD is crucial to control oligodendrocyte number during development (Raff et al., 1998). For example, about 50% of the oligodendrocytes generated in the developing optic nerve normally undergo PCD soon after they differentiate (Barres et al., 1992). It is thought that differentiated oligodendrocytes are dependent on survival signals from axons. In the Bcl-2 transgenic mouse mentioned above, the number of axons in the optic nerve is increased by elevated numbers of RGCs. In these mice, the number of oligodendrocytes in the optic nerve increases in proportion (Burne et al., 1996). These experiments led to a model whereby the number of oligodendrocytes is matched to the number and length of axons requiring myelination.

Consistent with this model, increasing the number of oligodendrocyte progenitors by overexpressing *PDGF* in transgenic mice, although it leads to an increase in the number of differentiated oligodendrocytes over the short term, has no long term effect on oligodendrocyte numbers because the extra oligodendrocytes die. This is to be expected because axon-derived survival factors are unaffected in the transgenics (Calver et al., 1998).

Another example where progenitor cell number is controlled by PCD is in the control of neuronal progenitor cell number, as revealed when proliferation becomes deregulated. Examples of this are found in mice lacking *p27 Kip1* (Levine et al., 2000), retinoblastoma protein (*Rb*) (Jacks et al., 1992) or *p57/Kip2* (Dyer and Cepko, 2001a). In the *p57Kip2* knockout mouse, many apoptotic nuclei were detected during retinal development in the inner neuroblastic layer where this protein normally participates in cell cycle exit. BrdU labelling shows that cells in the neuroblastic layer are dividing abnormally at this time too. Cells might die because they receive conflicting signals to differentiate and to proliferate. Cessation of proliferation is likely to be a multi-step process and when any one step is eliminated cells still exit the cycle but at an earlier or later time than usual (Dyer and Cepko, 2001b).

1.2 Control of cell size versus cell number

So far, I have discussed regulation of cell number during development. However in determining the final size of the organ or organism, regulation of cell size as well as cell number might be important. Experiments on *Drosophila* have demonstrated the importance of both cell size and cell number in determining organ size. For instance, experimentally increasing cell proliferation in the posterior wing imaginal disc by directed expression of the transcriptional regulator and elongation factor E2F, resulted in an increase in cell number coupled with a decrease in cell size. As a consequence the posterior compartment of the wing remained the same size. Conversely, slowing down the cell cycle by directed expression of the *Drosophila* homolog of retinoblastoma (*Rbf*),

a co-repressor of E2F, led to a decrease in cell number and an increase in cell size, but no change in compartment or wing size (Potter and Xu, 2001). Such experiments demonstrate that altered cell proliferation does not necessarily lead to changes in organ size (Su and O'Farrell, 1998) and suggest that there are size control mechanisms that monitor total tissue mass rather than cell numbers. However cell number control is still clearly important for determining organ size. For instance, the differences in organ size between species are most often a result of differences in cell number (Raff, 1996c). For example, an elephant heart is larger than a mouse heart because of an increase in cell numbers (Raff, 1996d). On the contrary, when the phosphoinositol 3-kinase (PI3K) signal transduction pathway is activated and expressed in the mouse heart this can lead to an increase in heart organ size due to an increase in cell size (Shioi et al., 2000). The above experiments show that regulation of cell number can be separated from organ size control. Nevertheless, organ size control may connect and co-ordinate with cell proliferation and cell growth to ensure correct organ size. It has been suggested from work in *Drosophila* that mechanisms that control the patterning genes (e.g *hox* genes) may be responsible for setting organ sizes. After initial specification by the patterning genes, the mechanisms that monitor organ size or total mass most likely function to coordinate cellular growth and proliferation.

1.3 The Ink4a family of cdk inhibitors

The *Ink4a* family all share a common structural feature- the presence of ankyrin repeats. They are expressed in a cell type specific manner. p16Ink4a is the only one classified as a tumour suppressor by the genetic criteria of loss of heterozygosity (LOH) (Ruas and

Peters, 1998). Mutation at this locus occurs in melanoma (Kamb, 1994). Each holoenzyme complex contains a regulatory subunit, the cyclin, and a catalytic subunit, the cyclin-dependent kinase. During progression through G1, the amount of D type cyclin increases in a mitogen regulated manner and activates cdk4/6 (Vidal and Koff, 2000). Ink4 proteins compete with D-type cyclins to bind cdk4/6. This frees cyclin D, which then becomes targeted for degradation and consequently extinguishes cdk4/6 activity. This allows cells to proceed through S phase. Cip/Kips are potent inhibitors of cyclin E- and A-dependent Cdk2, however they also act as positive regulators of cyclinD-cdk4/6 complexes by mediating their assembly early in G1 (Fig 1.1). When p27/Kip1 binds cyclin D-Cdk4/6 complexes, this frees up cyclinE-cdk2 complexes for activation. p27/Kip1 is then phosphorylated by cyclinE-cdk2 and targeted for degradation. Thus in cycling cells there is a reassortment of Cip/Kip proteins between cdk4/6 and cdk2 as cells progress through G1, alternately acting as positive and negative regulators of cdk activity.

Other Cdk inhibitors in development

What is the role of cdkis in development? Different cdkis appear to be acting in different cell types. *p27/Kip1*, *p57/Kip2* and *Ink4d* have been shown to be expressed in the retina during development, with roles in Muller glia, amacrine cells and horizontal cell differentiation for example. *Ink4b* is not expressed in the retina but has roles in the lens and cornea. *Ink4a* mRNA is reportedly expressed in the developing cortex (van Lookeren and Gill, 1998) and cerebellum (Watanabe et al., 1998a). In the cerebellum it is present in granule cells exiting the cell cycle in the external granular layer and is

sustained in these cells when they adopt their mature position in the internal granular layer (Watanabe et al., 1998b). It is also present in Purkinje cells of the cerebellum. p15 and p18 are also present in the cerebellum but the identity of the cells that express them is unknown. Later in this Thesis I present data on the role of Ink4a in the developing eye.

How do these cdkis act on the cell cycle during development? The brain, after being in a highly proliferative state during neurogenesis, enters a state of relative quiescence after birth except for specialised areas and certain cell types including glial cells. How do cdkis participate in replicative shutdown? In mouse retina, targeted deletion of *Kip1* causes hyperproliferation of specific cell lineages without affecting differentiation patterns. Likewise, oligodendrocyte progenitors deleted for *p27Kip1* continue to proliferate beyond the time they normally would have stopped (Durand and Raff, 2000). Ectopic expression of *Kip1* arrests cultured progenitors despite elevated mitogen levels but fails to trigger differentiation into mature oligodendrocytes unless mitogens are withdrawn. From these data, it appears that cdkis function only to regulate cell cycle arrest and withdrawal without directly affecting differentiation. In the retina, p27Kip1 cooperates with p19Ink4d to maintain neuronal quiescence independent of differentiation, and both are required to regulate exit from the cell cycle. It is only after both cdkis are deleted that proliferation continues inappropriately (Zindy et al., 1999b). It appears from these data that blocking both G1 and S phase kinases is critical to ensure permanent cell cycle exit and maintenance of longterm quiesecence. Retinae from mice deficient for *Ink4d* exhibit prolonged cellular division that is compensated by apoptosis

suggesting that continued expression of *Ink4d* might guard against inappropriate cell cycle entry. Mature *Ink4d* null animals show no apparent change in the architecture of the brain or retina compared with wild type, suggesting that deletion of *p19Ink4d* does not affect retinal differentiation patterns (Zindy et al., 1999a). However, p27/Kip1 and p57/Kip2 have been implicated in the differentiation of certain cell types as discussed before.

The *Ink4a* gene locus encodes two distinct growth inhibitors. One is the cyclin-dependent kinase inhibitor *p16/Ink4a*, which is a component of the Rb pathway. The other is the tumour suppressor protein *p19/ARF*, which has been functionally linked to p53 (Pomerantz et al., 1998). p19/ARF is thought to function as a tumour suppressor by physically interacting with Mdm2 to stabilize p53. Therefore, the *Ink4a* locus encodes separate proteins that function in the two central growth control pathways, Rb and p53.

1.4 Development of the vertebrate eye and retina

The eye is essentially a highly specialized extension of the brain. It forms as an evagination of the diencephalon in the early neurula. The vertebrate eye develops from an interaction of the neural tube with a series of epidermal thickenings called the cranial ectodermal placodes. The optic vesicle evaginates from the brain and an interaction between the neural tube and ectoderm induces a lens placode in the surface ectoderm. The transcription factor Pax-6 is required for the surface ectoderm to respond to the induction signal from the optic vesicle. The secreted signalling molecule, Sonic

hedgehog (Shh) is also thought to be required at this point in development. From its source, the ventral forebrain, it is thought to repress Pax-6 at the midline of the embryo, dividing the field of Pax-6 expression in two. In the absence of *Shh* a 'cyclops' phenotype develops i.e only one eye is present. The overlying ectoderm differentiates into lens cells as the optic vesicle folds in on itself and the lens placode becomes the lens vesicle (Fig 1.2). As the lens is internalised the optic vesicle then invaginates, becoming the optic cup. This occurs via molecular and mechanical cues provided by the lens, perhaps ensuring the lens is perfectly positioned with respect to the retina. The optic cup then differentiates into two layers. The outer layer produces melanin pigment and becomes the pigmented retina. The inner layer proliferates rapidly and generates a variety of glia, ganglion cells, interneurons and light-sensitive photoreceptor neurons. These cells constitute the neural retina. Fibroblast growth factors, (FGFs) secreted from the surface ectoderm promote neural retina fate whereas the ocular mesenchyme directs retinal pigment epithelium formation. Also at this time the lens vesicle induces the overlying ectoderm to become the cornea.

Tissue interactions are clearly important in development of the retina right from the outset of neural retina formation. In 1901 Spemann made the observation that ablation of

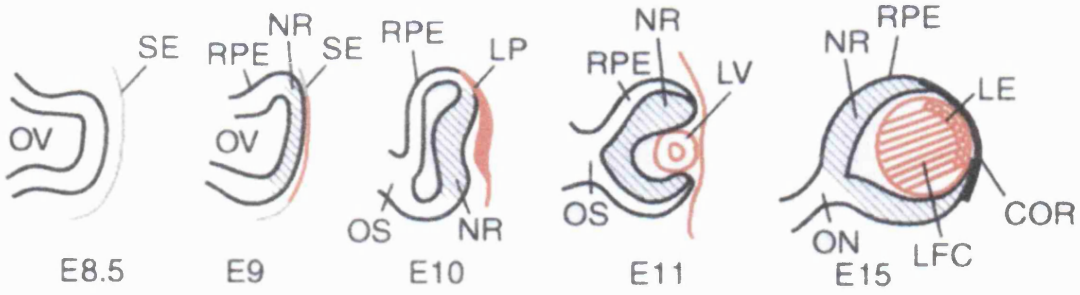

Figure 1.2 **Development of the vertebrate eye.** ***Adapted from Ashery-Padan and Gruss (2001), Figure 1.*** Schematic illustration of eye development in the mouse. At embryonic day 8.5 (E8.5) the evagination that will give rise to the optic vesicle (OV, black) is extending laterally from the brain. In response to inductive signals from the OV the oeverlying surface ectoderm (SE, orange) thickens, forming the lens placode (LP), which then internalises (E10) and detatches from the ectoderm (lens vesicle, LV) (E11). The posterior cells of the lens vesicle differentiate to lens fiber cells (LFC) while the anterior cells become the lens epithelial cells, a layer that maintains mitotic potential (E15).

the presumptive retinal region of neural plate stage *Rana temporaria* embryos resulted not only in the absence of retinal development but also in the loss of lens formation. Lens development was hence proposed to depend on presumptive retina. The idea of embryonic induction subsequently emerged from this evidence.

The neural retina develops into a layered structure of different cell types. During retinogenesis, the different retinal cell types are generated in a defined birth order from a population of multipotent retinal progenitor cells residing in the outermost layer of the optic cup. These retinal precursors generate the neurons and glia of the neural retina. The typical striated laminar pattern of the neural retina results from inward migration and differential death of cells from the germinal layer (Fig 1.3). Turner and Cepko (Turner and Cepko, 1987) performed retroviral lineage analysis and showed that a single precursor cell can give rise to at least three types of neurons or to two types of neurons and a glial cell. For example, a single precursor can give rise to a number of rods, a bipolar neuron and a Muller glial cell. Initially the neuroblastic layer is split into two main layers - the inner and outer neuroblastic layers. Retinal ganglion cells, cone photoreceptors and horizontal cells are born first, followed by amacrine and rod photoreceptor cells, while bipolar and Muller cells appear last (Fig 1.3).

1.5 Development and function of retinal astrocytes.

Glial cells outnumber neurons by at least 10:1 in the human brain (Bignami et al., 1991). Of these, astrocytes are the most numerous glial cells. They owe their name to their

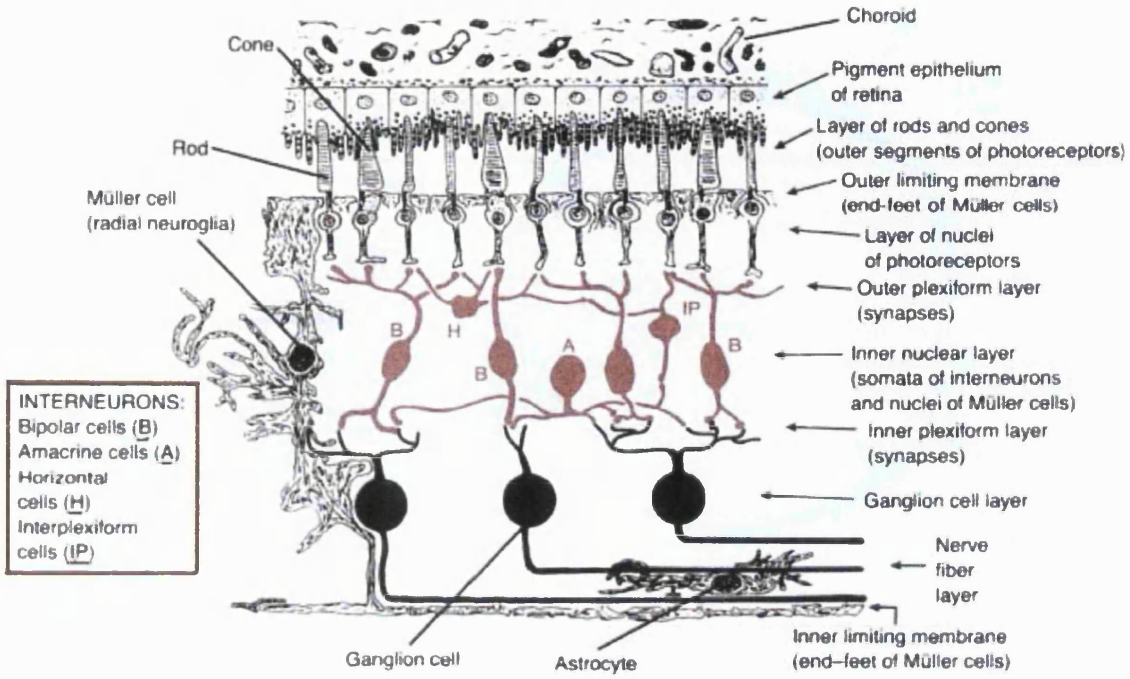

Figure 1.3 **Schematic diagram showing a cross section through the retina.** This diagram demonstrates the distinct layers of the retina composing neurons, pigmented epithelial cells and neurone support cells. The outermost layer consists of the pigmented epithelial cells. Below are the rod and cone cell processes. The outer nuclear layer contains the cell bodies of the rod and cone photoreceptors, as marked in the diagram. Underneath, the cell bodies of the intergrating neurons make up the inner nuclear layer. Deep to this, is the ganglion cell layer. The innermost layer of the retina contains the retinal vasculature and retinal astrocytes. The position of astrocytes in relation to nearby cells/structures (retinal ganglion cells, the end feet of Muller cells and the optic nerve fibres) is shown.

Source: //publish.uwo.ca/~jkiernan/retina.jpg

roughly star shaped processes, which also give clues to their function in the nervous system. Over 100 years ago, Golgi first suggested that astrocytes should play a role in the distribution of energy substrates from the circulating blood to neruons (Golgi 1886) . The long proceses of astrocytes can be seen touching nerve cells in the brain and spinal cord, and in contact with blood vessels. We are still only at the beginning of understanding astrocyte function, however.

Golgi (1886) first noticed the close association of astrocytes with blood vessels. More recently it has been established that astrocytes contribute to formation of the blood brain barrier (BBB) (Neuhaus et al 1991). The BBB is responsible for the selective exclusion from the CNS of blood cells and certain molecules that are carried in the blood. It is composed of a specialized microvascular endothelium, glial cell elements, astrocytes and microglia in physical proximity to the endothelium , and a basement membrane (Prat et al., 2001b; Abbott, 2002). Astrocytes form large processes or end-feet which contact and cover the surface of brain capillaries (Prat et al., 2001a). Constant input from glia is required to maintain the BBB-related properties in endothelial cells. Culture experiments have suggested that an astrocyte derived soluble factor is responsible for the maturation of endothelial cells into a BBB (Neuhaus et al., 1991). Factors released by astrocytes alter the phenotype of endothelial cells and can induce tight junction formation between brain endothelial cells. Following injury, activated astrocytes respond by producing many chemokines and cytokines that can increase the permeability of the endothelial cell barrier and allow entry of lymphocytes in to the parenchyma of the CNS.

Another function of astrocytes is to buffer the extracellular level of neurotransmitters around symapses. For example, *Glutamine synthetase* is expressed in astrocytes and is involved in recycling glutamate. Astrocytes take up synaptically released glutamate and convert it to glutamine which is released and taken up by neurons to replenish their glutamine pools. This is a protective role for astrocytes, given that accumulation of extracellular glutamate leads to exitotoxic damage and neuronal death, and is involved in the pathophysiology of ischemic brain damage and other neurodegenerative diseases (Perego et al., 2000). Astrocytes also protect neurons from exitotoxic damage from elevated potassium ions in the extracellular space, caused by neuronal activity. They are highly permeable to potassium and this allows them to maintain the right extracellular concentration of this ion (Walz, 2000).

Astrocytes have other roles involved with synaptic transmission. They respond to neuronal activity with an elevation of their intracellular calcium. This triggers the release of chemical transmitters that can influence neuronal activity (Barres and Barde, 2000; Araque et al., 1999). Astrocytes have been shown to enhance the number of functional synapses that form between neurons in cultures (Pfrieger and Barres, 1996)
On injury to the CNS, astrocytes are known to become activated in a process called 'gliosis' where they up-regulate GFAP and release cytokines, which are presumably beneficial to repair. Apart from their functions in the adult, astrocytes also have functions in the developing CNS. For example, they have been shown to release trophic factors for growing neurons and guidance cues for growth cones. In the next section I discuss the importance of astrocytes in development of the retinal vasculature.

1.6 Astrocytes and the retinal vasculature development

Retinal blood vessels are derived from an ingrowth of capillaries arising in or near the optic nerve head. The resulting pattern of vessels varies greatly among different vertebrates (Michaelson 1954). Some animals such as guinea pigs have almost no retinal vasculature and nutrition is supplied by diffusion from the choroid vasculature. Such species lack retinal astrocytes. In fact retinal astrocytes seem to go hand in hand with the retinal vasculature, reflecting an important functional association.

In the mouse, the retinal vasculature develops as a spreading network, entering the retina from the optic nerve head just after birth and spreading subsequently towards the peripheral retina. These vessels form a network at the inner surface of the retina, and are intimately associated with retinal astrocytes. The vessels are preceeded by a network of retinal astrocytes that also spreads from the optic nerve head. Initially, the retinal vessels appear to follow the retinal astrocyte network. Subsequently, when vessels have spread across the entire retina, they start to sprout downwards into the inner plexiform layer where they establish a second vascular network parallel to the first. This second vasculature is not normally associated with retinal astrocytes.

It has been proposed that the spread towards the periphery of the developing vasculature is signalled by migrating retinal astrocytes, which respond to the metabolic demands of the rapidly differentiating neural retina by expressing *VEGF*, which in turn stimulates

vascular growth by acting through VEGF receptors (Flt-1) on endothelial cells (Provis et al., 1997a). Astrocytes migrate onto the neonatal retina from the optic disc along the ganglion cell fibre layer and spread radially, forming a lacy network of cells. Retinal astrocytes in several species have been seen to progress slightly in advance of the vessels. As the vasculature develops, endothelial cells use the established astrocytic template to determine the retinal vascular pattern (Zhang and Stone, 1997c). Initially the vessels grow radially as spokes, but then become progressively more interconnected by capillary plexus formation. Vessels grow as a monolayer in the nerve fibre layer up to p10. Between p7 and p8 collateral branches begin to sprout from this primary plexus and penetrate into the retina to the outer plexiform layer. By p21 the entire network undergoes extensive remodelling and a tertiary or intermediate plexus forms at the inner surface of the inner nuclear layer. Other cells associated with the developing vasculature include pericytes which assemble over the surfaces of vessels, particularly arteries, and are thought to strengthen the vessel walls against the interior blood pressure (Lindahl et al., 1997). Microglia are also present in vascular and avascular areas prior to retinal development but more develop in association with the vasculature.

It has been proposed that maturation of photoreceptors and neurons leads to the development of a 'physiological hypoxia' in the retina, which in turn induces VEGF expression by astrocytes and proliferation of the vascular endothelium (Chan-Ling et al., 1995; Stone et al., 1995b). The oxygen brought in by those vessels down-regulates the expression of VEGF by local astrocytes making the process self-limiting (Stone et al., 1995a). Perhaps the spread of increased metabolic activity in progressively more

peripheral locations ensures the retina is vascularised to the periphery (Provis et al., 1997b). Astrocytes appear to be strategically located to control vessel growth being at the leading edge (Zhang and Stone, 1997a). Further evidence that astrocytes act as a template for the developing vasculature comes from Otani et al (Otani et al., 2002). These authors injected bone marrow stem cells into eyes at birth. The cells were seen to attach only to the astrocytes in poorly-vascularised or unvascularised areas of the retina. They then incorporated into vessels, after 2 weeks.

As mentioned in the previous section, astrocytes form the glia limitans of retinal vessels and induce barrier properties in them. Diseases of the retinal vasculature include the common and damaging growth of vessels out of the retina into the vitreous humour often with bleeding. This can occur in retinopathy of prematurity, diabetic retinopathy, venous occlusive disease and altitude retinopathy. It is often related to prolonged hypoxia of the retina, which can induce high levels of *VEGF* expression by the retina and accumulation of VEGF in the vitreous humour. VEGF has been shown to be upregulated under hypoxia in vitro and in vivo. When kept in low (6%) oxygen, adult mice showed upregulation of VEGF in the brain and in particular in glial and nerve cells here (Marti and Risau, 1998). So, just as retinal vascular development is driven by hypoxia, during ischemia (stroke), abnormal vascular growth is associated with a similar lack of blood/oxygen supply (Zhang and Stone, 1997b).

There are some subtle differences between the retinal vasculature of humans and mouse. The human retinal vasculature is asymmetric, unlike the symmetrical mouse vasculature.

Human vasculature develops into four vascular beds creating a butterfly shape along the temporal/nasal axis. Also the human retina, as for other primates, has a fovea in the temporal retina, which is a specialisation for high visual acuity. This is completely absent in mice. The fovea has a very high local density of cone photoreceptors and inner retinal cells during development but excludes astrocytes and retinal vasculature. Blood vessels actually grow around but not through this area.

Maintaining neuronal, glial and vascular relationships in the retina is important. Because the retina consists of well defined layers of neuronal, glial and vascular cells, relatively small disturbances such as those seen with vascular hyper-proliferation or edema can lead to significant loss of visual function. In fact, most diseases that cause vision loss involve abnormal angiogenesis.

It is not only in the retina that neuron-glial-vascular relationships determine vascular development. In the embryonic mouse limb skin, for example, peripheral nerves provide a template that determines the pattern of blood vessel branching and arterial differentiation via local secretion of VEGF (Mukouyama et al 2002). The glial cells in this part of the nervous system – the Schwann cells – are required for arterial differentiation and blood vessel-nerve alignment. Mukouyama et al (2002) proposed that the nerve promotes arteriogenesis via local secretion of VEGF by Schwann cells. However, it is unclear whether the source of VEGF is axons, Schwann cells or both; perhaps expression of *VEGF* by axons requires the presence of Schwann cells.

1.7 Hyaloid vasculature

The hyaloid vascular system (HVS) is a transient network of intraocular vessels that is present during normal development. The HVS in mouse is composed of endothelial cells and several types of perivascular cells forming the hyaloid artery, the vasa hyaloidea propria (VHP) branching from the hyaloid artery, the tunica vasculosa lentis surrounding the lens and the papillary membrane (Mann 1950). Hyaloid vessels nourish the growing lens and adjacent mesoderm during early development and then subsequently regress (Mann 1950).

The mouse HVS normally regresses during the first 2 weeks of postnatal development (Ito and Yoshioka, 1999b). HVS regression involves apoptosis in endothelial cells and pericytes. This apoptosis is at least partially p53-dependent because HVS regression is slowed or incomplete in inbred *p53*-/- BALB/c and C57BL/6 mice. Apoptosis in the HVS peaks between p7 and p8 in the mouse (Reichel et al., 1998) and the VHP regresses between p6 and p10 (Ito and Yoshioka, 1999a). Abnormalities of regression of the hyaloid vascular system are associated with ocular pathologies in humans including persistent hyperplastic tunica vasculosa lentis (PHTVL), persistent hyperplastic primary vitreous (PHPV) and persistent prepupillary membrane (PPM) (Zhu et al., 1999).

1.8 Oxygen as a mediator of cell proliferation/differentiation

Oxygen is essential to the life of all aerobic organisms. Virtually every cell tested is able to sense a reduced oxygen supply (hypoxia) and to induce a set of oxygen-regulated genes in response (Wenger, 2000b). Oxygen is also an important developmental cue in a number of different areas of the body.

During placental development, for example, low levels of oxygen control development of cytotrophoblasts, a type of epithelial stem cell. Differentiation of these cells determines whether chorionic villi - the placenta's functional units - float in maternal blood or anchor the conceptus to the uterine wall (Genbacev et al., 1997). In anchoring villi, some cytotrophoblasts detach from their basement membrane and aggregate to form cell columns. Cytotrophoblasts at the distal ends of these columns attach to and then deeply invade the uterus and its arterioles. The cells then replace the endothelial and muscular linings of uterine arterioles initiating maternal blood flow to the placenta and greatly enlarging the vessel diameter. Differentiation begins when the cytotrophoblasts form columns and ends when they have deeply invaded the uterus. In columns, the cells are proliferative but, more distally, proliferation stops and the cytotrophoblasts modulate expression of proteins including integrin cell adhesion molecules, matrix metalloproteinase-*9*, and human placental lactogen. Before cytotrophoblast invasion of maternal vessels and formation of a circulation between uterus and placenta after 10 weeks, the conceptus is in a relatively hypoxic atmosphere. Thus, as cytotrophoblasts invade the uterus during the first half of pregnancy, they encounter a steep gradient of

oxygen tension equivalent to 20 mmHg (~2% oxygen) at the surface to about 100 mmHg (~12% oxygen) in the interior of the tissue. In explant cultures of anchoring villi, cytotrophoblasts were found to proliferate under 2% but not 6% or 20% oxygen (Genbacev et al 1997). In addition, these cells started to express *integrin α1*-a stromal and cytotrophoblast cell differentiation marker- under normoxic conditions but failed to express it under hypoxic conditions. Integrin α (a laminin and collagen receptor) is required for invasiveness in vitro and is expressed by differentiated stromal cells and cytotrophoblasts. Under hypoxia, although cytotrophoblasts failed to express integrin α1, stromal cells were unaffected by hypoxia suggesting that the affect on differentiation is cell-type specific. Hypoxia affected the expression of another differentiation marker, human placental lactogen but not that of some other stage-specific antigens suggesting that hypoxia has selective effects on gene expression and differentiation.

Another example where hypoxia is reported to keep cells in an immature state is neuroblastoma. This childhood tumour arises from immature cells in the developing sympathetic nervous system (SNS), which derives from neural crest. In cultures of these cells or in neuroblastoma xenographs grown in mice, hypoxic regions show decreased expression of several neuroendocrine genes yet increased expression of neural crest sympathetic progenitor markers (*c-kit* and *Notch-1*) as well as *VEGF*, *HIF-1α* and *tyrosine hydroxylase*. In vivo, hypoxia was marked by expression of *VEGF*, *HIF-1α* and *tyrosine hydroxylase*. These de-differentiation effects could be mimicked by culturing tumour cells in hypoxic (1% oxygen) conditions.

Yet another example of hypoxia affecting proliferation is in the retina, as already discussed. Here, hypoxia-mediated proliferation is mediated by VEGF, a potent mitogen for endothelial cells. This dimeric glycoprotein resembles PDGF and is produced by a number of different cell types in response to hypoxia including endothelial cells themselves. The effects of VEGF are mediated via two receptor tyrosine kinases – Flt-1 (VEGFR-1) and Flk-1 (VEGFR-2). Both VEGF and its receptors are thought to be upregulated under hypoxia (Faller 1999). These receptors have slightly different specificities for the various VEGF isoforms (VEGF-A to E). Gene knockout experiments reveal the crucial role of *VEGFR*s for vasculogenesis and angiogenesis during embryonic development (Kliche and Waltenberger, 2001). Ligand binding induces auto/transphosphorylation of different tyrosine residues of the intracellular domain of the VEGFR. Phosphorylated tyrosines are then targets for adaptor proteins such as Shc, Grb2 and c-Src. Thereafter, various intracellular signal transduction pathways are activated. For activation of VEGFR-2, the downstream effects of activation include proliferation and migration, nitric oxide release, effects on survival, increase of vascular permeability and modulation of gene expression. The role of other angiogenic factors are summarised in Table 1 at the end of this chapter.

The mammalian oxygen sensing pathway

HIF-1α (Wang and Semenza, 1995a) is a transcriptional activator that mediates changes in gene expression in response to changes in cellular oxygen concentration. It plays important roles in normal development, physiologic responses to hypoxia and the pathophysiology of common human diseases. HIF-1α has been well studied since its

discovery and it is reportedly expressed in most cells tested, in response to lowered oxygen. It therefore seems to be involved in a universal oxygen-sensing pathway in mammalian cells.

The molecular oxygen sensor itself has been proposed recently to be prolyl hydroxlase (PH), based on its requirement for dioxygen as a cosubstrate and iron as cofactor (Jaakkola et al., 2001). Virtually all proteins capable of binding molecular oxygen contain iron, usually in the centre of a haem moiety (Wenger, 2000a), so it was always possible that the mammalian oxygen sensor could be a haem-containing protein. This 'haem hypothesis' was further supported by the evidence that iron chelators such as desferrioxamine and cobalt chloride are capable of mimicking hypoxia (Wenger, 2000c; Wang and Semenza, 1993). However, it has been determined that PH is not a haem-protein after all. PH modifies HIF-1α by a trans-4-hydroxylation. When hydroxylated, HIF-1α, unlike the non-hydroxylated form, is unable to up-regulate downstream genes involved in oxygen homeostasis such as *VEGF*. Inhibitors of PH - for example, oxaloglutarates - are able to block the hydroxylation modification on proline^{564} in HIF-1α in cell extract assays, leading to accumulation of HIF-1α. Although a non-haem protein, PH contains an iron centre and its oxygen sensing depends on iron. Supplementary Fe(II) (100μM) enhanced an interaction of HIF-1α with its binding partner, von Hippel Lindau protein (VHL) in a transcription/translation assay (reticulocyte lysates). Conversely, addition of 100μM desferrioxamine, an iron chelator, greatly diminished this interaction (Jaakkola et al; 2001).

Action of HIF-1α

HIF-1 is a member of a gene family that also includes *HIF-2* and *HIF-3*. HIF -2 has similar properties to HIF-1α but HIF-3 has not been characterised yet. HIF-1 is a ubiquitously and constitutively expressed heterodimeric transcription factor composed of a subunit that is unstable under normoxia and a common beta subunit HIF-1β (or ARNT), the latter being shared by other transcription factors. HIF-1α heterodimerisation with HIF-1β/ARNT in the nucleus is required for DNA binding and transactivation (Gassmann et al., 1997) but not for translocation into the nucleus (Chilov et al., 1999). HIF-1α has an oxygen dependent degradation (ODD) domain. Under normoxic conditions, this domain is hydroxylated by PH, which effectively primes HIF-1α for ubiquitination via the von Hippel Lindau protein (VHL). This tumour suppressor protein recognises and links HIF-1α subunits via a multiprotein complex, to the ubiquitination machinery (Maxwell et al., 1999). Cells deficient in *VHL* show constitutively high HIF-1α levels and expression of many oxygen-regulated genes.

Once activated by hypoxia, HIF-1α binds to the consensus *HIF-1α* DNA binding site present in the hypoxia response elements (*HRE*) of many oxygen-regulated genes. In 1995 Semenza et al discovered HIF-1 on the basis of its ability to bind to a hypoxia response element (*HRE*) in the 3' flanking region of the erythropoietin gene (Wang and Semenza, 1995b). Since then further HIF-1 target genes have been discovered including those involved in oxygen transport, regulation of erythropoiesis, angiogenesis and vascular tone. Such genes include *erythropoeitin*, *VEGF*, *Flt-1* and *transferrin*. HIF-1α

also upregulates genes involved in anaerobic metabolic pathways such as glycolysis and glucose uptake (e.g *aldolase A* and *glucose transporter-1*) (Wenger, 2000d) . With this range of target genes, HIF-1α has been labelled a master regulator of adaptive responses to hypoxia.

Studies of the *HIF-1α* null mouse have revealed it has a important role during development. *HIF-1α* -/- mice arrest in development by day 9 of gestation (E9) and die by E10.5, with severe cardiovascular and neural tube defects and massive cell death especially in the branchial and cephalic regions. It is thought to be required for mesenchymal cell survival during embryonic development. Heterozygous mice develop normally, but when subjected to long term hypoxia (10% for 3 weeks) erythrocytosis and pulmonary vascular remodelling is significantly impaired (Yu et al., 1999).

HIF-1α is also essential for angiogenesis in ischemic tissue. HIF-1α mediated VEGF expression may play a major role in the development of retinopathy of prematurity and other ischemic retinal disorders such as diabetic retinopathy (Semenza, 2001).

HIF-1α plays an important role in promoting tumor progression. It is overexpressed in the majority of common human cancers and its increased expression correlates with tumour grade and vascularisation. Its increased activity results in increased expression of target genes with important roles in tumour progression such as induction of tumour vascularisation by VEGF. As hypoxia is a common feature of solid tumours, this suggests that activation of HIF might underlie these patterns of tumour-associated gene

expression. However, this is not the only activator of HIF: inactivation of tumour suppressor genes, activation of oncogenes and diverse growth factor pathways are also known to activate HIF (Maxwell et al., 2001). Nevertheless, as a master regulator of adaptive responses to hypoxia, HIF has been proposed to help the tumour adapt to hypoxic conditions and promote tumour growth, leading to more aggressive vascularised tumours. Warburg first noted that glycolysis is greatly enhanced in cancer and this effect was named– 'the Warburg Effect'. HIF may promote this switch in metabolism by upregulating genes involved in the glycolytic pathway. However, in such studies of the role of HIF in cancer, there are still difficulties distinguishing cause and effect in the cancer phenotype. Is HIF driving the tumour or is it a co-selected result of other activated pathways? This is a particularly crucial distinction when devising strategies for therapy.

Hypoxia in astrocytes and in the retina

What are the specific effects of hypoxia on astrocytes? Hypoxia is already known to be important during retinal vascular development where it acts on astrocytes, as discussed in the previous section. As mentioned, Stone et al (1995) show that astrocytes respond to hypoxia by secreting VEGF in the retina, leading to endothelial cell proliferation. In this Thesis, I look further at the effect of hypoxia on retinal astrocytes.

In the adult, astrocytes are known to express *erythropoietin (Epo)* in response to hypoxia. This is the major hormone controlling the hypoxia-induced increase in the number of erythrocytes. Erythropoietin stimulates the proliferation and differentiation of erythroid progenitor cells in the bone marrow by providing protection against apoptosis. However,

Epo is also known to act in the nervous system and is expressed by astrocytes here. It is suggested that Epo has a neuroprotective role and acts in a paracrine way on neurons (Morishita et al., 1997). An anti-apoptotic effect of Epo protects brain cells against ischemic damage in vivo (Siren et al., 2001) and oxidative stress in vitro (Zaman et al., 1999). Direct administration of Epo to the CNS of mice significantly reduces neuronal death and reduces learning disability associated with cerebral ischemia (Bernaudin et al., 1999).

Epo expression can also be stimulated by mimics of hypoxia -cobalt chloride or desferrioxamine- in vitro and in vivo (Bernaudin et al., 2000). Both substances appear to potentiate the transcriptional activation of HIF-1α, perhaps by a replacement or a chelation of the central iron in the oxygen sensor (Goldberg et al., 1988b). They are thought to lock the sensor in a deoxy-conformation and thereby mimic the state of hypoxia (Goldberg et al., 1988a).

In the hypoxic retina, HIF-1α induced Epo protects against light-induced retinal degeneration (Grimm et al., 2002). In the adult mouse retina, acute hypoxia stimulates expression of *Epo* and *VEGF* via HIF-1α stabilisation. Epo acts on photoreceptor cells, protecting then from light induced damage and death. Epo blocks the apoptotic pathway by inhibiting caspase-1 expression. Hence, the normal retina requires a functional HIF-1α /Epo/EpoR system to react promptly to variations in oxygen tension and to protect retinal cells from apoptotic cell death. Given that astrocytes in other brain areas are

known to secrete Epo in response to HIF-1α stabilisation, it is possible that astrocytes are also responsible for HIF-1α up-regulation and Epo production in the retina.

Is hypoxia a physiologically relevant stimulus during development? Markers of hypoxia such as VEGF are upregulated during development in unvascularised inner layers of the retina suggesting that hypoxia is a normal condition during development. It is also thought that in the mature retina, the physiology of the outer retina keeps photoreceptors on the verge of hypoxia (Steinberg, 1987). My Thesis mainly concerns the functional role of hypoxia during retinal development, particularly retinal vasculogenesis.

Table 1: Vascular endothelial growth factor and other known angiogenic factors

VEGF-A	Uses receptors VEGFR2, VEGFR1, Neuropilin (NRP1 and NRP2). Isoform VEGF-120 has no heparin or matrix binding, highly angiogenic in tumours, dispensible for vascularization during organ development. Isoform VEGF-165 binds heparin and matrix, involved in arterial development in the retina, bone vascularization and repair-associated, tumour and myocardial angiogenesis. Isoform VEGF-189 binds heparin and matrix, involved in repair-associated tumour and myocardial angiogenesis, contributes to venular and arterial development in the retina and some role in bone vascularization.
VEGF-B	Uses receptor VEGFR1. Principal role in cardiovascular system, possible role in tumour angiogenesis.
VEGF-C	Uses VEGFR2, VEGFR3 and NRP2. Main lymphangiogenic factor, angiogenic, involved in metastatic spread.
VEGF-D	Uses receptor VEGFR3. Angiogenic and lymphangiogenic.
VEGF-E	Viral homologue that acts through VEGFR3. Lymphangiogenic and angiogenic.
PLGF	Acts through VEGFR1,VEGFR2. Stimulates angiogenesis and collateral growth in ischaemic heart and limb. No effect on prenatal vascular development.
Angiopoietin	Acts through Tie2 receptor. Angiopoietin-1 (Ang-1) stabilizes vessels by tightening endothelial smooth muscle interaction, inhibits permeability. Ang-2 destabilizes vessels before sprouting.
Ephrins	Regulate arterial/venous specification. Ephrin B2 and receptor EphB4 are essential to embryonic heart development.
bFGF	Stimulates angiogenesis and arteriogenesis
NOS (nitric oxide synthase)	Nitric oxide and prostaglandins stimulate angiogenesis and vasodilation.

2 Materials and Methods

Falcon sterile plastic ware by Becton Dickenson was used unless otherwise stated. Solutions were sterilized where necessary by autoclaving for 20 minutes at 15 lb/sq.in on liquid cycle. Heat labile solutions were filtered through a 0.22μm pore size filter (Millipore).

Unless otherwise stated, general chemicals were from Sigma-Aldrich Co Ltd.

Water used was, where necessary purified by the Milli Q system (Millipore).

The composition of phosphate buffered saline (PBS) was as follows: 1 litre of distilled water, 8g of NaCl, 0.2g of KCl, 1.44g of Na_2HPO_4 and 0.24 g of KH_2PO_4 adjusted to pH 7.4 with HCl.

2.1 Mammalian cell culture

2.1.1 Retina cultures

2.1.1A Poly-D-lysine coating coverslips

Circular coverslips (13mm diameter, No.1 thickness) were baked overnight to sterilize and then placed into sterile plastic 24 well plates. Each well was filled with 500 μl of 20μg/ml poly-D-lysine in PBS (Sigma; 10mg/ml stock kept at –20°C) and left for 30 min at room temperature. Poly-D-lysine was then removed and the plates left to dry under sterile conditions.

2.1.1B Breeding of wild type mice

Wild-type mice were used of C57B1/6J x CBA/Ca F1 progeny. Mice pups were collected at postnatal day 1 (P1) unless otherwise indicated.

2.1.1C Dissection and plating

Pups were killed by decapitation, the eyes enucleated and put into 2xPBS on ice for at least 5 min or until eyeballs had shrunk slightly. The outer sclera and cornea were then cut away using fine forceps and microscissors (Biology grade 4, dumoxel, Agar Scientific Ltd) and the retinae isolated and transferred to EBSS (Earle's balanced salt solution; Gibco BRL; without calcium and magnesium) on ice.

The following dissociation solution was made up in a 5ml bijou: 850 µl DMEM (Dulbecco's minimum essential medium with sodium pyruvate, 4500MG/L glucose and pyridoxine; Gibco BRL) 100µl collagenase D (from clostridium hi stolyticum; Roche; 10% (w/v) stock in DMEM kept at –20°C) and 50µl Papain (Roche, 10mg/ml stock). The solution was left for 3 min and then syringe filtered through a 0.22 µm filter. The dissected retinae were placed in the dissociation solution and incubated at 37°C for 30 min, gently shaking every 10 min.

After 30 min, 100µl fetal calf serum (FCS; Gibco BRL) and 10µl of DNAse (Deoxyribonuclease from bovine pancreas, 5.25mg/ml stock in DMEM) was added to the retinae in solution. A long Pasteur pipetter (polished to approximately 0.5mm internal diameter) was used to triturate the tissue. 9ml of 10% FCS/DMEM was added and cells were centrifuged at 1000rpm for 5'. Supernatant was removed and the cells resuspended

to a concentration of $3x10^6$ cells/ml in 10% fetal calf serum/DMEM/1x satos (10x satos stock contained 0.1mg/ml transferrin, 0.1mg/ml bovine serum albumin, 60ng/ml progesterone, 40ng/ml sodium selenite, 40ng/ml thyroxine, 30ng/ml triiodo -L-thyronine, 16μg /ml putrescine and 50μg /ml insulin dissolved in DMEM). Cells were plated at 500μl per well and then placed in a carbon dioxide incubator (RSBiotech) at 37°C, 20% oxygen, 5% carbon dioxide and a relative humidity of >98%.

2.1.1D Co-culture using insert membranes

Postnatal day one (P1) retinal cells were plated as described above, in 24 well plates. 400μl suspended P7 retinal cells at the same density, were then placed on top of culture membrane inserts (Millicell Culture Plate Inserts, Millipore) and the inserts placed on top of the P1 cells already in the 24 well plate. P7 cells could therefore be cultured with P1 cells but separated by a 3.0μm pore size membrane. Cells on the coverslip were labeled with BrdU as described in section 2.4.2, but in this case, inserts were removed to pipette in BrdU and then replaced for the 2-hour incubation period.

2.1.1E Culture in hypoxia

To incubate cells in hypoxic conditions, cells were placed in a Jouan IG 750 incubator at 1.5% oxygen (measured as actual chamber levels to +/-0.1%), 5% carbon dioxide, relative humidity >98%, and at 37°C unless stated otherwise. Control cultures that were plated at the same time were placed in an incubator at 20% oxygen, 5% carbon dioxide, at a relative humidity >98%, and at 37°C. Medium was replaced every 72 hours.

2.1.2 Human umbilical vein endothelial (HUVEC) cell culture

HUVECs were obtained from TCS CellWorks and grown in TCS CellWorks Large Vessel Endothelial Cell Basal Medium in 500ml plastic flasks, according to the manufacturers instructions. Cells were fed with medium every 48 hours and subcultured at a confluency of 60-80%. For co-culture with retina cultures, HUVECs from one confluent flask were diluted in 7ml of 10% fetal calf serum/DMEM containing mixed retinal cells (as prepared in section 2.1.1C) and then plated at $3x10^6$ cells per ml in 24 well plates. Control HUVEC cells were grown without retina cells in 10% fetal calf serum/DMEM/satos.

2.2 Wholemount retina preparation

Pups were killed by decapitation up to postnatal day 7, or by carbon dioxide asphyxiation above this age. Eyeballs were enucleated and placed onto 2xPBS solution on ice for 5 to 10 min allowing slight shrinkage, to facilitate dissection. 2xPBS was then replaced with 2% (w/v) paraformaldehyde in PBS for 2 min to fix. Eyeballs were left in 2xPBS again for at least 5 min and then dissected as described in section 2.1.1C above. After the retina was dissected away as a complete cup, four radial incisions were made with microscissors, to flatten out the retina. The PBS was then removed and replaced with methanol (BDH Inc.) kept at –20°C and the retinae were stored at –20°C.

2.3 Preparation of tissue sections

Freshly isolated retinal cups or whole eyes were placed in 4% paraformaldehyde in PBS and left at 4°C for 24 hours to fix. To cryoprotect, tissue was then transferred to 20% sucrose in PBS and left at 4°C for a further 24 hours.
Samples were embedded in OCT embedding compound (Sakura-Tissue-tek) and frozen slowly on dry ice. Tissue blocks were stored at –70°C until required.

15μm thick cryosections (using Bright Ltd. Microtome 5030) were collected on microscope slides, air-dried for 2 to 4 hours and then used for immunohistochemistry.

Tissue sections of *Ink4a* null mice were prepared by Peter Hitchcock, University of Michigan. Eyes were dehydrated through graded alcohols, starting at 50% and ending with 100% and infiltrated and embedded in glycomethacrylate (Polysciences, Inc. Warrington, PA. USA). Five-micrometer sections were cut using a rotary microtome, mounted onto glass microscope slides and stained with 2.5% toluidine blue.

Digital photomicrographs were taken with a Spot -RT digital camera (Diagnostic Instruments, Inc., Sterling Heights, MI. USA) attached to a Nikon compo und microscope. Illustrations were assembled using Adobe Photoshop

2.4 BrdU labeling

2.4.1 BrdU labeling in vivo by injection

For mice pups aged postnatal day 0 to postnatal day 7, pups were given a subcutaneous injection of 5-bromo-2'-deoxy-uridine (BrdU; Boehringer Manheim) into the scruff of the neck using a 30 gauge syringe needle (Becton Dickinson) and 1 ml plastic syringe (Terumo). BrdU was used at 50μg per gram body weight and was injected at 10mg/ml in sterile PBS. 2 hours after injection, animals were sacrificed and the retinae dissected out and fixed as described in the above sections.

2.4.2 BrdU labeling in vitro

To label culture cells in S phase in vitro, 10μM BrdU (diluted in DMEM) was added into each well and left to incorporate at 37°C for a standard 2 hours. Cells were then washed and fixed, before performing immunohistochemistry.

2.5 Immunohistochemistry

A list of antibodies used, is listed in Table 2 at the end of this chapter.

2.5.1 Immunohistochemistry on culture cells

After removing from the incubator, culture cells were washed in PBS and then fixed in 4% (w/v) paraformaldehyde for 15 min.

2.5.1A GFAP/BrdU immunohistochemistry

For GFAP (Glial Fibrillary Acidic Protein) staining, cells on coverslips were then blocked and permeabilised in 5% FCS/0.5% Triton X-100 in PBS for 15 min. A rabbit polyclonal anti-GFAP antibody (donation from Martin Raff) was applied for 1 hour at room temperature in a 1% FCS/0.1% Triton X-100 in PBS (1:200) on coverslips. Coverslips were then washed briefly in PBS and left to block for a further 10 min. A FITC (fluorescein isothiocyanate) conjugated anti-rabbit was applied (Pierce) for 45 min and cells then washed for 5 min in PBS.

Cells were then post fixed for 5 min in acid-alcohol (70% (v/v) ethanol, 20% (v/v) glacial acetic acid) to fix the antibodies from the previous step. Cells were then incubated in 70% ethanol (v/v) for 15 min at –20°C and permeabilised for 15 min in 1% triton-X-100 in PBS. 6M HCl/1% (v/v) Triton-X-100 in PBS was then applied for 20 min, followed by 0.1M $Na_2B_4O_7$ (pH 8.5) for 10 min. Cells were then incubated overnight at 4°C in anti-BrdU (hybridoma supernatent BU209; Magaud et al., 1989), diluted 1:4 in 0.1% (v/v) Triton X-100 in PBS. After a 5 min wash in PBS, cells were incubated in goat-anti-mouse IgG (Pierce; 1:100 in 0.1% Triton X-100 in PBS,) for 30 minutes. After another wash in PBS for 5 minutes, coverslips were mounted onto microscope slides in anti-fade reagent (Citifluor Ltd) and sealed around the edges using translucent nail varnish.

For each sample, at least 3 coverslips were prepared and counted; with approximately 200 astrocytes on each coverslip. BrdU labeling index was calculated as the proportion of GFAP positive cells that were BrdU positive.

2.5.2 Immunohistochemistry on wholemount retina

Wholemount prepared retinae stored in methanol were fixed in 4% paraformaldehyde in PBS for 5 minutes. Retinae were blocked for 20 minutes in 5% fetal calf serum in PBS. For collagen IV staining, the primary antibody was applied overnight at 4°C (Biogenesis, rabbit IgG anti-collagen), diluted 1:100. Retinae were then washed for 30 minutes in PBS, followed by an incubation in the secondary antibody for 4 hours at room temperature (FITC conjugated goat-anti-rabbit) diluted at 1:100.

If required, wholemount retinae were processed for detection of incorporated BrdU. Wholemounts were washed in PBS for 15 minutes and then fixed for 10 minutes in 4% (w/v) paraformaldehyde. 6M HCl /1% (v/v) Triton X-100 in PBS was then applied for 45 minutes, followed by at least 3 washes of 30 minutes in PBS. Tissue was incubated overnight at 4°C in anti-BrdU (hybridoma supernatent BU209, Magaud et al., 1989) diluted 1:4 in 1% (v/v) Triton X-100 in PBS. They were then washed twice for 30 minutes in PBS before incubating in rhodamine conjugated anti-mouse (diluted 1:100 in 1% (v/v) Triton X-100 in PBS) at room temperature for 3 to 4 hours. Finally, wholemounts were washed at least 3 times for 30 minutes in PBS and mounted in glycerol on microscope slides.

2.5.3 Immunohistochemistry on tissue sections

2.5.3A GFAP/BrdU Immunofluorescence

Once dry after sectioning, tissue sections were incubated in block for 20 minutes (5% fetal calf serum in PBS). Sections were then treated as described in section 2.5.1A for GFAP and BrdU immunofluorescence, although throughout, the slides containing sections were placed in a humidified chamber.

2.5.3B TUNEL (TdT-mediated dUTP nick end labeling) analysis

Tissue sections on slides (section 2.3) were fixed in 4% (w/v) paraformaldehyde in PBS for 15 minutes and then in 70% ethanol for 30 minutes. Slides were rinsed twice in water and then incubated for 10 minutes in proteinase K (Roche; 15.6 mg/ml) diluted to 20μg /ml in 10mM Tris-HCl pH 7.4. After rinsing in PBS, slides were incubated for 5 minutes in 3% H_2O_2 (v/v) (Sigma; stock solution at 30% (w/w)) and then washed twice in water, for 5 minutes each. Sections were then blocked in TUNEL buffer (Roche), 30mM Tris/HCl, 140mM sodium cacodylate and 1mM $CoCl_2$) for 15 minutes at room temperature. Slides were then incubated in the following reaction mixture for one hour at 37°C: in 50μl volume (used for one slide), 10 μl 5x buffer, 1μl terminal transferase (Roche; from calf thymus), 5μl cobalt chloride (Roche; 2.5mM), 0.2 μl biotin-dUTP (Roche; 1mM) and 33.8μl distilled water. For the negative control, terminal transferase was omitted. After this time, slides were left in 1x SSC (20x stock: 175.3g NaCl, 88.2g sodium citrate in 1 litre water at pH 7.0) for 10 minutes at room temperature, then

incubated in 1% bovine serum albumin in PBS for 20 minutes. Slides were washed in PBS twice for 5 minutes each and then incubated for one hour in anti avidin-peroxidase (1:100 in PBS) at room temperature. Slides were then washed twice in PBS for 5 minutes and then exposed to peroxidase substrate (Peroxidase Substrate Kit, Vector Ltd.) for 10 minutes. Following this, slides were mounted as described in section 2.5.1A.

2.6 In situ hybridisation

This technique was used to analyse mRNA expression in cells and therefore it was essential to ensure that all solutions and equipment used were RNase free to protect the mRNA as much as possible. Solutions were therefore treated with diethylpyrocarbonate (DEPC) made up to 0.1% (v/v) and then autoclaved. Those solutions that couldn't be autoclaved were made up in DEPC treated water and containers. All dissection equipment was washed in DEPC treated water and plastic ware used was sterile and kept sealed until just before use.

2.6.1 In situ hybridisation on tissue sections

2.6.1A Preparation of digoxygenin-labelled probes

To first prepare the template, 10 µg of pDNA containing the gene of interest was linearised in a 100µl volume for 2 hours. Linearisation was checked by running a sample on an agarose gel. 5 µl of 10% SDS and 1 µl of Proteinase K (20mg/ml) was then added

and the mixture incubated at 55°C for 15 minutes. Following this, the mixture was extracted twice with phenol:chloroform:isoamyl alcohol (25:24:1). To do this, 100 µl of phenol-chloroform was added to the digested template, mixed thoroughly and then centrifuged for 2 minutes at 13000 rpm. The aqueous phase was then isolated and extracted once with choloroform:isoamyl alcohol (24:1). To precipitate DNA, sodium acetate (final concentration of 0.3M) and twice the volume of ethanol were added. This mixture was kept at –20°C for 30 minutes and then centrifuged at 4°C for 10 minutes. The pellets were then washed in 70% ethanol, air dried and dissolved in 50µl of distilled water.

To transcribe from the template the mixture was incubated in the following: 1 µg linearised template, 5µl 5X Transcription Buffer (Stratagene), 7.5µl DTT (100mM stock), 2.5µl DIG labeling mix (10mM of ATP, CTP, GTP, 6.5mM UTP, 3.5mM DIG-UTP (Roche)), 1µl RNAsin (Promega), 2µl polymerase (T7, T3 or SP6 as required, Promega) and made up to 25µl total volume with distilled water. To stop the reaction, 2µl of 200mM EDTA pH 8.0 was added (0.5 M stock: 186.1g disodium ethylenediaminetetraacetate.$2H_2O$ in 1 liter of water, NaOH to adjust the pH) and the reaction mixture made up to 100µl with distilled water. The probe was run on an RNAse free agarose gel to check it and then stored at –20°C.

2.6.1B Preparing microscope slides for in situ hybridisation

Microscope slides (BDH 76x 26mm) were thoroughly washed in detergent and distilled water and baked at 200°C for 24 hours before immersing in acetone for 5 minutes. Slides

were then immersed for a further 5 minutes in Vectorbond reagent and then rinsed and air dried.

2.6.1C Preparing tissue sections

Tissue was prepared as describe in section 2.3 although all solutions: (e.g. 2xPBS, 20% sucrose) were DEPC treated and dissecting tools washed in DEPC treated water.

2.6.1D Hybridisation with digoxygenin-labelled probe

PDGFRα anti sense probes were transcribed from a EcoRI fragment coding for most of the extracellular domain of mouse *PDGFRα* (gift from Chiayeng Wang, University of Chicago) cloned into pBluescript-KS (Stratagene). Human *PDGF-A* antisense probes were transcribed from a fragment encompassing most of the human *PDGF-A* cDNA (Betsholtz et al 1986)(See section 2.6.1A).

Probes were diluted in hybridisation buffer usually at 1:1000 but a concentration series from 1:500 to 1:2000 was performed for each new transcription product. Hybridisation buffer was made up as follows:-

1x salts (10X salts: 2M NaCl, 50mM EDTA, 100mM Tris-HCl pH7.5, 50mM NaH_2PO_4, $2H_2O$, 50mM Na_2HPO_4)
50% deionised formamide (added 10% (w/v) 'Amberlite' IRN-150L monobed mixed resin (BDH) to formamide (Sigma) for 30 minutes, then filtered to remove beads)
0.1mg/ml yeast total RNA (Roche)

10% (w/v) dextran sulphate (Roche)

1x Denhardt's (50X stock, Sigma)

Once diluted, the probe mix was denatured for 5 to 10 minutes at 70°C, then vortexed to mix. Approximately 150µl of probe solution was added to each microscope slide and a baked coverslip lowered on top. Slides were kept in a sealed box on blotting paper soaked in 50% (v/v) deionised formamide/1XSSC and hybridised overnight at 65°C.

2.6.1E Post-hybridisation washes and antibody staining

Slides were transferred to coplin jars where they were washed in wash buffer (1XSSC, 50% formamide, 0.1% Tween-20) prewarmed to 65°C, for 15 minutes. Coverslips were then removed easily and slides washed again in wash buffer at 65°C (twice for 30 minutes). Slides were washed twice in 1xMABT (5x stock: 500mM maleic acid pH7.5, 750mM NaCl, 0.5% (v/v) Tween-20) at room temperature (30 minutes each).

Slides were then transferred to a humidified chamber and incubated in blocking solution (MABT with 2% blocking reagent (Boehringer) and 10% heat-inactivated sheep serum (Gibco BRL)) for at least 1 hour at room temperature. Anti-digoxygenin AP-conjugated antibody (Fab fragments, Roche) was diluted 1:1500 in blocking solution and placed onto slides, incubating overnight at 4°C.

2.6.1F Post antibody washes and colour reaction

Slides were transferred into coplin jars again and washed 5 times for 10 minutes in MABT at room temperature. A further two washes, 10 minutes each, were performe d in prestaining buffer (100mM Tris-HCl pH9.5, 100mM NaCl, 50mM $MgCl_2$) made up fresh. Slides were then incubated in the dark in staining buffer (100mM Tris-HCl pH9.5, 100mM NaCl, 50mM $MgCl_2$, 5% polyvinyl alcohol (Sigma), 0.2mM 5-bromo-4-chloro-3-indolyl-phosphate (Roche), 0.2mM nitroblue tetrazolium salt (Roche)) until staining was satisfactory. To stop the reaction, slides were rinsed in several changes of water for 30 minutes, then dehydrated through an ascending series of alcohols (30% to absolute), cleared in xylene and mounted under coverslips in XAM mountant (BDH Ltd).

2.6.2 In situ hybridisation on wholemount retina

2.6.2A Preparation of tissue for in situ hybridisation

Wholemount retinae once removed from storage in –20°C methanol, were fixed for 5 minutes in 4% paraformaldehyde/PBS, and then washed twice in PBS/0.1% Tween-20 for 10 minutes. Retinae were then slightly digested for 5 to 10 minutes in proteinase K diluted 1:200 in 6.6% SDS. Tissue was further fixed in 4% parformaldehyde/0.2% glutaraldehyde (Sigma) for 5 minutes, then washed twice, for 10 minutes each, in PBS/0.1% Tween-20.

2.6.2B Hybridisation with digoxygenin-labelled probe

Retinae were transferred into 6 well plates and the PBS/Tween removed. Drops of hybridisation buffer (see section 2.6.1D) were placed on each retina and then incubated at 65°C for 10 minutes. Probe was then applied overnight at 65°C as described previously in section 2.6.1D. Instead of covering tissue with a coverslip, the 6 well plate was sealed with tape to prevent evaporation.

2.6.2C Post hybridisation washes and antibody staining

Retinae were washed in wash buffer (section 2.6.1E) preheated to 65°C, for 10 minutes and then 3 more times at 30 minutes each, all at 65°C. They were then washed in MABT at room temperature twice for 20 minutes each. Blocking buffer was then added, incubating for 20 minutes before replacing with anti-digoxygenin AP-conjugated antibody (Fab fragments, Boehringer) diluted 1:1500 in blocking buffer. This was left overnight at 4°C.

2.6.2D Post antibody washes and colour reaction

Wholemount retinae were washed in 1XMABT for 5 minutes initially, then twice for 30 minutes. Washing was continued overnight at room temperature. MABT was then replaced with staining buffer (100mM Trisma Base, 100mM sodium chloride) for 10 minutes and before staining solution (100mM Trisma Base, 100mM sodium chloride, 0.25mM nitroblue tetrazolium salt (NBT) 0.2mM 5 -bromo-4-chloro-3-indolyl-phosphate (BCIP) was applied overnight at 37°C or until staining was satisfactory.

Retinae were then washed with staining buffer twice for 10 minutes then twice again for one hour. Immunohistochemistry was then performed on the wholemounted retinae (see section 2.5.2).

2.6.3 In situ hybridisation on culture cells

2.6.3A Preparation of culture cells and hybridisation with digoxygenin-labelled probe

Culture cells were removed from the incubator, washed briefly in PBS (DEPC treated) and then fixed for 30 minutes in 4% (w/v) paraformaldehyde/5% (v/v) acetic acid. After washing again in PBS, cells were dehydrated through an ascending series of alcohols (70% to absolute). After this, coverslips were air dried and then stuck onto microscope slides using translucent nail varnish. Slides were transferred into coplin jars and left in xylene twice for 5 minutes. After rehydrating in a descending alcohol series and a 2-minute wash in PBS, slides were placed for 10 minutes at 37°C in 0.1% pepsin/0.1M HCl. They were then washed for 30 seconds in 0.2% glycine (stock 10%) and further washed in PBS twice for 2 minutes. Cells were post fixed in 1% formaldehyde/PBS for 10 minutes and then washed in PBS twice for 2 minutes. Again, cells were dehydrated in an ascending series of alcohols (70% to absolute) and air-dried. Probes were diluted in hybridisation buffer and applied onto slides as described for tissue sections in section 2.6.1D. Slides were incubated at 65°C overnight, as before.

2.6.3B Post hybridisation washes and antibody staining

Slides were washed 4 times, for 10 minutes in 4XSSC and then 4 times, for 10 minutes in MABT. They were then transferred into a humidified chamber and incubated for 1 hour at room temperature with blocking solution (section 2.6.1E). Slides were then left overnight at 4°C incubated in anti-digoxygenin AP-conjugated antibody diluted 1:1500 in blocking solution.

2.6.3C Post antibody washes and colour reaction

After transferring slides to coplin jars, cells were washed 3 times, for 5 minutes in MABT. Washes in prestaining buffer, incubation in staining buffer and mounting slides were then performed exactly as for tissue sections described in section 2.6.1F.

2.7 Analysis of transgenic mice

2.7.1 Isolation of genomic DNA

Tail clips were taken from mice and incubated in 500 µl of DNA preparation buffer (50mM Tris-HCl pH8, 100mM NaCl. 1% (w/v) SDS) with 10 µl of 10mg/ml proteinase K. Tails were left in this solution overnight at 55°C and then vortexed. 200µl ammonium acetate was added to a final concentration of 1.5M and the sample was vortexed again and left on ice for 15 minutes. After this time, samples were centrifuged at 13000rpm for 10 minutes at 4°C. The supernatant was collected and after adding

500µl cold isopropanol, was vortexed. Pellets were retrieved by centrifuging and were washed in 70% ethanol before being dissolved in 70µl water and stored at 4°C.

2.7.2 Quantitation of genomic DNA

To calculate the concentration of DNA, the optical density of a sample was measured using a spectrophotometer (Shimadzu). After diluting 1:200 in water, the optical density at 260nm and 280nm (OD^{260},OD^{280}) was taken and concentration calculated as follows: [OD^{260} x 200 (dilution factor) x 50 (DNA multiplication factor)] µg/ml. To assess the purity of each sample, the ratio OD^{260}/OD^{280} was calculated which is 1.8 for pure DNA.

2.7.3 PCR analysis of genomic DNA

In order to distinguish heterozygous and homozygous null *INK4a/ARF* mice, polymerase chain reaction (PCR) analysis was used. Each PCR reaction was performed in 25 µl thin walled tubes with reagents as follows: -

2.5µl 10x PCR buffer (Promega; 500mM KCl, 100mM Tris-HCl pH 9.0, 1% (v/v) Triton X-100)

0.25µl dNTPs (20mM each dATP, dCTP, dGTP, dTTP; Amersham Pharmacia Biotech)

0.1µl each primer (100pmol/µl; MWG Biotech)

0.1µl Taq polymerase (5U/µl; Promega)

1.5µl 25mM Magnesium chloride (Promega)

2µl genomic DNA sample (0.1 to 0.5 µg /µl)

18.45µl sterile water (Baxter)

PCR was performed in a MWG Biotech thermal cycler using two sets of primers: 'WT' for detection of the wild-type allele (5' *ATGATGATGGGCAACGTTC* and *CAAATATCGCACGATGTC*) and 'targeted allele (TA)' for detection of the targeted allele (5' *CTATCAGGACATAGCGTTGG* and 5' *AGTGAGAGTTTGGGGACAGAG*). WT primers yielded a product of 236 base pairs and TA primers yielded a product of 723 base pairs. For WT primers, 40 cyles were performed with melting temperature at 94 °C for 30 seconds, annealing temperature at 55 °C for 30 seconds and elongation at 72°C for 2 minutes. For TA primers, 40 cycles were performed with melting temperature at 94 °C for 30 seconds, annealing temperature at 57 °C for 30 seconds and elongation at 72°C for 2 minutes. For both primers, an initial denaturation was carried out at 94 °C for 4 minutes before the 40 cycles and after the cycles, a final extension at 72°C was performed for 10 minutes. PCR products were visualized on a 1% agarose gel stained with ethidium bromide.

2.7.4 Agarose gel electrophoresis

Agarose gels were prepared by dissolving multi-purpose agarose (Bioline) in 1x TAE (50X TAE: 2M Tris-acetate pH7.5, 50mM EDTA) at 1% (w/v). The agarose was boiled in a microwave oven and then cooled to less than 60 °C before adding ethidium bromide

at 0.5μg /ml. The hot agarose was poured into a horizontal electrophoresis system (Gibco BRL Life Technologies Ltd) and left to set. Loading buffer was added to the samples (10x stock: 0.4% (w/v) bromophenol blue, 0.4% (w/v) xylene cyanol FF, 25% (w/w) Ficoll (Type 400; Amersham Pharmacia Biotech)) and once loaded, the gel was run at 5V/cm. A gel documentation system (Alpha Innotech Corporation) with an ultra violet transilluminator at 302nm and CCD camara was used to visualize DNA.

2.8 Hyperoxia chamber

Mice were transferred into the hyperoxia chamber with their mother at postnatal day zero unless stated otherwise. Mouse pups and their nursing mothers were exposed to increased oxygen levels in a modified, airtight cage. Oxygen concentrations were measured with a sensor placed inside the cage and regulated by an oxygen controller (PROOX 110; Reming Bioinstruments CO., Redfield, USA). Oxygen was supplied by a gas tank (BOC, size F, medical oxygen). A small fan was installed inside the cage to mix inflowing pure oxygen with the cage air. Cage air was removed and replaced with normal room air a t a constant rate (approximately 6 cage volumes per hour) to prevent buildup of carbon dioxide and humidity. Half the litter at P0 were used as controls and kept with a foster mother in normal cage racks. Pups were taken out of the hyperoxic chamber to inject with BrdU (section 2.4.1) and then returned for 2 hours before sacrificing.

2.9 Microscopy

Fluorescence was viewed under a Zeiss Axiophot microscope connected to a digital camara (Hamamatsu). Images were captured using simplePCI (C Imaging Systems) imaging software and manipulated where necessary using Adobe Photoshop software.

Table 2: Antibodies used for immunohistochemistry

GFAP	Rabbit polyclonal	Donation from Martin Raff	Used 1/200 in 1% FCS/0.1% Triton X-100/PBS, 45 minutes at room temperature
BrdU	Mouse monoclonal	Hybridoma supernatant BU209 (Magaud et al 1989)	Used ¼ in 0.1% Triton X-100/PBS, overnight at 4°C
Collagen IV	Rabbit polyclonal	Biogenesis Ltd.	Used 1/100 in 1% FCS/0.1% Triton X-100/PBS, 2 hours at room temperature
Pax-2	Rabbit polyclonal	Covance Research Products Inc., Berkely USA.	Used 1/100 in 1% FCS/0.1% Triton X-100/PBS, 2 hours at room temperature

Chapter 3. Description of astrocyte proliferation during development in wild type and in mice overexpressing *PDGF-A* in astrocytes

3.1 Introduction

Retinal astrocytes in mice, are born in the optic nerve head and then migrate into the retina shortly before birth (Ling and Stone, 1988; Watanabe and Raff, 1988). They spread radially across the inner surface of the retina until they reach the periphery of the retina at P7 (Mudhar et al., 1993). One factor known to affect astrocyte numbers at this time is PDGF-A, derived from nearby retinal ganglion cells (RGC) (Fruttiger et al., 2000) (Fig 3.1A).

In a transgenic mouse overexpressing *PDGF-A* in retinal ganglion cells under control of the neuron specific enolase (*NSE*) promoter, the numbers of astrocytes increased (Fruttiger et al., 1996). Proliferation at postnatal day 3 (P3) was elevated in transgenic compared to wild type animals suggesting that increased proliferation may be responsible for the increased number of cells that develop. PDGF-A could also act via increasing survival however, but this was not addressed in this study. Conversely, blocking PDGF signaling with a neutralizing anti-PDGFRα antibody reduced development of the astrocyte network.

The experiments described here suggest that PDGF-A controls retinal astrocytes in the developing retina by regulating proliferation. This is similar to its effect on

oligodendrocyte progenitors in the spinal cord. Van Heyningen et al (van Heyningen et al., 2001) proposed a model whereby PDGF-A controls numbers of progenitors by becoming a limiting factor for proliferation during development. As the rate of supply approaches rate of consumption, competition increases for PDGF and its extrac ellular concentration drops, preventing further increases in cell number.

Is PDGF-A the only limiting factor controlling the numbers of astrocytes that develop? Even in the NSE-PDGF-A mouse, the extra source of PDGF-A is eventually used up by the increased numbers of retinal astrocytes, so it is not possible to answer this question. To address this, another transgenic mouse was made by Fruttiger et al (Fruttiger et al., 2000), this time expressing the human *PDGF-A* gene (*hPDGF-A*) in astrocytes themselves, under the *GFAP* promoter (Fig 3.1B). Astrocytes in these mice therefore express both the ligand and the receptor for *PDGF* signaling, creating an autocrine loop in these cells. It can be predicted that the source of PDGF-A is unlimited in these mice because as the number of cells and subsequent demand for PDGF-A increases, so the source of it also increases.

Autocrine growth factor signaling involving PDGF is thought to occur in the pre-implantation embryo but thereafter becomes paracrine (see introduction). It has been suggested that autocrine growth factor stimulation also occurs in gliomas because *PDGF* ligand and receptor mRNA are often seen to be co-expressed. Indeed, over-expression of *PDGF-B* in mouse brain can drive tumour growth with tumour cells co-expressing both *PDGF-B* and *PDGFRα* (Uhrbom et al., 2000). Furthermore, these tumour cells were

found to be dependant on PDGF-B for proliferation in vitro, as a PDGF receptor tyrosine kinase inhibitor blocked proliferation.

If PDGF-A is limiting for retinal astrocyte proliferation, can over-expression in an autocrine loop cause uncontrolled proliferation with a tumour like growth? Retinal astrocyte numbers do appear to increase in *GFAP-PDGF-A* mice with the formation of an abnormal 'growth' covering the inner surface of the retina (Fig 3.1C). However, the population growth still stops sometime after birth although there are no obvious physical barriers present inside the eye. Hence, PDGF-A does not appear to be the only limiting factor for retinal astrocyte population growth. What other factors ultimately control astrocyte population growth and how might they achieve this?

In this chapter, I investigate what factors could be limiting the size of the retinal astrocyte population. I investigate two possibilities here: 1) a decline in proliferation and 2) an increase in apoptosis. I look at proliferation across time and space in the retina, in both wild type and mice overexpressing *hPDGF-A* in an autocrine loop. From this data it appears that control on proliferation is limiting the numbers of astrocytes. Surprisingly, despite the higher levels of proliferation in the transgenic mice, proliferation in both wild type and transgenic mice stopped at the same time in development. By manipulating mitogen supply so that it no longer becomes limiting during development, the existence of another control on population growth has emerged.

Fig 3.1 **A transgenic mouse expressing *hPDGF-A* in an autocrine loop leads to a large bolus of astrocytes in the retina.** **(A)** The development of neurons, astrocytes and vasculature is co-ordinated in the retina. Retinal ganglion cells secrete PDGF-A, which acts as a mitogen on retinal astrocytes. Retinal astrocytes secrete VEGF, which promotes vessel development. **(B)** a transgenic mouse (*GFAP-hPDGF-A*) expresses *PDGF-A* in retinal astrocytes. These cells express both *hPDGF-A* and *PDGFRα*, creating an autocrine loop. **(C)** P7 wholemount preparations of retina were immunolabelled for GFAP. The right hand image shows the dense bolus of retinal astrocytes in the *GFAP-hPDGF-A* mice, compared to the fine astrocyte network in the wild type mice (left hand image).

Figure adapted from Marcus Fruttiger (unpublished).

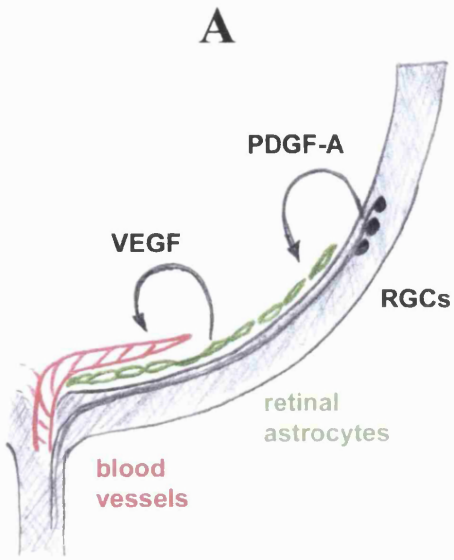
A
PDGF-A
VEGF
RGCs
retinal
astrocytes
blood
vessels

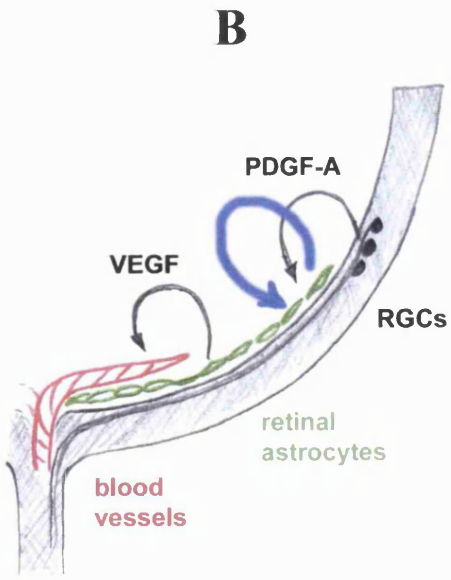
B
PDGF-A
VEGF
RGCs
retinal
astrocytes
blood
vessels

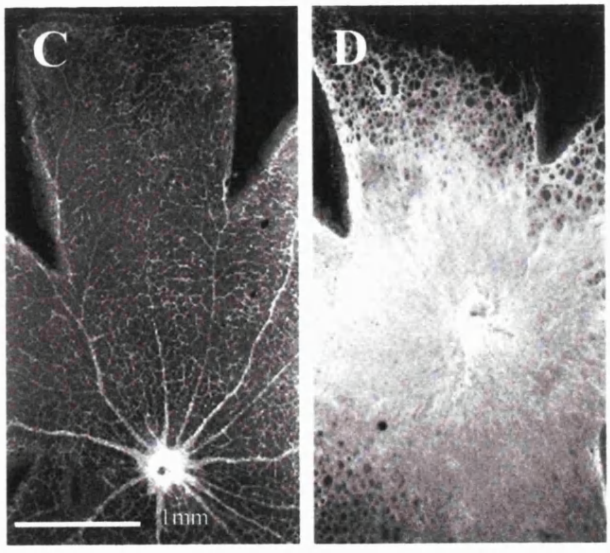
C
D
1mm

3.2 Results

3.2.1 Astrocyte proliferation stops a week after birth whether *PDGF-A* is overexpressed or not

Astrocyte proliferation was analyzed by immunostaining either cross-sections of the retina or mixed retinal cells that were dissociated and cultured overnight. In both cases, BrdU was used to mark cells in S phase and GFAP to label astrocytes. Since retinal astrocytes first enter the retina shortly after birth and fully cover the inner surface of the retina by P7, pups were analyzed at P7 and after.

Retinal astrocytes can be identified in cross sections based on their characteristic location internal to retinal ganglion cells (Stone and Dreher, 1987; Ling et al., 1989) and their expression of GFAP and *PDGFRα* (Mudhar et al., 1993).

Wild type and transgenic pups overexpressing *PDGF-A* in astrocytes (*GFAP-hPDGF-A* mice) were given a 2-hour pulse of BrdU by intra-peritoneal injection. BrdU is incorporated into the DNA of all cells in S phase and can be detected with an antibody. The percentage of labelled nuclei in a given population of cells is indicative of the level of proliferation, assuming that S phase remains constant in length.

By analyzing cross sections, the thickness of the astrocyte layer and presumably numbers of astrocytes in the astrocyte layer together with the spatial distribution of proliferating

cells could be visualised. Under certain pathological conditions, antibodies against GFAP can stain Muller cells as well as astrocytes in the retina but unlike astrocytes, Muller cells span the inner to outer surface of the retina whilst astrocytes lie horizontally throughout the astrocyte layer. However, in this study antibodies against GFAP did not reveal Muller cells. As seen in Fig 3.2, the GFAP positive ($GFAP^+$) astrocyte layer in the transgenic mice is thicker than in wild type mice, consistent with the increase in number reported previously. BrdU labelled cells are seen in the first week after birth (data not shown) in the astrocyte layer but after P7 most BrdU labelled cel ls disappear in both wild type and GFAP-hPDGF-A mice (Fig 3.2, Fig 3.3 and Fig 3.4).
Although the BrdU labelled cells are within the astrocyte layer, they cannot be identified with 100% certainty as astrocytes because BrdU is localized to the nucleus where as GFAP is in intermediate filaments in the cytoplasm. Hence, it is not possible to distinguish BrdU labelled astrocytes from endothelial cells, which also reside in this layer. However, by dissociating BrdU labelled retina and culturing overnight, it wa s possible to distinguish individual retinal astrocytes by immunohistochemistry and observe the presence or absence of BrdU in the nucleus. This method permitted a quantitative analysis of the rate of retinal astrocyte proliferation.

Fig 3.4 shows that after an initial high BrdU labelling index after birth (approximately 25%), the levels of proliferation declind in both wild type and *GFAP-hPDGF-A* mice. The labelling index and hence number of cells in S phase was similar in wild type and *GFAP-hPDGF-A* mice at P1; but it was higher in *GFAP-hPDGF-A* mice at P2 and P5.

Fig 3.2 **Proliferation in the inner retina declines after P7 and becomes restricted to the periphery.** Wild type and *GFAP-hPDGF-A* litter mate pups at ages P7 to P11 were given intra-peritoneal injections of 50ug/g body weight of BrdU. Two hours later pu ps were killed and the retinas fixed and embedded for cryosectioning. 15 μM sections were cut and immunostained for GFAP (green) and BrdU (red). **(A,C,E and G)** show wild type sections at P7, P8, P9 and P11 respectively. **(B,D,F and H)** show sections from *GFAP-hPDGF-A* mice at P7,P8,P9 and P11 respectively. BrdU labelled cells ar e most numerous towards the periphery at P7 in both wild type and transgenic animals. In both cases, levels decline to zero by P11.

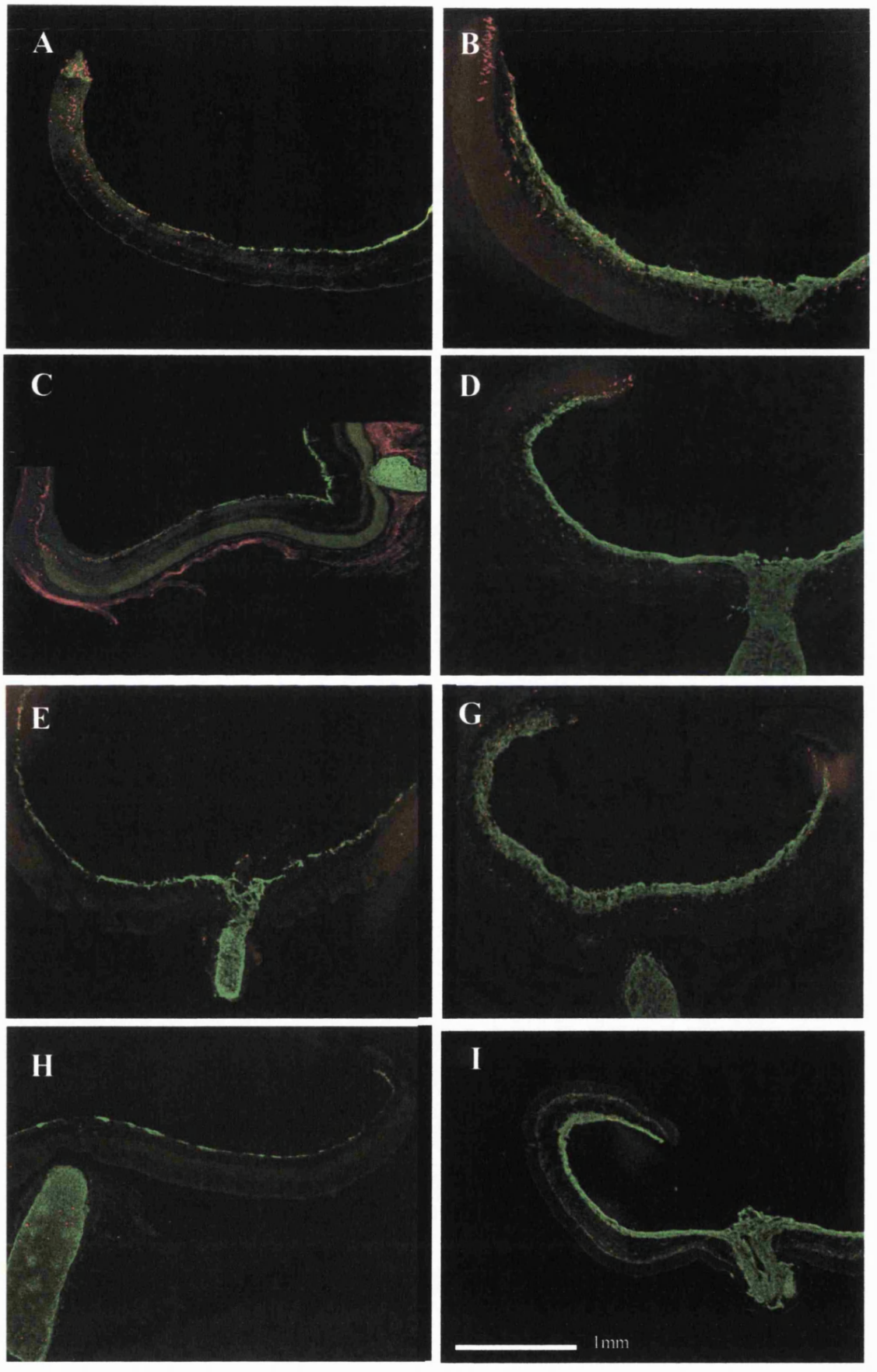
A
B
C
D
E
G
H
I
1mm

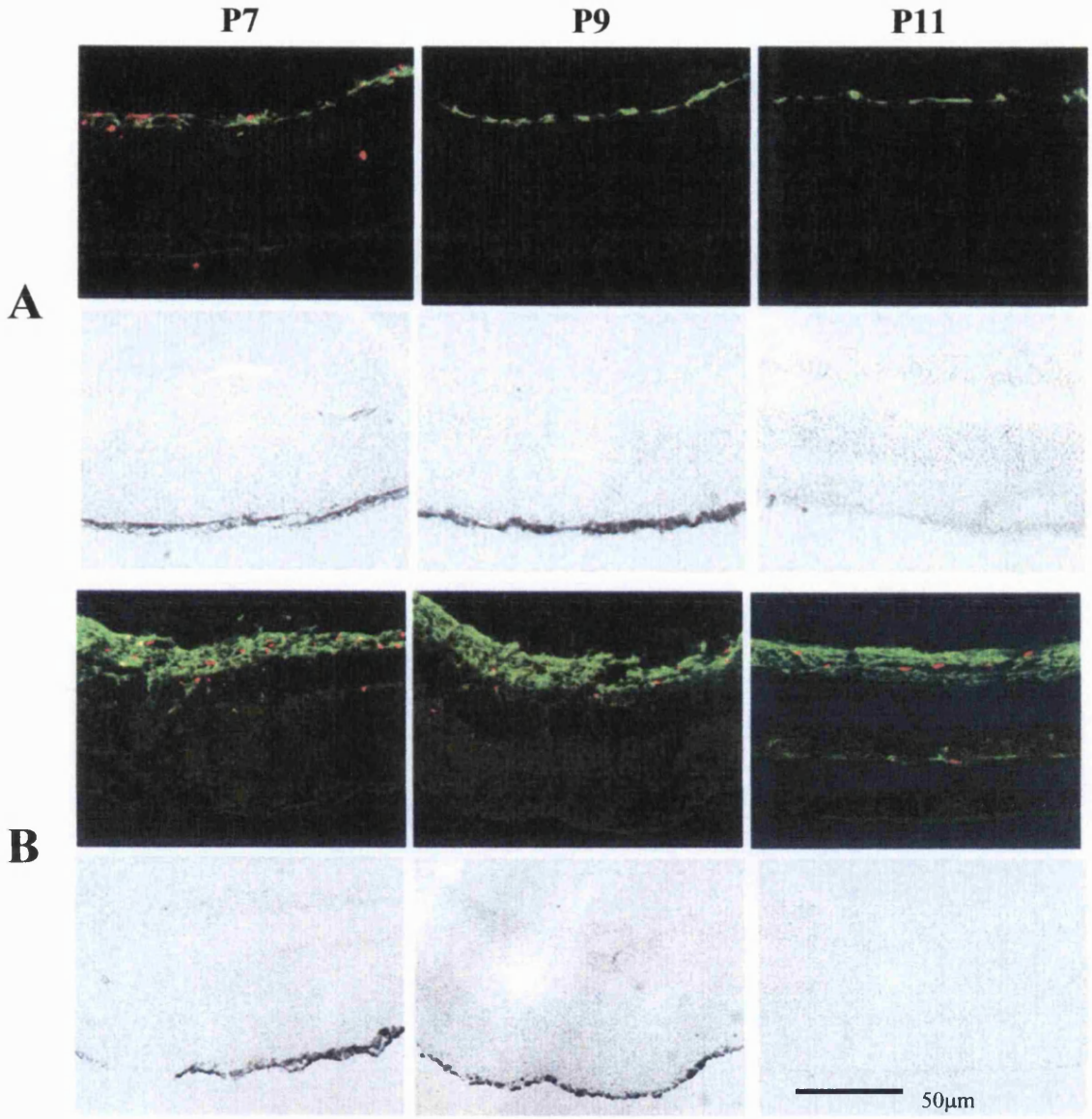

Fig 3.3 **Proliferation declines at the same time in both wild type and *GFAP-hPDGF-A* mice.** (A) and (B) are x20 images of the mid retina. **(A)** upper panels show immunofluorescence for GFAP (green) and BrdU (red) on wild type retinae. Lower panels show light microscope images of the same sections. **(B)** upper panels show immunofluorescence on *GFAP-hPDGF-A* retinae. Lower panels show light microscope images as in (A). BrdU labelled cells are detected in the GFAP stained layer but decline from P7 to P11 in both wild type and *GFAP-hPDGF-A* retina.

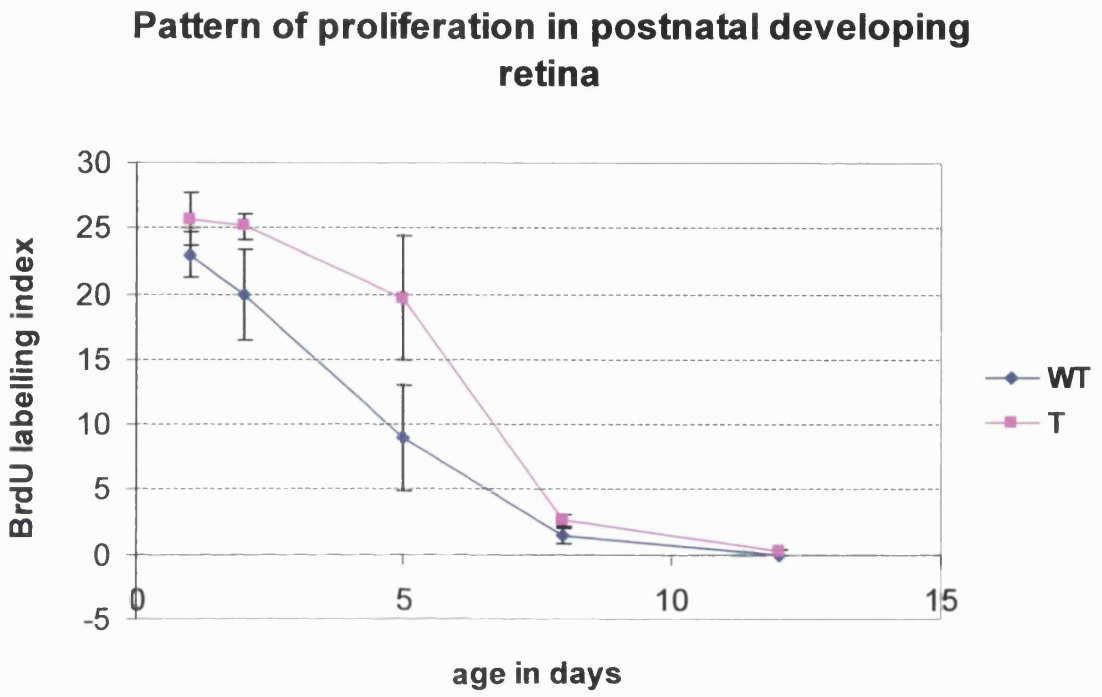

Fig 3.4 **Proliferation declines at the same time in both wild type and *GFAP-hPDGF-A* mice: analysis by dissociation assay.** Wild type and *GFAP-hPDGF-A* litter mate pups were given a BrdU pulse. Retina from 4 pups were dissociated and plated overnight in medium containing 10% fetal calf serum. Cells were then fixed and stained by immunofluorescence for GFAP and BrdU. $GFAP^+$, $BrdU^+$ double positive cells were counted as a proportion of the total $GFAP^+$ astrocyte population. Labelling index was plotted against the age of the animal from which retina were taken (P1, P2, P5, P7 and P12). Each point represents the mean $^+$/- s.d of cultured cells in triplicate taken from four animals.

By P12, this rate has declined to zero in both strains. Thus from an initial high level of proliferation, proliferation declined in both wild type and *GFAP-hPDGF-A* mice although the decline was delayed in the *GFAP-hPDGF-A* mice. Despite this, in both strains proliferation appeared to stop at the same time. At P7 for instance, both strains have declined to levels below a 5% BrdU labelling index.

3.2.2 Changes in proliferation rather than cell survival appear to control astrocyte population growth

In the cross sections in Fig 3.3, retinal astrocytes are clearly present after P7 but have stopped proliferating. If cell death were limiting astrocyte numbers, high levels of apoptosis would be expected at this time in the astrocyte layer. To detect apoptotic cells, a TUNEL (Tdt-mediated dUTP nick end labeling) assay was performed on cross sections through the retina. This method labels DNA strand breaks generated during apoptosis, by using the enzyme terminal deoxynucleotidyl transferase to introduce labelled nucleotides at the ends of the degraded DNA. No signal was detected at P7 in wild type and transgenic mice (Fig 3.5) despite a strong signal in the outer nuclear layer, which has also been reported by Pimental et al (Pimentel et al., 2002). This data supports the idea that a control on proliferation rather than cell survival stops the astrocyte population growth.

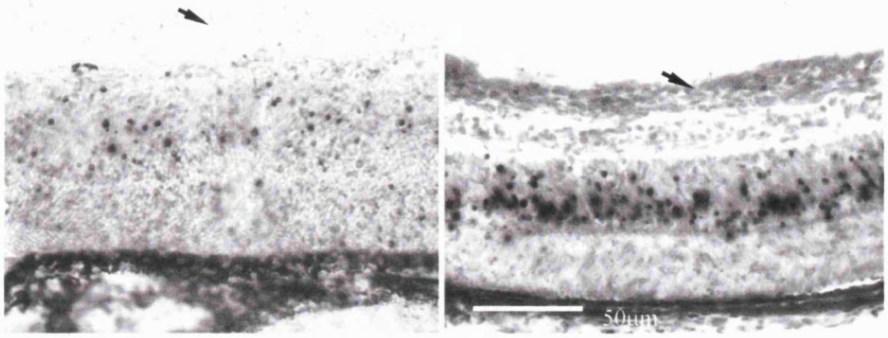

Fig 3.5 **A TUNEL assay to analyse apoptosis in the astrocyte layer.** A TUNEL assay was performed on P7 cross sections from wild type (left panel) and *GFAP-hPDGF-A* mice (right panel). Labelled cells are detected in the mid layers of the retina but not in the inner layer (arrow) where astrocytes reside.

3.2.3 Proliferation stops despite continued expression of PDGF-A and PDGFRα

There is a possibility that the decline in proliferation seen in both wild type and transgenic mice could be due to down regulation of the receptor *PDGFRα* or the ligand *PDGF-A* after P7. In wild type mice however, it is known that PDGF-A protein is still expressed strongly in the nerve fibre layer at P15 and even in the adult- a time after which proliferation is seen to decline (Mudhar et al., 1993). Also in rats, *PDGF-A* mRNA is still expressed at P15 and only declines in the adult, therefore at least in wild type animals, PDGF-A does not appear limiting for proliferation of astrocytes. To check that the transgene, *hPDGF-A*, does not become limiting in the *GFAP-hPDGF-A* mice, in situ hybridisation was performed on cross sections and on wholemount preparations of the retina.

hPDGF-A mRNA can be seen strongly at P7 in cross sections through the retina of transgenic mice (Fig 3.6A). The probe against *PDGF-A* mRNA used for this in situ hybridisation was specific to the human form of *PDGF-A*, which is only expressed in the transgenic mice. This probe does not detect endogenous mouse *PDGF-A* mRNA, therefore no expression is seen in wild type mice. By P16 this layer of *hPDGF-A* expression in transgenic mice has thinned (Fig 3.6A). If proliferation was limited by expression of the transgene, a decline in expression would be expected by P7 when proliferation has already declined.

Fig 3.6 **Astrocytes continue to express *PDGF-A* after proliferation has declined. (A)** 15μm cross-sections of retina from wild type and *GFAP-hPDGF-A* litter-mates were stained by in situ hybridisation for *hPDGF-A*. Expression was detected in *GFAP-hPDGF-A* mice but not in wild type mice. This analysis showed expression at the inner surface of the retina (arrow head) where astrocytes reside. **(B)** to get a different perspective, *PDGF-A* expression was also analysed in wholemount retina. Wholemount retina were prepared from wild type and *GFAP-hPDGF-A* mice and stained by in situ hybridisation for *hPDGF-A* (black stain). A strong signal was detected at all time points analysed in *GFAP-hPDGF-A* mice. As expected, no signal was detected in wild type mice, which do not express *hPDGF-A*.

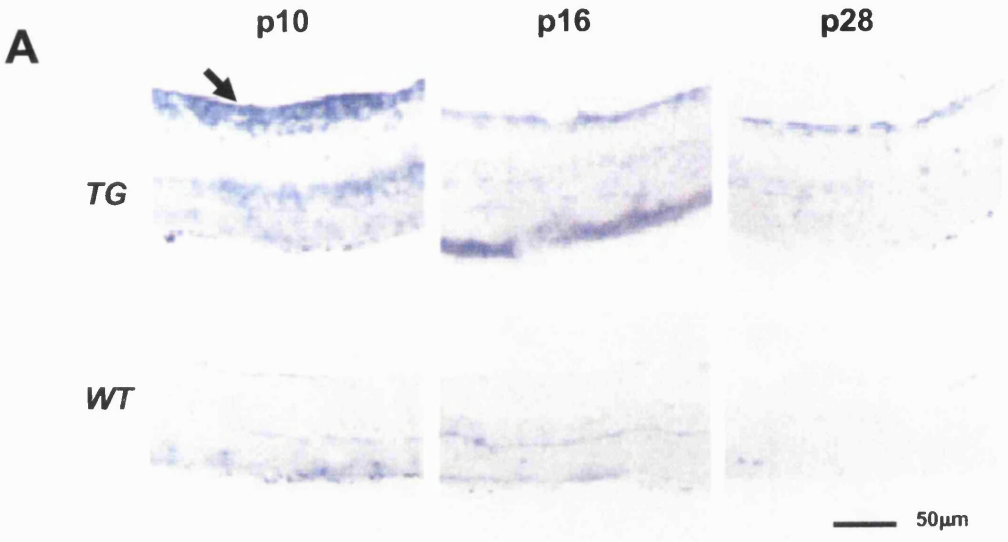
A
p10
p16
p28
TG
WT
50μm

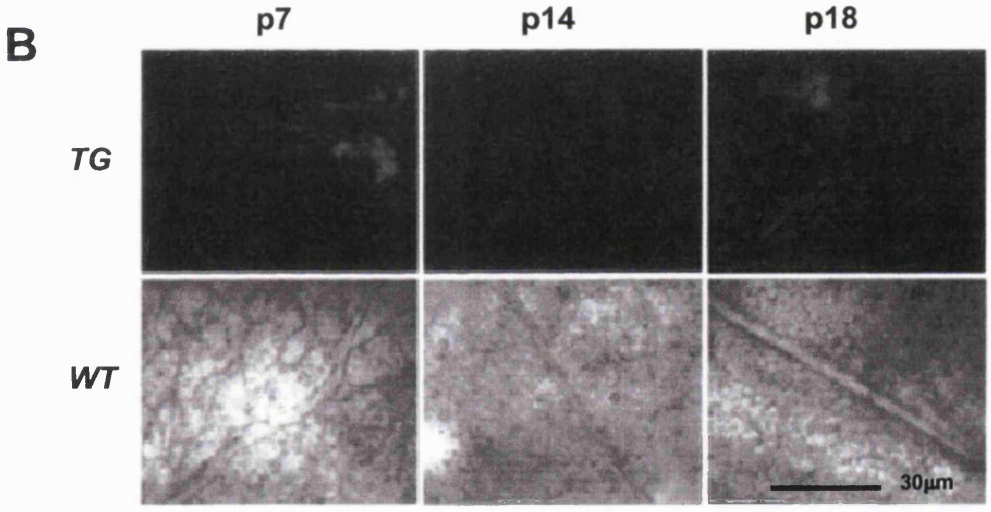
B
p7
p14
p18
TG
WT
30μm

From another angle, wholemounts stained with a probe to *hPDGF-A* mRNA, show a very strong signal all over the inner retinal surface in *GFAP-hPDGF-A* mice but not in wild type (Fig 3.6B). These results suggest that expression of the transgene is not limiting for proliferation in transgenic mice.

To check that the receptor for *PDGF-A* is still being expressed, in situ hybridisation was performed on wholemount preparations with a probe against *PDGFRα* mRNA. As shown in Fig 3.7, expression of *PDGFRα* can still be detected weeks after birth in both transgenic and wild type mice. In a high power image (Fig 3.7A), GFAP labelled astrocytes can clearly be seen co-expressing *PDGFRα* in the cell body. The expression of PDGFRα protein has not been addressed in this study. However, Marcus Fruttiger (unpublished) has demonstrated by immunohistochemistry the expression of PDGFR α protein in P14 wild type mice retina. This suggests that expression of the receptor is not limiting the proliferation of astrocytes in wild type or transgenic mice. It is possible however, that the signaling downstream of this receptor is blocked, as part of a control mechanism limiting retinal astrocyte proliferation.

3.2.4 Astrocyte proliferation occurs non-uniformly across the retina and correlates with avascular regions and regions at the edge of the vasculature

Cross section analysis of BrdU labelled cells reveals an unequal distribution of proliferating cells in the astrocyte layer. After P7, the few proliferating cells present are

Fig 3.7 **Astrocytes continue to express *PDGFRα* after proliferation has declined.**

Wholemount retina were stained by in situ hybridisation for *PDGFRα* (black stain) and then immunostained for GFAP (white). **(A)** shows expression of *PDGFRα* in $GFAP^+$ astrocytes at P21. **(B)** expression of *PDGFRα* can be detected at P7, P14,P21 and P28 (left to right) in both wild type (upper panels) and *GFAP-hPDGF-A* mice (lower panels).

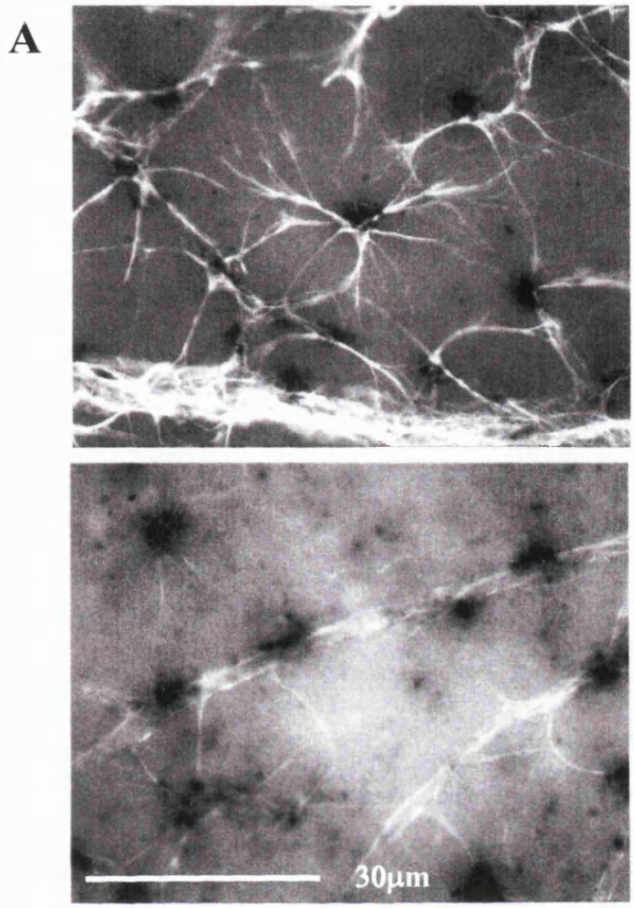
A
30μm

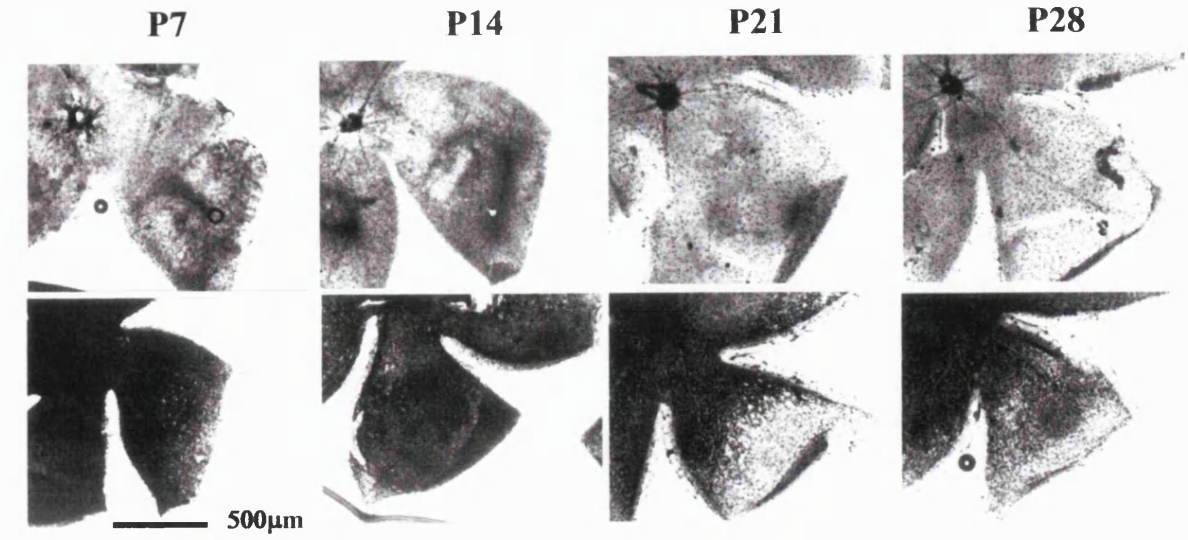
B
P7
P14
P21
P28
500μm

found mainly at the periphery. To observe these spatial differences more closely, wholemount preparations of retina were hybridised by in situ hybridization with a probe for *PDGFRα* mRNA to mark astrocytes, and then immunostained for BrdU.

Wholemounts were also co-stained for collagen IV to mark endothelial cells of the vasculature. Since astrocytes reside in the same layer as the vasculature, it was necessary to distinguish astrocytes from endothelial cells.

Just after astrocytes first enter into the retina at P0, they appear to be proliferating across most of the astrocyte network (Fig 3.8A). This data is consistent with the high BrdU labelling index observed in the dissociation assay. At this time the vasculature has not fully entered into the retina, and can be seen just emerging from the optic nerve head (Fig 3.8A). At P3, BrdU labelled astrocytes can be seen in the avascular regions of the spreading astrocyte network (Fig 3.9). However, where the vasculature is present most proliferating cells appear to co-localise with collagen IV (Fig 3.9B), suggesting endothelial rather than astrocyte proliferation in these areas. A similar trend is seen at P8 (Fig 3.10) where proliferating astrocytes are seen outside the vascularised area or just at its edge. Again, most of the proliferating cells within the areas covered by the vasculature co-localise with vessels.

A quantitative analysis was performed at P5, a time when the vasculature has spread partially across the inner surface of the retina. For the purpose of this analysis, the retina was split into mid retina, intermediate area (at the edge of the spreading vasculature) and peripheral retina (Fig 3.11B). The number of $BrdU^+$, $PDGFR\alpha^+$ double positive cells

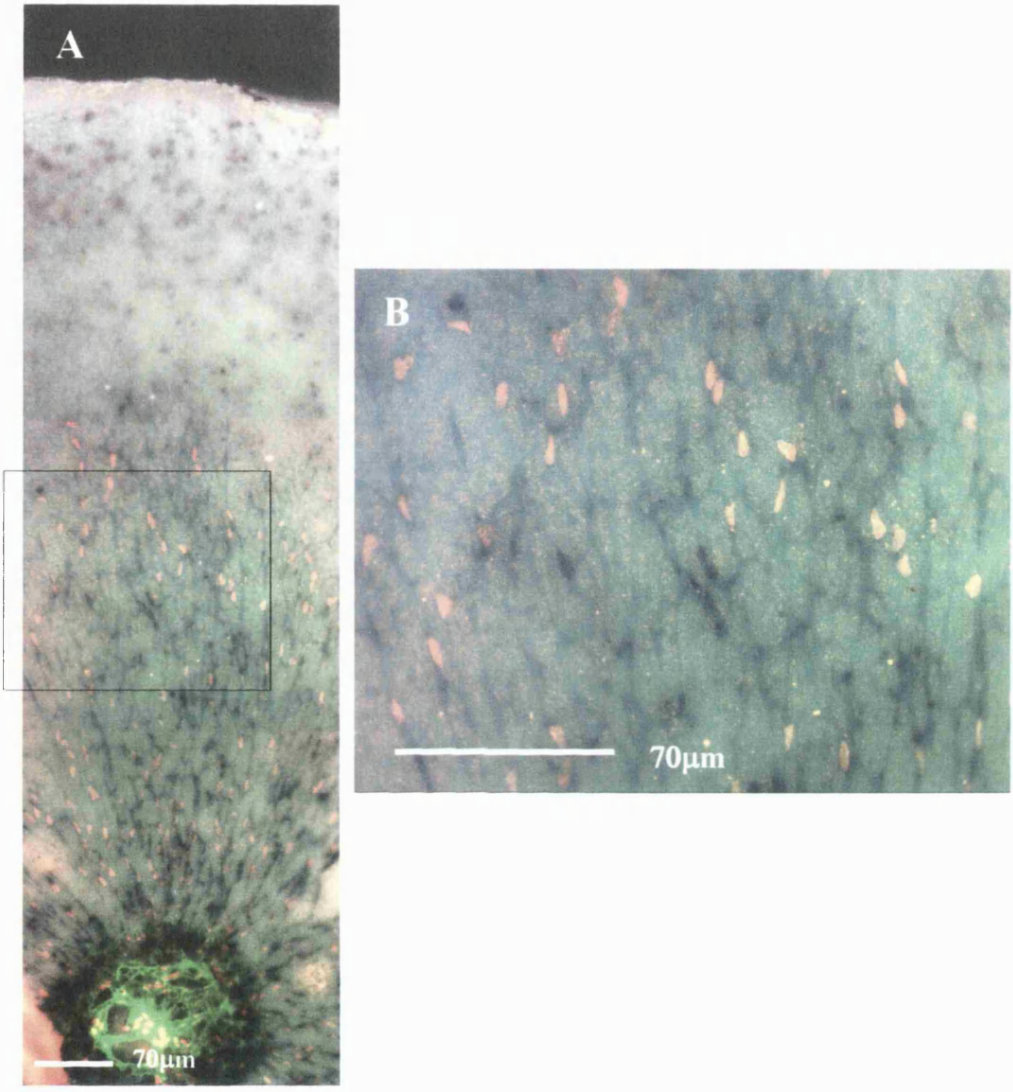

Fig 3.8 **Astrocyte proliferation is restricted to the avascular regions and regions at the edge of the developing vasculature: P0. (A)** Wild type retina were pulse labelled with BrdU as in Fig 1.2. Retina were then fixed and stained by in situ hybridisation for *PDGFRα* (blue/black stain). Retina were then stained by immunofluorescence for collagen IV (green) and BrdU (red). **(B)** shows a high power image of the black box shown in (A), demonstrating many *PDGFRα*$^+$, BrdU$^+$ double labelled cells. Collagen IV$^+$ vasculature is seen only at the very centre of the retina and is not in contact with most of the astrocyte network.

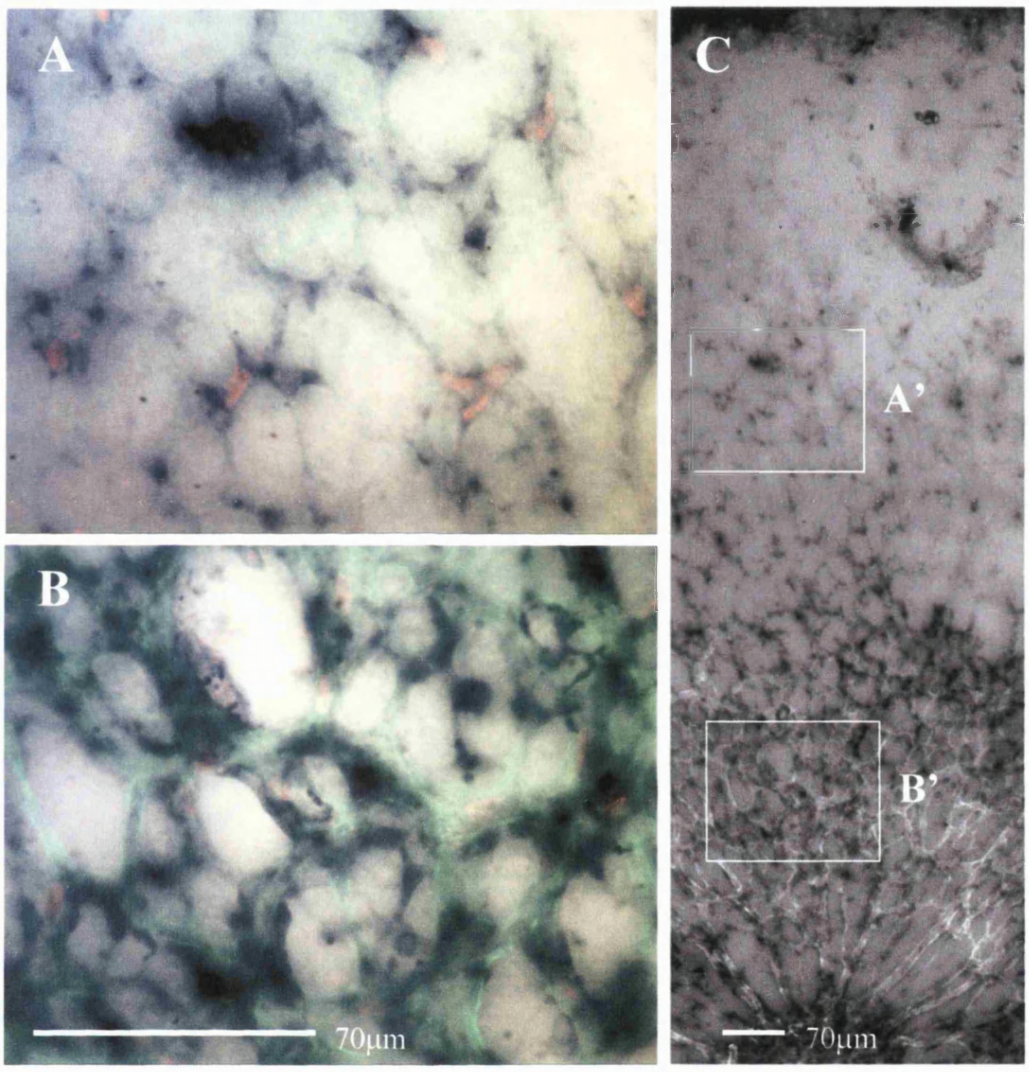

Fig 3.9 **Astrocyte proliferation is restricted to the avascular regions and regions at the edge of the developing vasculature: P3.** P3 wholemount retina were stained by in situ hybridisation for *PDGFRα* and by immunohistochemistry for collagen IV and BrdU. **(A)** shows *PDGFRα*$^+$, BrdU$^+$ double positive cells in an area with no collagen$^+$ staining. **(B)** shows a collagen IV$^+$ vascularised area. BrdU$^+$ cells co-localise with collagen IV$^+$ areas in this panel. **(C)** a low power image showing the areas of the retina from which panels A and B were taken, marked by white boxes A' and B' respectively.

Fig 3.10 **Astrocyte proliferation is restricted to the avascular regions and regions at the edge of the developing vasculature: P8.** Wild type P8 wholemount retina were stained by in situ hybridisation for *PDGFRα* and immunostained against collagen IV and BrdU **(A)** shows the fully vascularised inner retina with the positions of panels B and C marked by *B'* and *C'*. **(B)** shows a high power image of the white boxed area (A') demonstrating collagen IV$^+$, BrdU$^+$ co-localised stain but no obvious *PDGFRα*$^+$, BrdU$^+$ double positive cells. **(C)** shows a high power image of the white boxed area (B') from the mid retina demonstrating a few BrdU$^+$, collagen IV$^+$ double positive cells but no *PDGFRα*$^+$, BrdU$^+$ double positive cells.

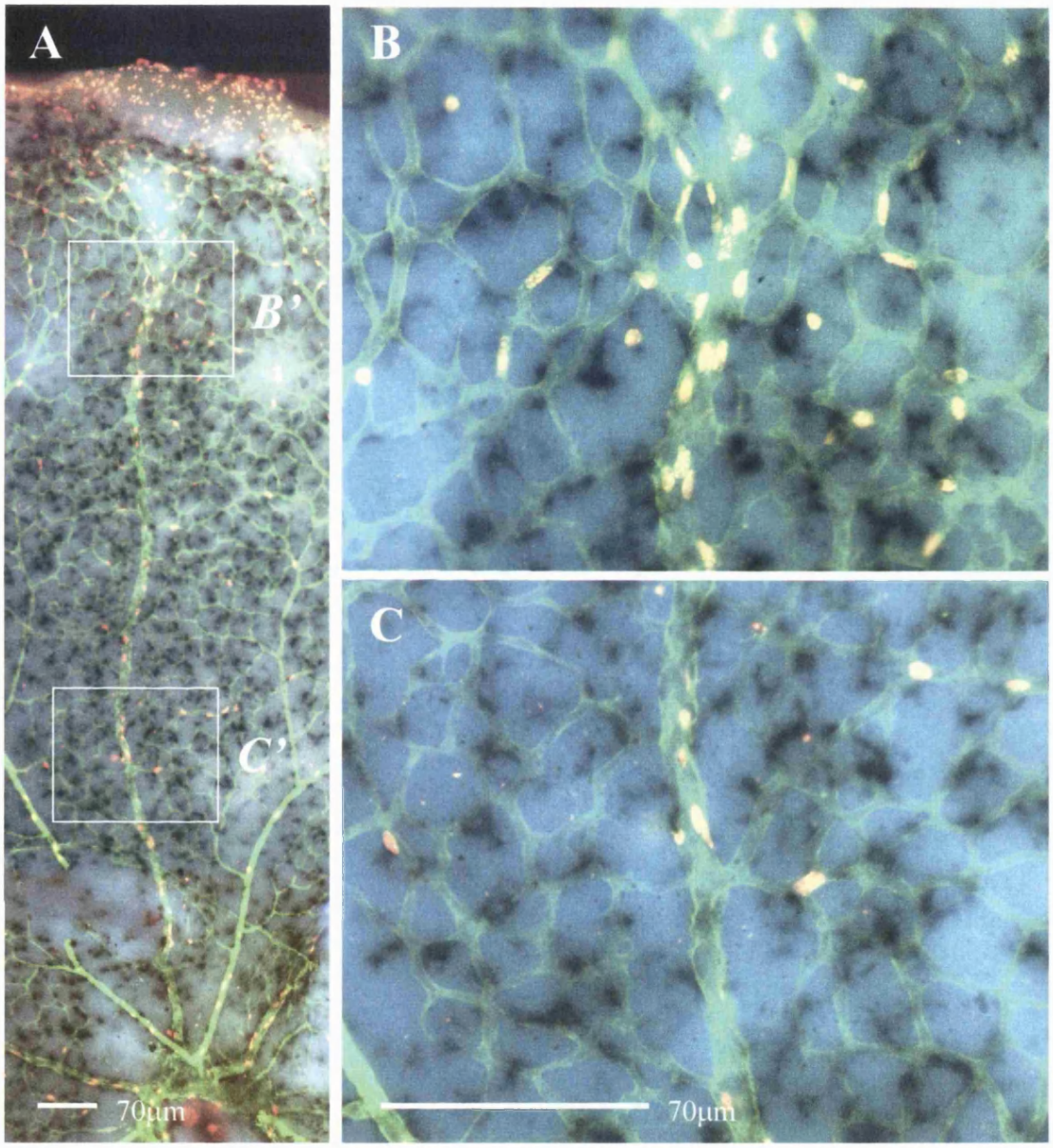
A
B'
C'
70µm
B
C
70µm

Fig 3.11 **Astrocyte proliferation is restricted to the avascular regions and regions at the edge of the developing vasculature: a quantitative analysis.** P5 pups were pulsed with BrdU and wholemount retina prepared. Wholemount retinae were stained by in situ hybridisation for *PDGFRα* (blue/black stain) and immunolabelled for BrdU (red). **(A)** shows part of the peripheral retina (left panel)with many BrdU $^{+}$ cells. **(B)** shows a high power image demonstrating *PDGFRα*$^{+}$, BrdU^{+} double positive cells in this region. **(C)** shows schematically, the distribution of BrdU^{+} cells across the inner surface of the retina. For the purpose of this analysis, the retina has been split into mid retina, intermediate area and peripheral retina as shown. x20 fields of view were analysed in these separate regions and the numbers of *PDGFRα*$^{+}$, BrdU^{+} double positive cells were calculated as a proportion of the total BrdU^{+} cells **(D)**. Each bar on the graph represents the mean $^{+}$/- s.d of counts from three specimens. Most BrdU^{+} cells at the periphery are *PDGFRα*$^{+}$ astrocytes, whereas, at the mid retina, few *PDGFRα*$^{+}$ astrocytes are BrdU^{+}

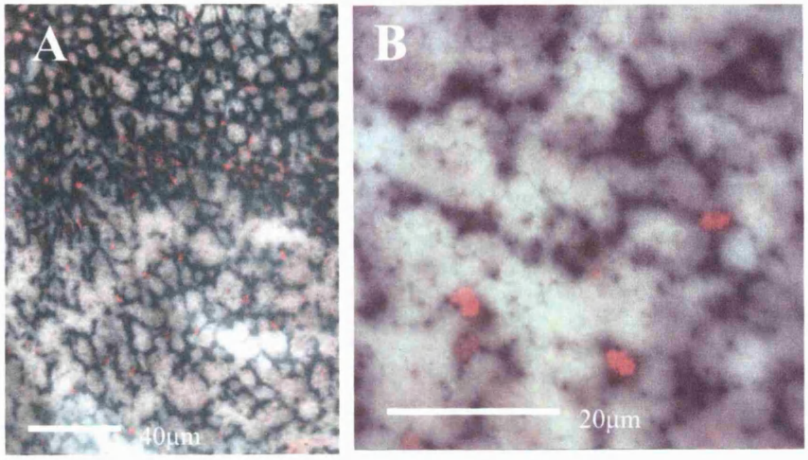
A
40µm
B
20µm

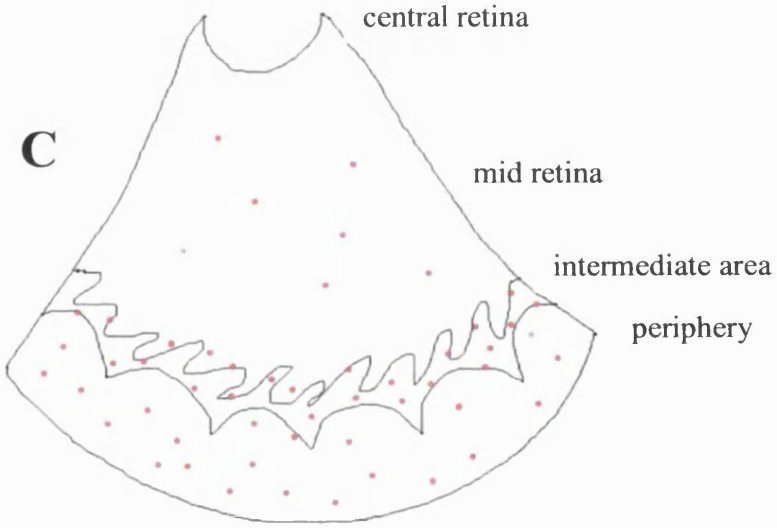
C
central retina
mid retina
intermediate area
periphery

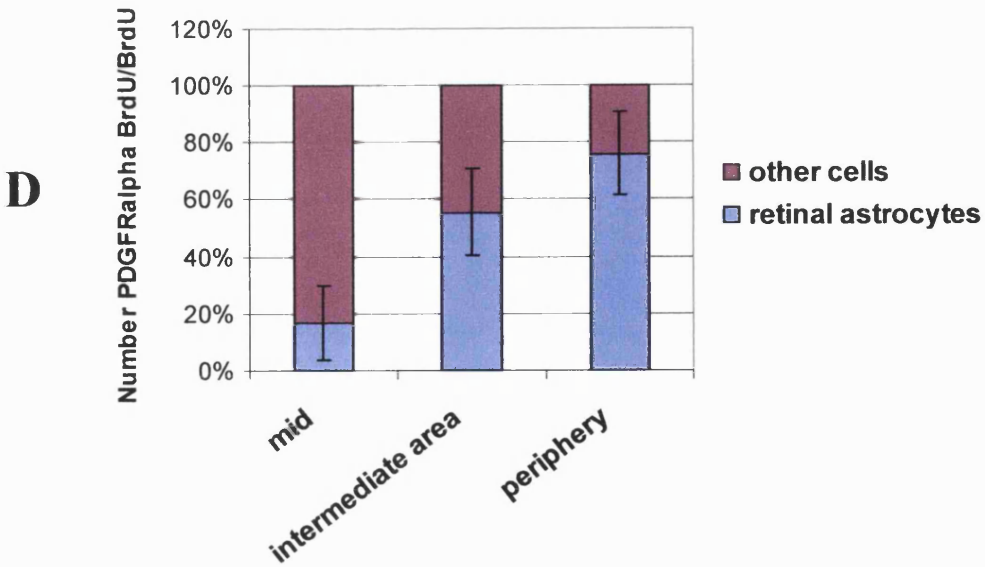
D
Number PDGFRalpha BrdU/BrdU
120%
100%
80%
60%
40%
20%
0%
mid
intermediate area
periphery
other cells
retinal astrocytes

(Fig 3.11D) was calculated as a proportion of the total BrdU $^{+}$ cells. This revealed that most of the proliferating cells in the avascular regions were retinal astrocytes, whereas the majority of proliferating cells in the vascularised regions were not astrocytes. In the intermediate area, at the edge of the vasculature, many cells are BrdU^{+} including retinal astrocytes and cells of the vasculature. In this area, approximately half the number of BrdU^{+} cells, are retinal astrocytes.

3.2.5 GFAP expression is downregulated in retinal astrocytes in avascular, hypoxic regions of the retina

GFAP has been suggested as a marker of astrocyte differentiation, where levels are thought to increase with normal differentiation in vitro and in vivo (Mi et al., 2001; Catalani et al., 2002; Zerlin and Goldman, 1997).

In Fig 3.11, *PDGFRα* was used as a marker for retinal astrocytes in P5 wholemount retina. However, *GFAP*, another astrocyte marker, shows a different expression pattern when analysed by in situ hybridisation at the same age (Fig 3.12). Fig 3.12 shows that in the peripheral retina, where I have clearly demonstrated *PDGFRα*$^{+}$ retinal astrocytes, *GFAP* expression is very low. This contrasts to high *GFAP* expression seen in central areas of the retina.

P5 wholemount retinae were also analysed for expression of vascular endothelial growth factor (*VEGF*), a gene that is expressed by astrocytes and upregulated in vitro and in vivo under relatively low oxygen concentrations (see introduction). As expected, Fig 3.12

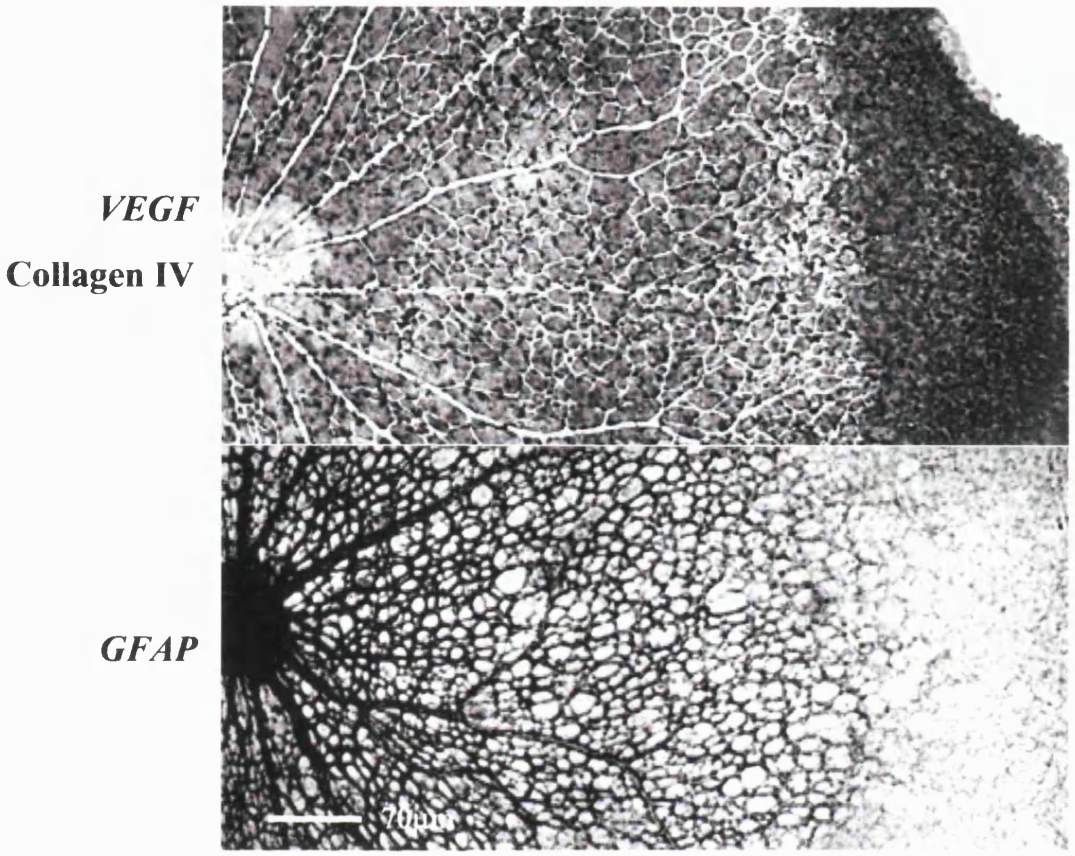

Fig 3.12 **Retinal astrocytes in peripheral, avascular areas show strong *VEGF* expression yet weak *GFAP* expression, compared to retinal astrocytes in vascularised areas.** P5 wholemount retina, were stained by in situ hybridisation for *VEGF* (black, top panel) and *GFAP* (black, bottom panel). The retinae stained for *VEGF* were also immunostained against collagen IV (white, top panel) to mark the vasculature. *VEGF* is expressed strongly in the peripheral areas of retina, that lack collagen IV^+ vasculature. *VEGF* is down-regulated in the collagen IV^+ areas (top panel). *GFAP* is strongly expressed in the collagen IV^+ vascularised areas (bottom panel), but weakly expressed in the peripheral areas lacking collagen IV^+ staining.

Figure from Marcus Fruttiger (unpublished)

(upper panel) shows strong *VEGF* expression in avascular, peripheral retina. It is also in this region that *GFAP* is expressed at low levels by retinal astrocytes (lower panel) and where these cells are proliferating highly. These results are consistent with GFAP levels marking astrocyte differentiation. Thus it appears that presence of blood vessels correlates with a decrease in proliferation, a decrease in *VEGF* expression and an increase in *GFAP* expression.

3.3 Discussion

In this chapter, I have analysed retinal astrocyte proliferation using immunohistochemistry and in situ hybridisation on cross sections, wholemount preparations of retina, or on overnight retinal cell cultures. I have shown that the level of astrocyte proliferation declines after birth, limiting the number of cells that develop. Overexpressing *PDGF-A* in an autocrine loop leads to higher levels of proliferation and greater number of cells yet the effect is limited. Proliferation still stops at the same time as in wild type mice, preventing further increases in cell number. Furthermore, I show that areas of astrocyte proliferation are confined to avascular areas and to the edges of the vasculature during development.

3.3.1 Cross section and wholemount analysis versus a dissociation assay

I have used several different methods to analyse proliferation of retinal astrocytes during development of the retina, each has its advantages and disadvantages. An advantage of using cross sections to analyse the astrocyte layer is that the thickness of the layer gives a quantitative impression of the number of astrocytes in the network. For instance, in the *GFAP-hPDGF-A* mouse, the GFAP stained astrocyte layer is thicker than that in the wild type mice. Consistent with this, in a dissociation assay numbers of astrocytes were on average 10x greater in transgenic than in wild type mice at P7 (data not shown). Cross section analysis was useful in the TUNEL analysis, where no signal was detected in the astrocyte layer compared to a strong signal detected in the outer nuclear layer, in another cell type. When used for in situ hybridisation with a probe against *hPDGF-A*

mRNA, cross section analysis clearly identified expression of the *hPDGF-A* transgene mRNA specifically in the astrocyte layer. A disadvantage of cross sections is that it is not possible to distinguish astrocytes easily from other cells in the layer e.g from endothelial cells which can be tightly associated with retinal astrocytes. Furthermore, the spatial distribution of proliferating cells across the inner surface of the retina is not easily discernable, so wholemount analysis is a good complement to cross section analysis.

In order to distinguish individual cells with certainty, a dissociation assay was performed. This method allows a quantitative analysis of astrocyte proliferation at different ages. Since spatial information is lost by this method, cross section and wholemount analysis complement each other. However, measurements of proliferation in the dissociation assay have to be treated with caution because astrocytes may proliferate in vitro, therefore distorting the total number of cells. The main advantage of this method is that retinal astrocyte proliferation can be quantified reproducibly.

Since astrocytes reside on the inner surface of the retina, wholemount analysis has the advantage of being able to visualise the whole astrocyte network. Only in these preparations can the correlation between the presence of vasculature and retinal astrocyte proliferation be seen. The limitation of the wholemount analysis is that individual astrocytes are difficult to count, so a labelling index cannot be calculated for different sections of the retina. It is possible however to say whether the BrdU labelled cells in a particular area are astrocytes or not, and to quantify this (Fig 3.11). The remaining BrdU positive cells could possibly be endothelial cells, pericytes, smooth muscle cells or

microglia associated with the vasculature (Provis et al., 1997). In the wholemount analysis, many of these $BrdU^+$ cells appeared to co-localise with collagen IV, suggesting they are vascular cells.

3.3.2 A control on proliferation limits population growth of astrocytes

Cell number depends on both cell division and cell death. Cell death can be important in the developing vertebrate nervous system in controlling cell numbers. Many types of neurons are overproduced and then compete for limited amounts of survival signal, secreted by the target cells they innervate (Raff, 1996). This ensures the matching of numbers of neurons to target cells (see introduction). Cell death also appears to control the numbers of glial cells too. Developing neurons and glial cells can interact to adjust glial cell numbers appropriately when neuronal numbers are increased. This is seen for example in mice overexpressing *bcl-2* in neurons (Bonfanti et al., 1996). This molecule antagonises apoptosis and leads to an increase in neuron numbers during development. The decreased loss of retinal ganglion cell axons leads to a decrease in the death of postmitotic oligodendrocytes. However, oligodendrocyte precursors increase in number due not to reduced death but an increase in proliferation, as do astrocytes in the optic nerve (perhaps via FGF). This is similar to retinal astrocytes, which appear to increase in number due to increased proliferation rather than reduced cell death.

It is possible that programmed cell death may decrease the numbers of retinal astrocytes at a later time point not tested in this study. However, the critical event for limiting

astrocyte numbers in the retina appears to be a cessation in proliferation. Any cell death after this time point may lead to the slight thinning of the astrocyte layer after its peak size seen at P7. In P5 mouse retina, one study reported no TUNEL signal around the ganglion cell layer at this time (including the astrocyte layer), but a strong signal in the neuronal nuclear layer (Pimentel et al., 2002). This is consistent with the results presented here two days later at P7, showing a similar distribution. Later at P16 most apoptotic cells are seen in the outer nuclear layer (Pimentel et al., 2002). It seems unlikely therefore, that programmed cell death plays a significant role in limiting retinal astrocyte numbers during development.

3.3.3 Use of BrdU to analyse rates of proliferation

Throughout this study, I have used BrdU incorporation as a marker for cells in S phase. A common alternative method uses tritiated thymidine. An advantage of this method is that thymidine is the only nucleotide base incorporated into DNA but not into RNA. This avoids labelling of mRNA or other RNA species being synthesised during labelling, which is not associated with DNA replication. However, a disadvantage of using tritiated thymidine is the handling of expensive radioactive isotopes, long exposure times that delay evaluation of data and poo r spatial resolution (Chan-Ling, 1997). BrdU avoids this because a monoclonal antibody is used that recognises single-stranded DNA containing 5-bromo-2'-deoxyuridine (Gratzner, 1982) an analog of thymidine, and can be used to identify cells in S phase. I assume here that the proportion of the mitotic cycle

spent in S phase does not vary significantly among the various conditions examined (Chan-Ling, 1997).

3.3.4 Astrocyte proliferation is confined to avascular regions and to the edge of the vasculature

Chapter 3 provides evidence that astrocyte proliferation is restricted mainly to the avascular regions and regions at the edge of the vasculature. At P8, the vasculature has covered the retina and astrocytes have stopped proliferating. Consistent with this, the dissociated cell assay s hows a very low BrdU labelling index at this time. In contrast, at P0 astrocyte proliferation is high both in wholemount analysis and in the dissociation assay. This correlates with an absence of retinal vasculature at this time. Later at P3, half the astrocyte network is covered by the vasculature and those in contact with vessels have stopped proliferating. At P3, the labelling index in the dissociation assay has decreased accordingly.

Interestingly, the arrival of the vasculature occurs in both *GFAP-hPDGF-A* and wild type mice at the same time. This could explain why the decline in proliferation occurs in both strains at the same time. If this is the case, it suggests that the influence of the vasculature overrides the effect of the mitogen PDGF-A on astrocyte proliferation. What model could explain the results observed?

At P0, no vasculature is present and the rate of proliferation is similar in both wild type and transgenic mice. This may be because proliferation of astrocytes is saturated. There is no vasculature inhibiting astrocyte proliferation and a fixed supply – presumably greater than the demand – of PDGF-A from retinal ganglion cells is already present in the retina. Later at P3, roughly half the retina is covered by vasculature and the astrocyte network has increased. At this time however, proliferation is almost double in the transgenic mice. One explanation is that in wild type mice, the fixed source of PDGF-A from RGCs has become limiting for retinal astrocyte proliferation, as the demand or number of cells has increased. In the transgenic mice however, the supply grows with the demand. As the numbers of astrocytes increases, the supply of PDGF-A never runs out because it is produced by the astrocytes themselves. The effect of the transgene is then limited by P7/8, because by this time the vasculature has come into contact with all astrocytes, and exerts an overriding effect on their proliferation.

Previous reports have demonstrated a close link between astrocytes and the vasculature during development and in the adult, as discussed in the introduction. Consistent with the results presented here, (Stone et al., 1995) show that retinal astrocytes migrate ahead of the vasculature during development. They are found to proceed blood vessel spread by a small margin in the human, cat and rat retina (Chu et al., 2001) consistent with the results in mice presented here. Stone and colleagues have shown that astrocytes respond to hypoxia and attract blood vessels to those avascular areas in the developing retina (Stone et al., 1995).

Provis (Provis, 2001) suggests that most of the proliferating cells in the nerve fibre layer are astrocytes and that these cells proliferate in advance of the spreading vasculature. However, the authors of this study do not look at the changes in retinal astrocyte proliferation at different stages of retinal development, or relate these changes to the vasculature. Provis and colleagues suggest that astrocyte proliferation during vasculature development in the astrocyte layer outnumbers endothelial cell proliferation by 4:1. Sandercoe et al (Sandercoe et al., 1999) show that 65-85% of proliferating cells at the advancing vascular front are GFAP positive, consistent with my results in the mouse retina at P5 (Fig 3.11). These authors show that 15-52% are CD34 positive, a marker for endothelial cells. This is also consistent with my wholemount analysis showing that many of the cells proliferating in regions covered by the vasculature, co-localise with collagen IV, marking vascular cells.

What is the nature of this effect of the vasculature on astrocyte proliferation? One possibility is that it is the effect of endothelial cells themselves, perhaps releasing a differentiation factor that acts upon astrocytes. One report suggests that endothelial cells in rat optic nerve cultures can induce the differentiation of astrocytes (Mi et al., 2001). Optic nerve endothelial cells were purified and mixed cultures made with optic nerve astrocytes. Endothelial cells were found to induce the differentiation of astrocytes via Leukaemia Inhibitory Factor (LIF).

Astrocytes migrate into the retina at birth (Fruttiger et al., 1996; Watanabe and Raff, 1988). At this time, the retinal vasculature is absent and astrocytes are experiencing

relatively low oxygen levels. Could hypoxia drive astrocyte proliferation during development of the retina? In order to populate the retina, astrocytes need to proliferate to cover the inner surface of the retina. Could the hypoxic retina be a trigger for this proliferation? Once the vasculature has arrived and oxygenated the retina, astrocyte population growth is no longer necessary. The rising oxygen levels may trigger differentiation – or at least a cessation of proliferation – of retinal astrocytes.

3.3.5 VEGF is upregulated in the avascular peripheral areas of the developing retina

In support of the latter idea, vascular endothelial growth factor (*VEGF*), a gene that is up-regulated under hypoxia (see introduction) and expressed by retinal astrocytes, is up-regulated in the avascular region of the retina (Fig 3.12 top panel). In vascularised areas, *VEGF* mRNA appears to be expressed weakly. These results are consistent with studies on *VEGF* expression in the developing human retina (Provis et al., 1997).
This data suggests that the avascular retina is indeed experiencing hypoxia during development and is consistent with the idea that oxygen levels may control retinal astrocyte proliferation. Does *VEGF* expression correlate with retinal astrocyte proliferation during development? This question is addressed in the next chapter.

3.3.6 Variation in GFAP expression throughout the astrocyte network

A comparison of P5 wholemounts stained against two markers for retinal astrocytes: *PDGFRα* and GFAP, reveal different staining patterns. At P5, *PDGFRα* mRNA is clearly visible in the avascular peripheral retina. As described (Fig 3.11), retinal astrocytes appear to be most highly proliferative in this region. However, at the same age, an in situ hybridisation against *GFAP* reveals weak staining in the peripheral areas compared to strong expression in the vascularised areas (Fig 3.12 lower panel). Hence, *GFAP* expression appears to be up-regulated in retinal astrocytes in contact with blood vessels.

The data presented here is consistent with increased *GFAP* expression marking differentiation of retinal astrocytes. Indeed, weak *GFAP* expression correlates with retinal astrocytes that are highly proliferative and less mature, given the central to peripheral wave of differentiation in the retina (Rapaport and Stone, 1982; Stone et al., 1995; Provis et al., 1997). A study by Chu et al (Chu et al., 2001) has shown in human retinal development, that astrocytes progress from a *GFAP* -negative to a *GFAP* -positive phenotype. This data also correlates with the central to pe ripheral pattern of differentiation in the retina: at any one time the more immature astrocytes can be seen at the periphery of the retina with the more mature *GFAP* -positive cells in the centre. This is consistent with a model whereby a property of the v asculature – perhaps increasing oxygen levels – induces loss of proliferative potential and differentiation of retinal astrocytes. This model is investigated further in Chapter 5.

Chapter 4. investigating the effect of hypoxia on retinal astrocyte proliferation in vivo

4.1 Introduction

In the last chapter, I proposed that a property of the developing vasculature – perhaps increasing oxygen levels -could be responsible for the de cline in astrocyte proliferation observed. In this chapter, I investigate levels of hypoxia in the developing retina by visualising *VEGF* mRNA, which is upregulated under hypoxic conditions. I correlate expression of *VEGF* mRNA with levels of proliferation throughout retinal development. In order to manipulate the areas of hypoxia in the retina, I grow mice in hyperoxic conditions, which has the effect of inhibiting vasculature development. In such conditions, areas of hypoxia could be expanded and levels of astrocyte proliferation increased suggesting that the presence of vessels leads to a cessation in astrocyte proliferation. Despite the absence of retinal vessels, I observed a small area of normoxia in the centre of the retina, most likely caused by o xygen diffusion from the central hyaloid artery. Interestingly, astrocyte proliferation was virtually zero in this area. This data suggests that the property of the developing vasculature that reduces retinal astrocyte proliferation, is the increasing oxygen levels.

Studies by Stone and colleagues (Stone et al., 1995) have already shown that astrocytes in the developing retina respond to low oxygen levels by up -regulating *VEGF*

expression, which induces the growth of blood vessels. However, it is not known is how these cells that control vascular development are controlled themselves.

VEGF has been shown in vitro and in vivo to be upregulated under hypoxic conditions. In a study on human retina, cells (presumably astrocytes) just ahead of the vascular front have been shown to express VEGF in response to their hypoxic environment. The maturation of photoreceptors and neurons leads to the development of a 'physiological hypoxia' in the retina. The rapidly increasing metabolic demands of the differentiating neural retina, are thought to deplete oxygen in the tissue and lead to its hypoxic status (Chan-Ling et al., 1995). Increasing retinal metabolism also limits the flow of oxygen from the choroidal vasculature to the inner layers of the retina. Astrocytes are strategically placed to sense hypoxia of the inner surface of the retina, and then attract in and act as a template for the incoming vasculature (Stone et al., 1995). Oxygen brought by the incoming vessels then down regulates the expression of *VEGF* by astrocytes making the process self-limiting (Stone et al., 1995).

Stone et al have used a common model for retinopathy of prematurity (Stone et al 1996) whereby manipulation of the vasculature can be achieved by growing mice in hyperoxic conditions. High levels of oxygen in arterial blood cause a down -regulation of *VEGF* around the central hyaloid artery in the optic nerve head, preventing the emergence of retinal vessels from the optic verve head. This leads to hypoxia in large parts of the retina even though the animal is breathing hyperoxic air. This model has been used in the past to study the effects of high oxygen on the vasculature, but here I use it to study

astrocyte behaviour under hypoxic conditions, where *VEGF* mRNA expression is up-regulated in most of the retina apart from a small area around the optic nerve head. In areas of high *VEGF* mRNA expression and presumably hypoxia, I found increased retinal astrocyte proliferation, whereas in areas of low *VEGF* mRNA expression, I found virtually no retinal astrocyte proliferation.

4.2 Results

4.2.1 Upregulation of *VEGF* expression correlates with astrocyte proliferation

Having demonstrated a link between blood vessels and and astrocyte proliferation, I investigated whether the proliferative areas of the retina in vivo correlated with hypoxic, avascularised areas. To do this I looked at *VEGF* mRNA expression during astrocyte development in the retina. *VEGF* is known to be upregulated by astrocytes in culture in response to hypoxia and thought to be upregulated in the retina under hypoxic conditions (Stone et al., 1995). Previous studies have looked at *VEGF* expression in the retina but it is not clear how this correlates with astrocyte proliferation during mouse retinal development. Many studies before have looked only at GFAP expression to mark astrocytes whereas I use here, *PDGFRα*. This marker was preferable because of the variability in GFAP expression observed in astrocytes at different states of maturity (data presented here, (Chu et al., 2001).

The results here show clear *VEGF* mRNA up-regulation in the avascular areas and at the edge of the vasculature, which correlates well with the areas of increased astrocyte proliferation. In Fig 4.1, at P0, many *PDGFRα* positive cells are labelled with BrdU. In different preparations, these BrdU positive cells – presumably astrocytes - are expressing *VEGF* also. In vascularised areas at P3, the few BrdU labelled cells appear to co-localise with collagen IV and hence appear to be endothelial cells (Fig 4.2). However in the avascular areas, the BrdU labelled cells co-localise with the areas strongly expressing

***Fig 4.1* *VEGF* is up-regulated in avascular regions of the retina where astrocytes are proliferating: P0 retina** P0 wild type pups were given an injection subcutaneously of 50μg/g body weight BrdU. Two hours later pups were killed and the retina dissected to prepare wholemounted specimens. Retinae were stained by in situ hybridisation for *PDGFRα* or *VEGF* (blue/black stain) and then immunostained for BrdU (red) and collagen IV (green). **(A)** shows the distribution of *PDGFRα*$^+$, BrdU$^+$ astrocytes at this age. **(B)** is stained with *VEGF* and BrdU. **(C)** is a high power image of the white boxed area in (B) showing *VEGF* expression in a BrdU$^+$ region. Collagen IV staining is only found at the centre of the retina, since the retina is not yet vascularised **(D)**.

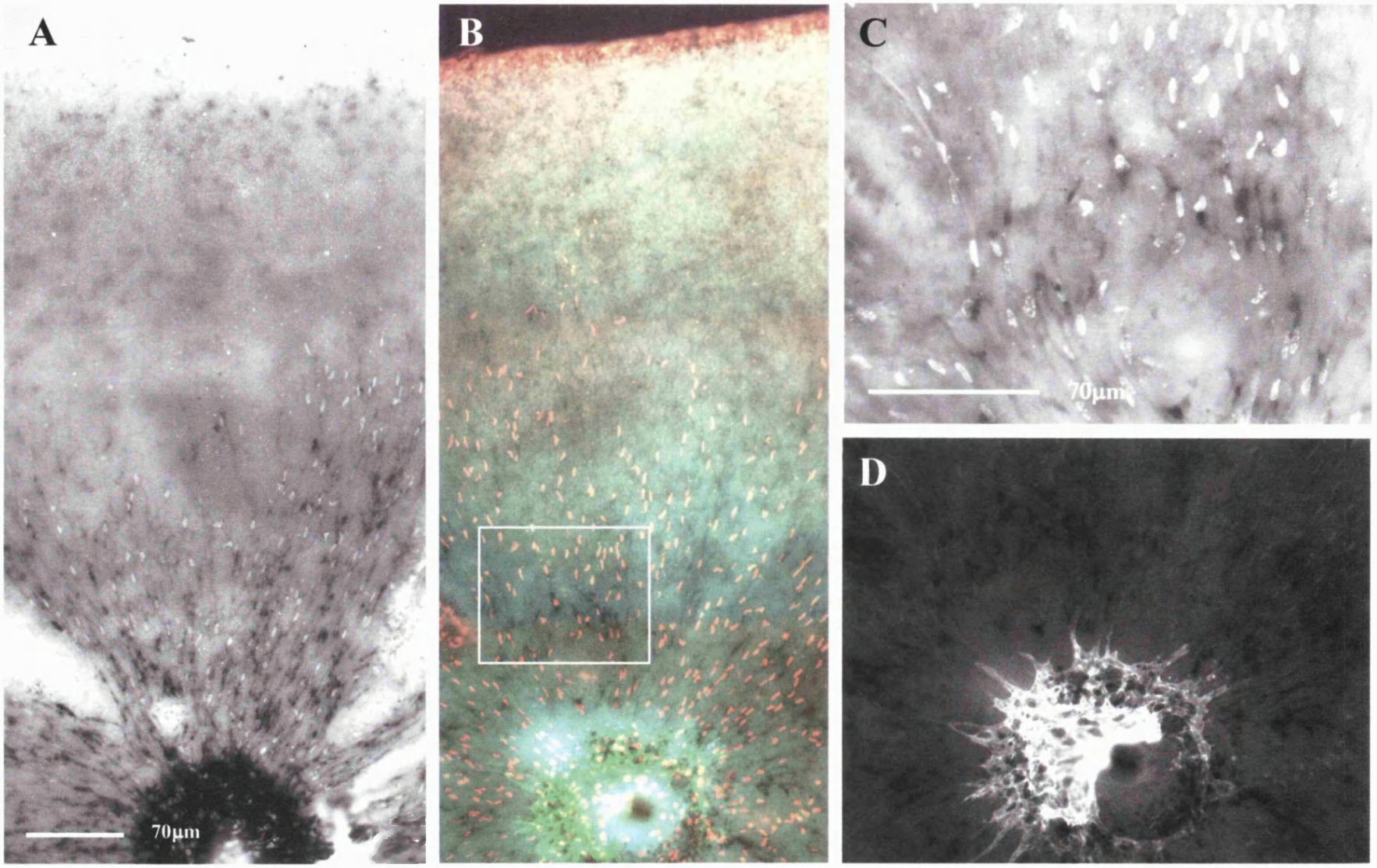

PDGFRα VEGF BrdU Collagen IV

Fig 4.2* *VEGF* is upregulated in avascular regions of the retina where astrocytes are proliferating: P3 retina.** P3 pups were pulsed with BrdU, the retina dissected and stained by in situ hybridisation for *PDGFRα* or *VEGF* and immunostained against collagen IV and BrdU. **(A)** and **(B)** show retina stained against *PDGFRα*, collagen IV and BrdU. These high power images are taken from the boxed areas marked **A'** and **B'** respectively. The distribution of *PDGFRα*$^+$, BrdU$^+$ cells are compared with the distribution of *VEGF*$^+$, BrdU$^+$ cells. **(C)** shows many *VEGF*$^+$, BrdU$^+$ double positive cells located in the avascular region (taken from the boxed area marked ***C' in the centre panel). **(D)** collagen IV visualises blood vessels in this region (taken from the boxed area ***D'*** in the centre panel). *VEGF* expression is low in this area and most BrdU$^+$ cells appear to be collagen IV$^+$ endothelial cells.

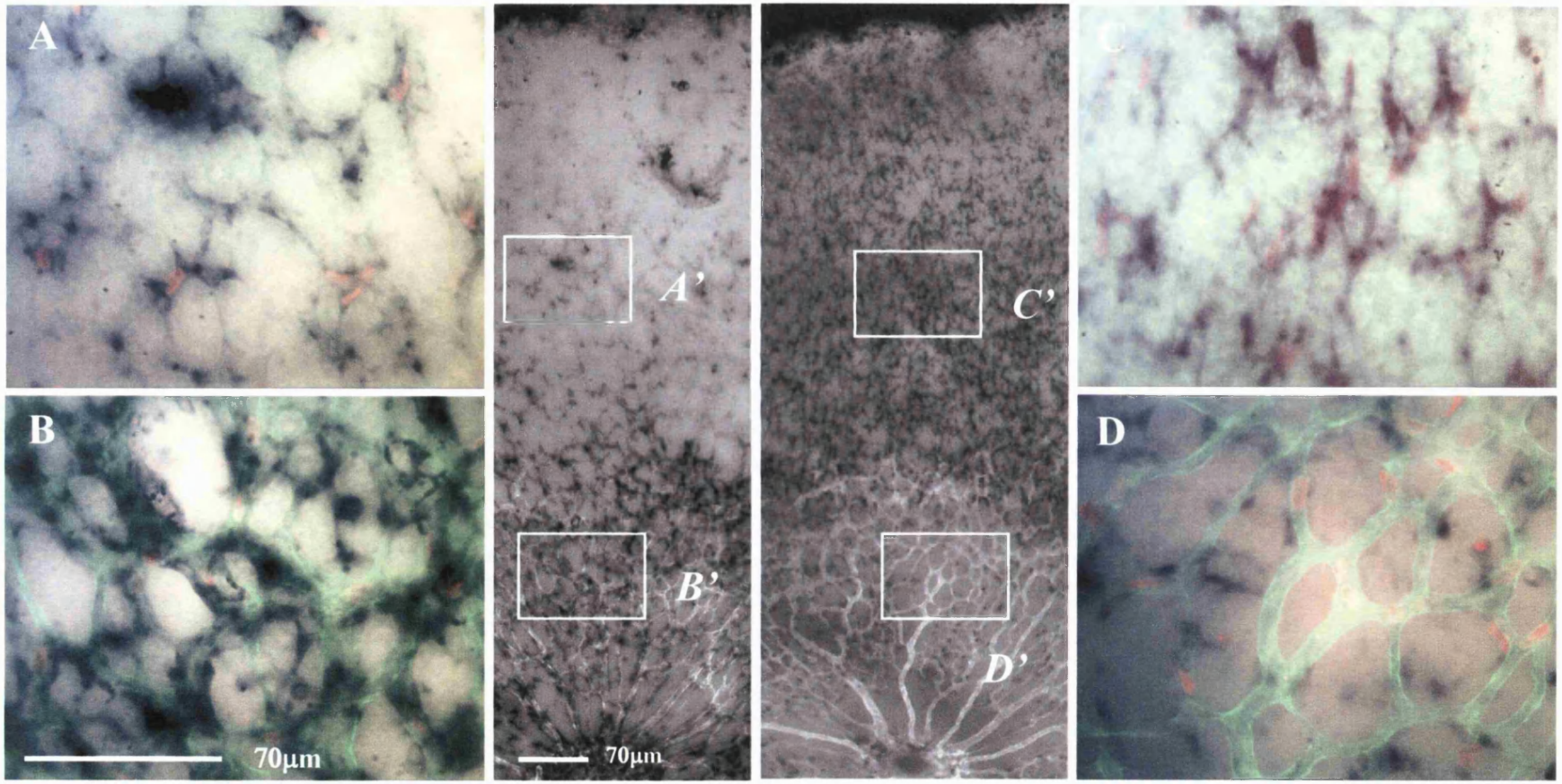
A
B
70μm
A'
B'
70μm
C'
D'
C
D
PDGFRα
VEGF

VEGF mRNA. At P8 the few BrdU labelled cells appear in the hypoxic *VEGF* mRNA expressing zone at the peripheral retina (Fig 4.3). This is consistent with the model that hypoxia or absence of vasculature is permissive for astrocyte proliferation during retinal development.

4.2.2 Obliteration of the vasculature leads to increased *VEGF* expression and increased astrocyte proliferation

Pups were grown with a mother in hyperoxic conditions of 80% oxygen from birth until P8. Control pups were grown with a foster mother in normo xic conditions for the same time-period. Pups were then given a 2-hour BrdU pulse injection at P8 before processing the retina for staining.

Immunostaining retinae against collagen IV, revealed that the vasculature is present in the control group but not in the hyperoxic-treated retinae (Fig 4.4). In a comparison of *PDGFRα* mRNA and BrdU staining in both groups, astrocyte proliferation had clearly spread over a larger area in hyperoxic-treated compared to control retina (Fig 4.4). Furthermore, the density and number of $PDGFR\alpha^+$ cells appeared greater in the hyperoxic-treated litter.

In order to test that hyperoxia treatment really does result in an enlargement of hypoxic areas in the retina, I visualised *VEGF* mRNA by in situ hybridisation of retinal wholemounts. This is based on the assumption that hypoxic retinal astrocytes express

***Fig 4.3* *VEGF* is upregulated in avascular regions of the retina where astrocytes are proliferating: P8 retina.** **(A)** this P8 wholemount retina was immunostained against collagen IV (green/blue), BrdU (red/yellow) and stained by in situ hybridisation against *VEGF* mRNA (black). The collagen IV^+ vasculature is spread almost entirely across the inner retinal surface. An avascular rim is present at the periphery where *VEGF* expression is upregulated **(B')**. The boxed area B' is shown at higher power in **(B)**. $BrdU^+$, $VEGF^+$ double positive cells can be found in this region (arrows). **(C)** shows a higher power image of the boxed area **C'**, taken in a vascularised region. None or few BrdU labelled cells are found here.

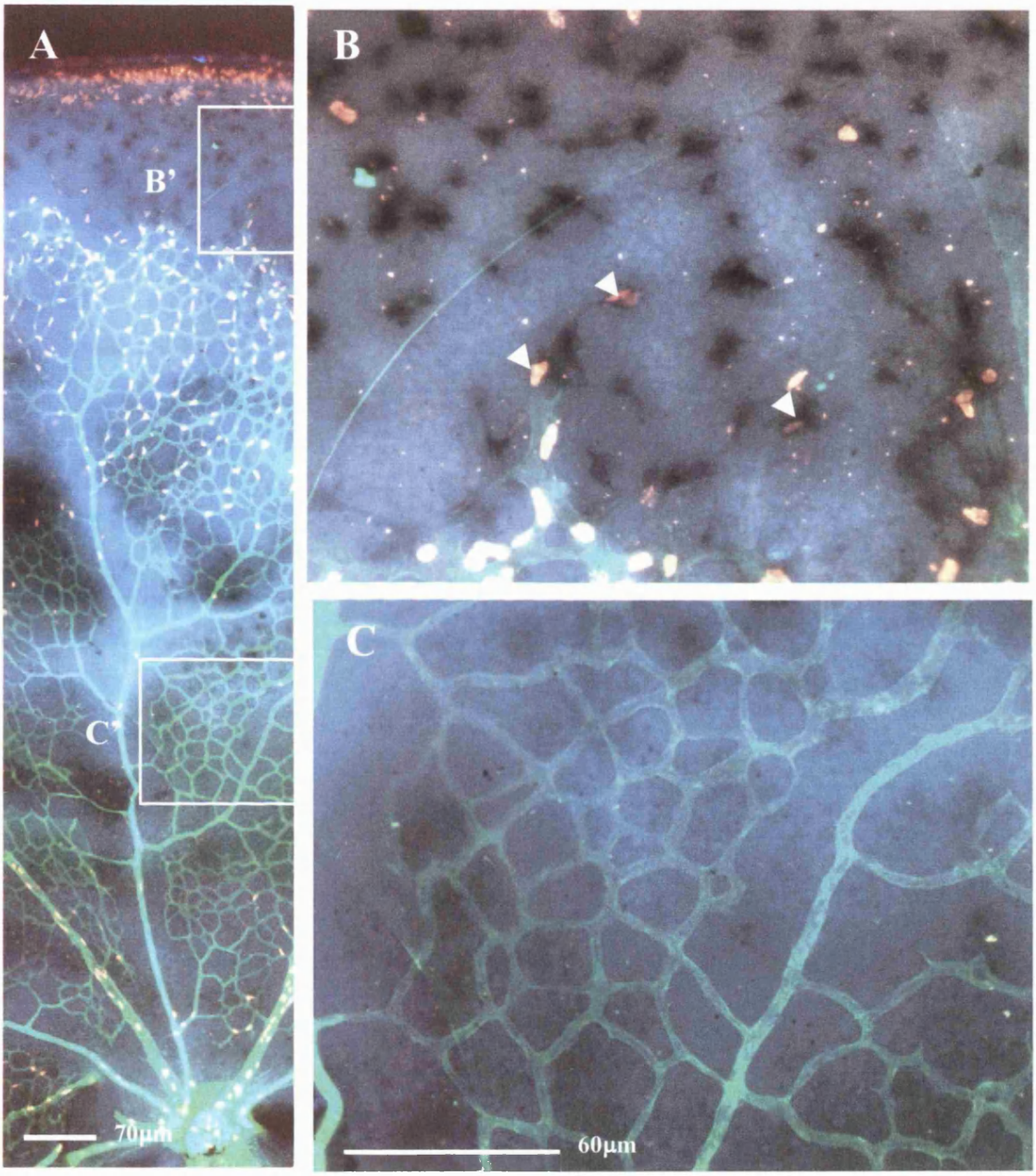

VEGF **BrdU** **Collagen IV**

Fig 4.4 **A correlation between avascular regions and regions of astrocyte proliferation, after manipulation of the developing vascualture.** Newborn pups together with their mother were placed in a cage maintained at 80% oxygen levels. Half the litter were kept as a control group and placed with a foster mother in normal atmospheric conditions. At p8, the pups from both groups were pulse labelled with BrdU for 2 hours. Wholemount retinae were stained by in situ hybridisation for *PDGFRα* and immunostained for BrdU and collagen IV. The far left panel shows a retina from the control animals, which is fully vascularised. The far right panel shows a retina from the animals kept in hyperoxic conditions. This retina lacks collagen IV^+ vasculature. Many $BrdU^+$, $PDGFR\alpha^+$ cells can be seen and an increase in *PDGFRα* staining. The boxed area marked **A'** is shown at higher magnification in **(A)** where many $BrdU^+$, $PDGFR\alpha^+$ double positive cells are labelled. In contrast, **(B)** taken from control animals shows a vascularised area at the same position in the retina, where very few BrdU labelled cells can be found. (B) is a higher power image of the boxed area marked (**B'**).

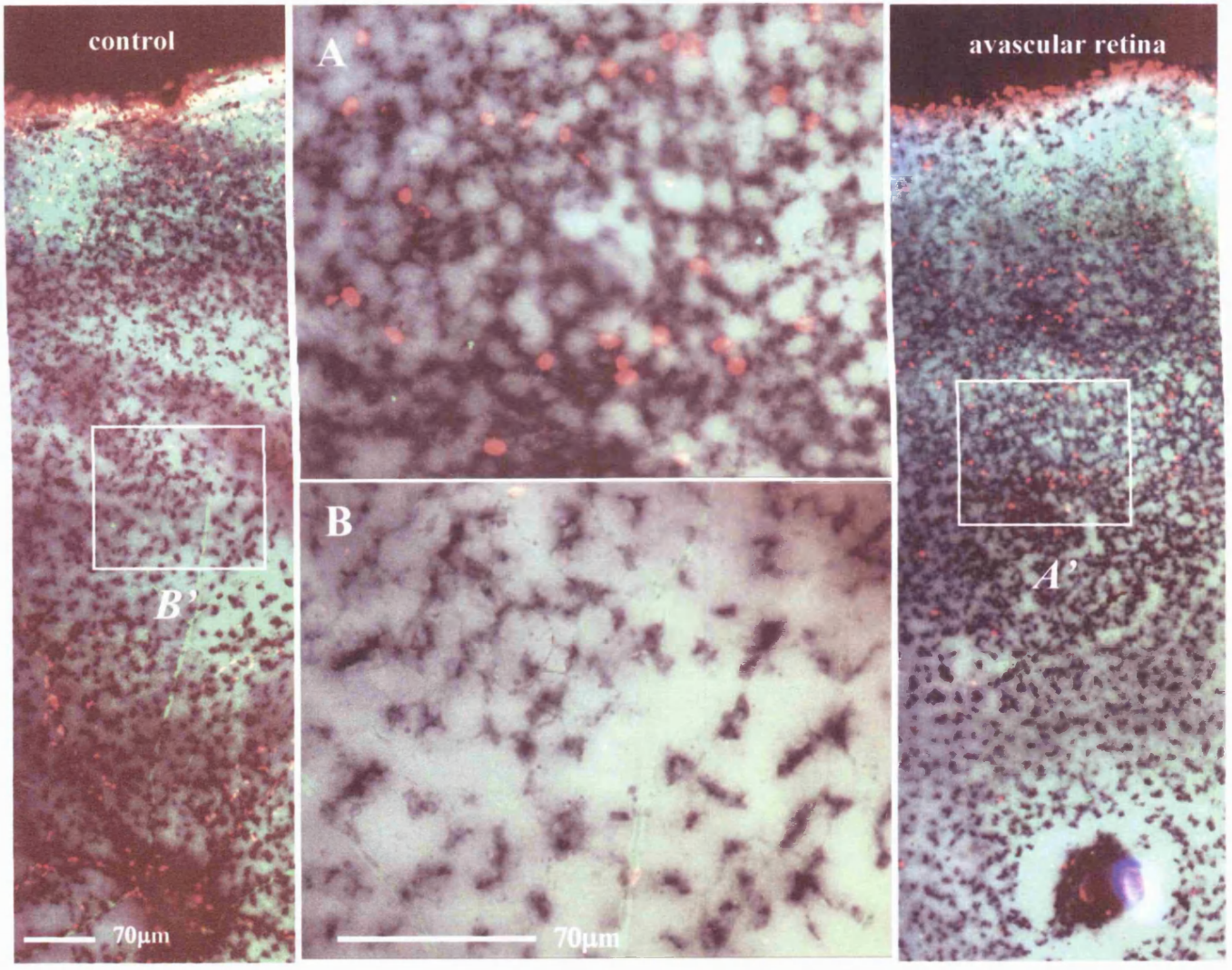
control
A
avascular retina
B'
B
A'
70µm
70µm
PDGFRα BrdU Collagen IV

high levels of *VEGF* mRNA whereas retinal astrocytes exposed to normoxia down-regulate *VEGF* mRNA. As expected I found *VEGF* mRNA expressed strongly across much of the avascular regions compared to low expression in vascularised retinas of control mice (Fig 4.5A/B). The number of BrdU labelled retinal astrocytes was greater and spread over a larger area in hyperoxia-treated retinae compared to normoxia controls. BrdU labelled cells in the control group did not co-localise with *PDGFRα* mRNA and their association with collagen IV suggested that these were endothelial cells rather than astrocytes.

A dissociation assay was performed in order to distinguish between endothelial cells and retinal astrocytes more reliably. The retinae from a litter of 8 pups were dissected out from control and from hyperoxic-treated animals, and astrocyte proliferation quantified (Fig 4.5C). The results in the graph show a four fold increase from a small baseline, in the number of BrdU labelled astrocytes in hyperoxic-treated retinae It was noticeable that in the wholemount analysis not all individual pups had been affected equally severely. In some pups the vasculature was still partially present, reducing the observable effects in retinal astrocyte proliferation.

Fig 4.5 **A correlation between areas of *VEGF* up-regulation and areas of astrocyte proliferation, after manipulation of the developing vasculature.** Newborn pups were kept in hyperoxic (80%) oxygen or atmospheric oxygen until P8. Pups were then pulse labelled with BrdU. Wholemount retina were stained by in situ hybridisation against *VEGF* and immunostained for BrdU and collagen IV. The far right panel shows a control retina with fully developed collagen IV^+ vasculature. The boxed area ***A'*** is shown at higher power in **(A)**. Here, the $BrdU^+$ cells visible are collagen IV^+ endothelial cells. The far left panel shows an avascular retina from an animal kept at 80% oxygen. *VEGF* is strongly expressed across this retina in contrast to the control, and many $BrdU^+$ cells can be seen. The boxed area ***B'*** can be seen at higher magnification in **(B)** showing double labelled $BrdU^+$, $VEGF^+$ cells. **(C)** Pups from control and hyperoxic-treated pups were given a BrdU pulse. After 2 hours, retinae were dissected, dissociated and plated overnight in medium containing 10% fetal calf serum. The BrdU labelling index of retinal astrocytes was then calculated. In the avascular 'hypoxic' retinae, the labelling index for retinal astrocytes was higher than in control animals.

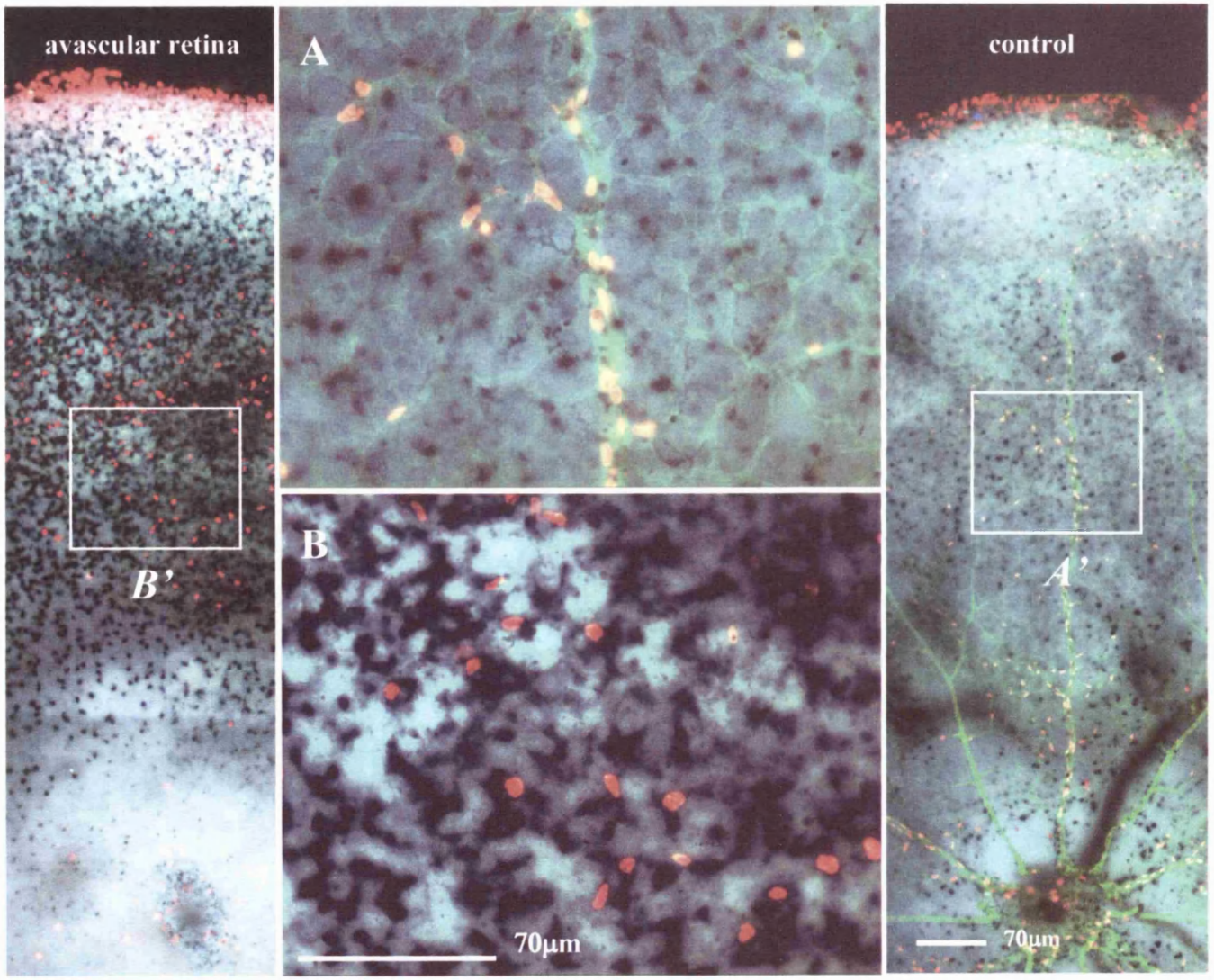

PDGFRα BrdU Collagen IV

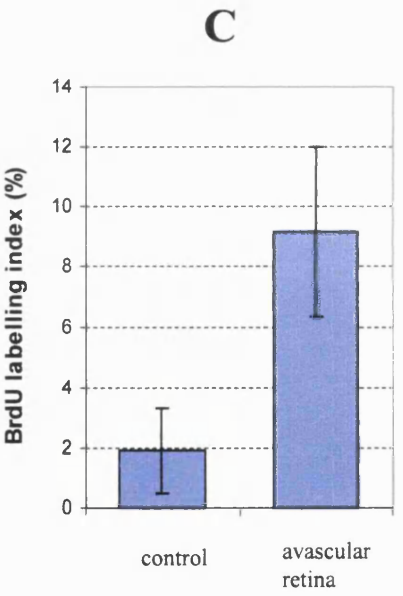

4.2.3 Retinal astrocyte proliferation correlates with *VEGF* expression independently of the presence or absence of vasculature

Although wholemount analysis of *VEGF* mRNA distribution revealed that hyperoxia treatment resulted in most retinal astrocyte expressing *VEGF* mRNA, I also observed a small area around the optic disc where retinal astrocytes did not express *VEGF* mRNA (Fig 4.5 left panel). This suggests that the area around the optic disc did not become hypoxic even though no retinal vessels could be seen. What could cause this area of relative normoxia despite lack of retinal vasculature? Studies on the retinal vasculature by Fruttiger (unpublished) led to the suggestion that this area remains normoxic because of the supply of oxygen from the large central hyaloid artery, which can diffuse through the vessel wall and reach cells in the immediate vicinity of this artery. Consistent with the idea that oxygen levels – as reflected by *VEGF* expression– are affecting astrocyte proliferation, astrocytes in this normoxic area were not proliferating (Fig 4.5 left panel). Furthermore, the *PDGFRα* mRNA staining was less dense around the optic disc, suggesting a reduced number of astrocytes developing in this area (Fig 4.4 right panel). In summary, this data suggests that the increasing oxygen levels brought by the developing vasculature lead to a reduction in retinal astrocyte proliferation and may induce differentiation.

4.2.4 Regulation of *GFAP* mRNA under hyperoxic conditions

As described in chapter 3, *GFAP* levels may give some indication about the differentiation of retinal astrocytes. Marcus Fruttiger (unpublished observations) has shown that under hyperoxic condtions, *GFAP* is up-regulated in the normoxic regions surrounding the central hyaloid artery. This contrasts to the low *GFAP* expression elsewhere in the retina. Again, this decrease in *GFAP* expression does not occur because retinal astrocytes are degenerating, since *PDGFRα*$^+$ cells remain throughout the retina (Fig 4.4 and Fig 4.6). These results are consistent with increasing oxygen levels brought by the developing vasculature leading to retinal astrocyte differentiation.

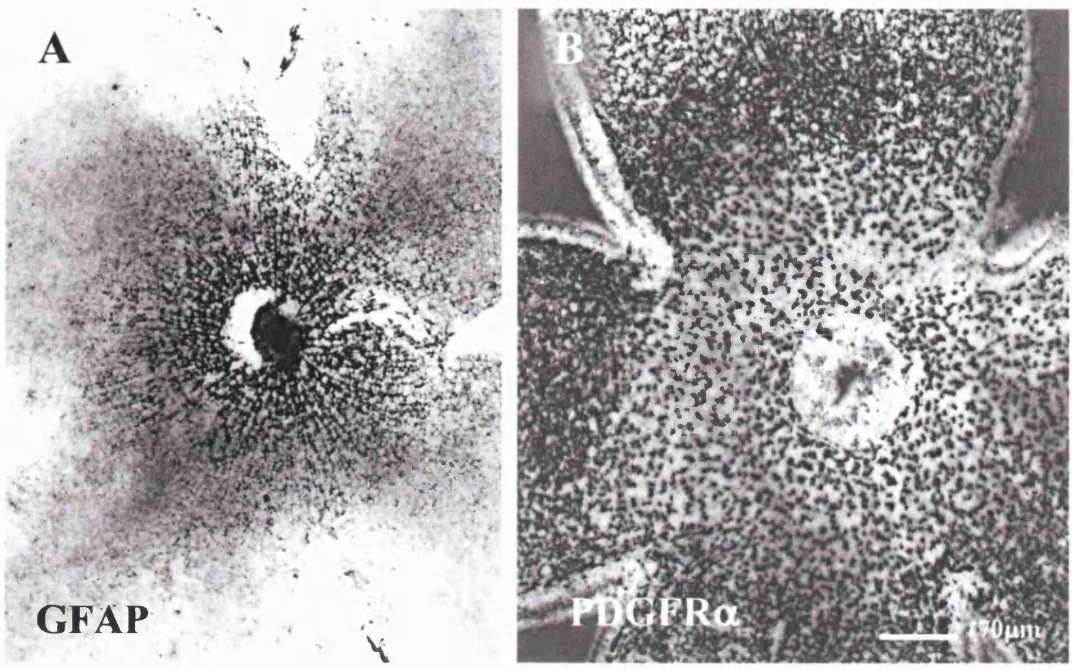

Fig 4.6 **GFAP mRNA expression in the retina under hyperoxic conditions.** Newborn pups were kept in hyperoxic (80% oxygen) conditions or in atmospheric air until P8. Retina were then dissected and wholemount preparations stained by in situ hybridisation with a probe against GFAP mRNA or PDGFRα mRNA. **(A)** GFAP mRNA is strongly expressed in the centre of the retina but is expressed at low levels elsewhere. **(B)** PDGFRα is expressed across the inner surface of the retina, showing that retinal astrocytes survive the hyperoxic treatment.

4.3 Discussion

4.3.1 *VEGF* expression in the retina in response to hypoxia

VEGF expression by astrocytes is known to be regulated by oxygen levels (Stone et al., 1996). Such a mechanism has also been demonstrated in cell culture systems (Aiello et al., 1995; Stone et al., 1995), clinical tumour specimens (Shweiki et al., 1992) and in several animal model systems. In the cat retina for example, exposure to hyperoxia down-regulates *VEGF* expression across the inner surface (where astrocytes reside). Consistent with the data in mouse shown here, maximal *VEGF* expression in the cat is seen towards the edge of the vasculature and at the periphery, with low expression in vascularised areas.

4.3.2 Use of hyperoxic conditions to manipulate the retinal vasculature

In the retina, it is possible unlike other areas of the CNS to create hypoxia by exposing animals to oxygen-enriched atmospheres. In other areas, autoregulation by adjacent vessels prevents obliteration of vessels during hyperoxia and any consequent proliferative vasculopathy (Chan-Ling et al., 1992). In the retina, the nearby choroidal circulation fails to autoregulate in the absence of the retinal vasculature and the inner surface becomes hypoxic.

In a previous study by Stone et al (Stone et al., 1996), cats were exposed to four days of hyperoxia and then for varying amounts of time to normoxia, in order to test how V EGF and astrocytes are involved in the pathogenesis of retinopathy of prematurity. Hyperoxia led to inhibition of vessel growth and upon return to the lower oxygen concentration in room air, a relative hypoxia developed in the inner retina due to lack of blood vessels. *VEGF* was strongly upregulated upon return to room air causing a subsequent pathological hyperproliferation of the vasculature. Once vascularised the oxygen brought by the newly grown vessels down-regulated *VEGF* expression again.

One discrepancy between this study and my observations presented here is the degeneration of astrocytes described by Stone et al (Stone et al 1996). In contrast, I was able to see astrocytes after hyperoxic-treatment, by using *PDGFRα* as a marker for retinal astrocytes. Stone et al propose that because of a lack of GFAP staining, that these cells may have degenerated. I propose that the majority of astrocytes survive but the hyperoxia-treatment down-regulates *GFAP*. This is consistent with other studies (Fruttiger et al., 2000; Chu et al., 2001) suggesting that less mature retinal astrocytes which have not yet associated with blood vessels, express lower levels of *GFAP*.

Pierce et al (Pierce et al., 1995) show a similar response of retinal cells to relative hypoxia. P7 mice were exposed to 75% oxygen for 5 days (i.e 5 days of hyperoxia) and then retuned to room air at P12. 12 hours after returning to room air, *VEGF* triples in quantity and then gradually declines again over the next few days. In this study, expression is seen in the inner nuclear layer. It is proposed that Muller cells whose

nuclei reside here, are the hypoxia sensors in the middle layers of the retina and secrete VEGF in response. *VEGF* is expressed normally after P7 in these inner nuclear layers.

Is HIF involved in the upregulation of *VEGF* seen in the retina? Ozaki et al (Ozaki et al., 1999) have looked at *VEGF* and HIF-1α during normal development and under hyperoxia treatment at P7. Lysates of mouse retina were analysed for HIF expression, so no spatial information was obtained for analysing normal development. These authors report low expression at P0, a sharp rise at P4 and then a decline to intermediate levels by adulthood. Under hyperoxic treatment, *VEGF* expression correlated with HIF-1α levels. So, although it is unclear if *VEGF* and HIF-1α are involved in oxygen sensing during normal development, they appear part of the response induced by experimental hyperoxia.

4.3.3 Does hypoxia regulate retinal astrocyte proliferation?

In this chapter, *VEGF* mRNA expression was found to correlate with retinal astrocyte proliferation. This data suggests that retinal astrocyte s where they are proliferating most are experiencing relative hypoxia. But is low oxygen itself a developmental cue or are some other properties of the vasculature influencing astrocytes?

It is possible that endothelial cells express a factor – cell bound or soluble – which induces a slow down in retinal astrocyte proliferation and differentiation. In vivo observations in chapter 3 are unable to distinguish between this possibility and the possibility that oxygen concentration regulates astrocytes. Und er hyperoxic conditions,

the area around the optic disc is endothelial cell free but normoxic. This could mean that oxygen concentration affects retinal astrocyte proliferation or that a long -range diffusible factor from endothelial cells of the central h yaloid artery affects them. An in vitro system is used to distinguish these two possibilities in the next chapter.

Chapter 5. A culture system for investigating controls on retinal astrocyte proliferation

5.1 Introduction

In Chapter 3 I demonstrated that control on proliferation can limit cell numbers in a growing population of retinal astrocytes during development. I also showed that areas of high astrocyte proliferation correlate with retinal regions not yet vascularised, and propose a model whereby the vasculature is leading to differentiation of astrocytes.
In order to study the factors that regulate retinal astrocyte proliferation and differentiation in more detail, I developed a retinal astrocyte culture system. Culturing of astrocytes allows direct manipulation of the culture conditions surrounding these cells. In Chapter 3 I suggested two possibilities for how the vasculature may affect astrocyte differentiation:-

1) direct interactions between endothelial cells and retinal astrocytes
2) an effect mediated via oxygen levels.

In this chapter, I test these two ideas in a culture system. I investigate whether endothelial cells influence astrocyte proliferation by co-culturing these cells. To test the effect of oxygen on astrocyte proliferation I cultured dissociated retinae at different levels of oxygen. At low levels of oxygen (1.5% oxygen), astrocytes maintained high rates of proliferation compared to a sharp decline in proliferation seen in cultures at

higher oxygen concentrations (20% oxygen). From these experiments, I suggest that levels of oxygen rather than presence of endothelial cells themselves influence astrocyte proliferation in vitro.

5.2 Results

5.2.1 Proliferation rates of P1 and P7 retinal astrocytes in vitro are similar to those seen in vivo

To characterise astrocytes in culture, P1 and P7 retina were dissociated and plated in culture dishes. After 3 days, cells were fixed and immunostained against GFAP, collagen IV and neurofilament, demonstrating the presence of astrocytes, endothelial cells and neurons respectively (Fig 5.1A). All these cell types were detected at both ages, although more retinal astrocytes, endothelial cells and neurons were apparent at P7 compared to P1.

The level of proliferation in P1 and P7 cultures was compared after 24 hours in culture (Fig 5.1B). In order to monitor levels of proliferation, BrdU was added to the culture medium 2 hours before cells were fixed. This analysis revealed a higher rate of proliferation in P1 retinal astrocytes (approximately 30% BrdU labelling index) compared to P7 cells (less than 5% labelling index), reflecting the situation seen in vivo. In chapter 3, I demonstrated that astrocyte proliferation declined from its highest postnatal level at P0, to less than 5% at P7. Hence, after 24 hours, cells in this culture system retain the differences in proliferation rate seen in vivo.

It must be noted however, that the recovery of cells after dissociation was not calculated in this study. The recovery of P1 and P7 cells could potentially be different, making comparisons between the two cell populations more difficult. Nevertheless, more P7 cells were found and at lower rates of proliferation than P1 cells, similar to the findings in vivo.

Fig 5.1 **Characterising retinal astrocyte in culture.** **(A)** P1 and P7 wild type retina were dissociated and plated in 24 well plates in medium containing 10% fetal calf serum. Cultures were left 72 hours and then immunostained for GFAP $^{+}$ astrocytes, collagen IV^{+} enodothelial cells and neurofilament^{+} neurons. **(B)** After 24 in culture, BrdU was added and 2 hours later, cells were fixed. Cells were then stained by immunofluorescence for GFAP and BrdU. GFAP^{+} BrdU^{+} double positive cells were counted as a proportion of the total GFAP^{+} astrocyte population (BrdU labelling index) Each bar represents the mean $^{+}$/- standard deviation of cultured cells in triplicate taken at each time point. **(C)** cells were grown in medium containing 10ng/ml PDGF-A and increasing amounts of fetal calf serum (FCS). The BrdU labelling index is less than 5% in medium containing 0.5% serum. PDGF-A is able to stimulate retinal astrocyte proliferation but only in the presence of sufficient quantities of serum (greater than 0.5% serum). The labelling index is not increased further in 20% FCS medium compared to 10% FCS. **(D)** P1 cells were grown in 10% FCS, boiled 10% FCS and dialysed 10% FCS. A BrdU pulse was given after 24 hours to compare rates of proliferation under these different conditions. Dialysing serum did not prevent its mitogenic affect on retinal astrocytes, whereas boiling serum abolished this affect. **(E)** shows that the morphology and survival of retinal astrocytes appeared to be unaffected in the presence of low levels of serum or boiled serum.

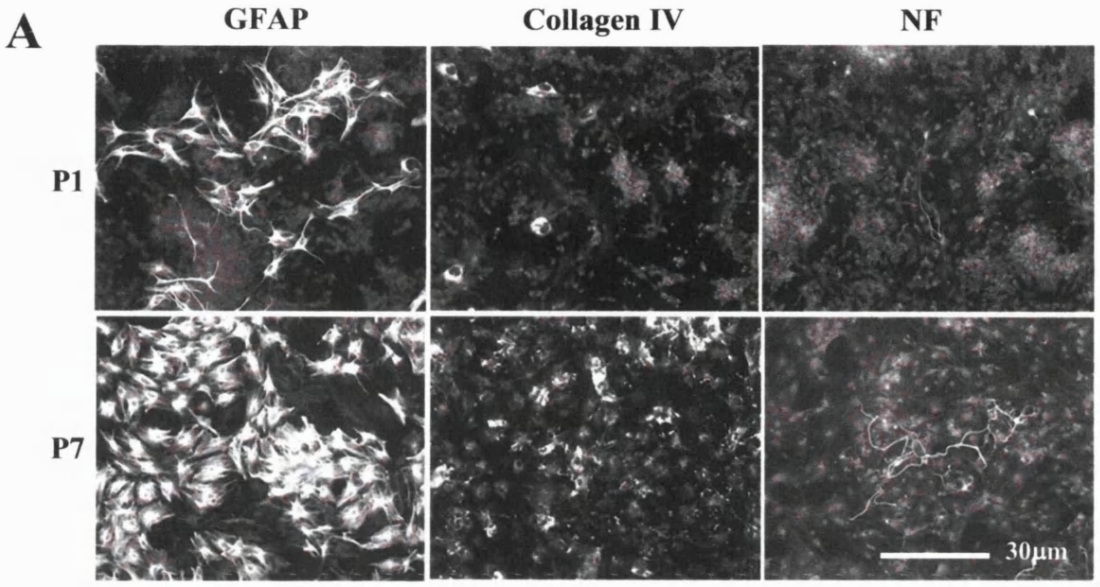
A
GFAP
Collagen IV
NF
P1
P7
30µm

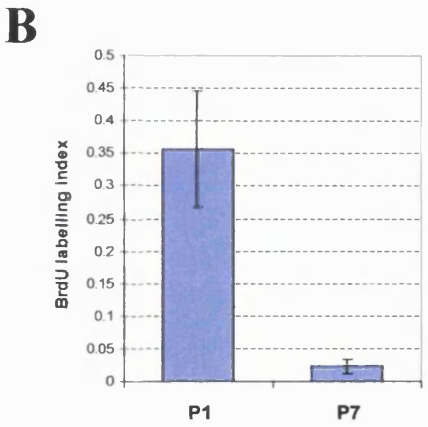
B
BrdU labelling Index
0.5
0.45
0.4
0.35
0.3
0.25
0.2
0.15
0.1
0.05
0
P1
P7

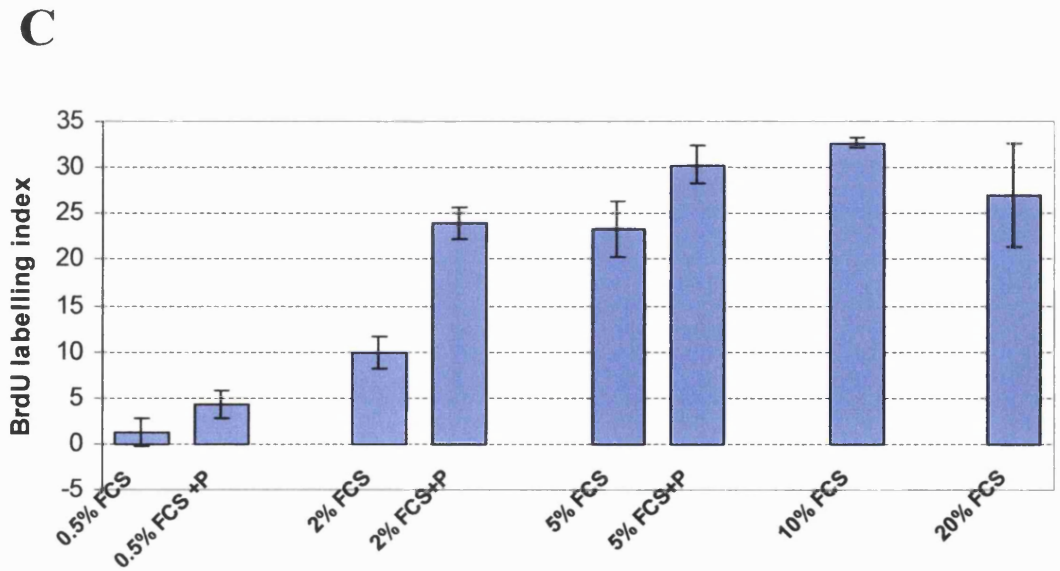
C
BrdU labelling index
35
30
25
20
15
10
5
0
-5
0.5% FCS
0.5% FCS +P
2% FCS
2% FCS+P
5% FCS
5% FCS+P
10% FCS
20% FCS

D

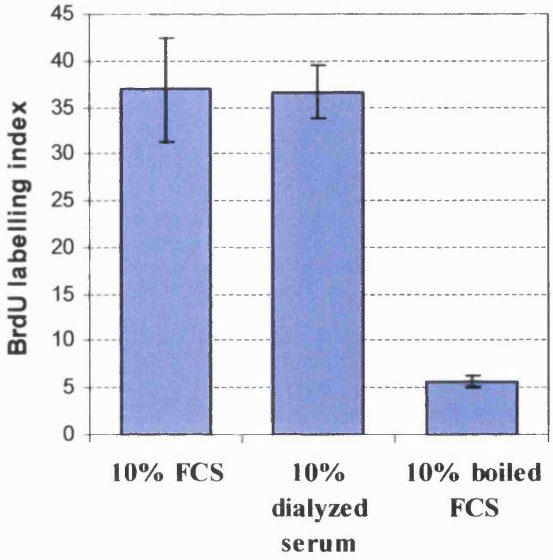
BrdU labelling index
45
40
35
30
25
20
15
10
5
0
10% FCS
10% dialyzed serum
10% boiled FCS

E

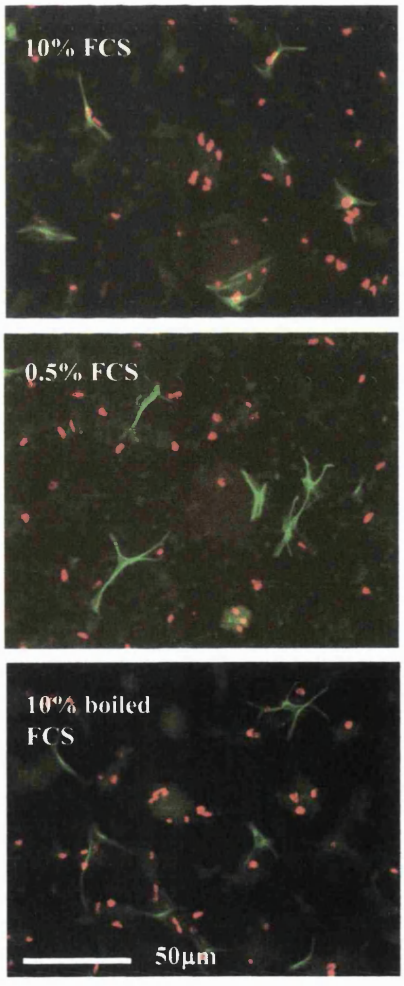
10% FCS
0.5% FCS
10% boiled FCS
50µm

5.2.2 Limitations of a pulse BrdU label to analyse cell proliferation

The rates of proliferation of P1 retinal astrocytes appears to decrease over 72 hours, as previously described. However the analysis of proliferation by a pulse BrdU label is limited. It is not possible to tell in this situation whether the proliferation of a sub-population of cells has decreased or whether proliferation of the whole population has decreased. In order to distinguish these two possibilities, a cumulative BrdU label can be used.

A cumulative analysis has also been performed on cultured retinal astrocytes and involved exposing cells to BrdU for increased periods of time until all cells are labelled (Fig 5.2E). A cumulative analysis of P1 cells showed that after 48 hours, approximately 100% of the cells are labelled with BrdU. This suggests that the whole population rather than just a sub-population is being analysed. On the contrary, after 100 hours only 40% P7 cells can be labelled, suggesting that only a sub-population of cells are undergoing proliferation (Fig 5.2E). This interpretation is consistent with the wholemount analysis showing a sub-population of cells at the periphery of the retina proliferating at P7, in contrast to the BrdU labelling across the entire retinal astrocyte network at P1 (see Fig 3.8, 3.9 and 3.10).

Having established from a cumulative label that most of the retinal astrocyte population are proliferating, I used a pulse label in subsquent experiments to analyse changes in proliferation rate of the cell population. It has not been tested however, whether a sub-population rather than the whole population, subsequently stops proliferating.

5.2.3 PDGF-A and another serum component/s stimulates retinal astrocyte proliferation in vitro

The analysis in Fig 5.1B was carried out on cells cultured in 10% fetal calf serum (10% FCS). However, if P1 cells were cultured at 0.5% FCS, the BrdU labelling index was severely reduced to less than 5% (Fig 5.1C). $GFAP^+$ Retinal astrocytes were still present in these cultures but were proliferating little (Fig 5.1E). This suggests that some mitogen within serum is necessary for retinal astrocyte proliferation. The effect of a range of serum concentrations from 0.5% to 20% FCS was also analysed (Fig 5.1C). The labelling index steadily increased with increasing amounts of FCS up to 10% FCS. At 20% FCS, rates of proliferation did not appear to increase further. This suggests that proliferation is saturated between 5 and 10% FCS.

Since PDGF-A has been shown to act as a mitogen for retinal astrocytes in vivo, its role in vitro was analysed here. When 10ng/ml PDGF-A was added to cells in 0.5% FCS, the BrdU labelling index remained low. PDGF-A was then added to medium at a range of different serum concentrations (0.5% to 20% FCS). At 2% and 5% FCS the addition of PDGF-A stimulated retinal astrocyte proliferation. This response to PDGF-A is consistent with the in vivo data suggesting that PDGF-A stimulates astrocyte proliferation.

Clearly, PDGF-A alone is insufficient for astrocyte proliferation in vitro, because at low levels of serum, PDGF-A is unable to stimulate proliferation. Some other component/components of serum are necessary for retinal astrocyte proliferation in vitro.

To investigate the nature of this mitogenic factor in serum, serum was dialysed through a 12kDa membrane to remove low molecular weight molecules that are freely diffusible through the membrane. This treatment did not affect the mitogenic effect of FCS suggesting the mitogen may be a larger molecule such as a protein or a small molecule bound to a protein (Fig 5.1D). To denature the protein components of serum, it was boiled. When grown in boiled serum, retinal astrocytes were present in the culture but proliferated little (Fig 5.1E). Since this treatment abolished the mitogenic ability of serum on retinal astrocytes, it is likely that the mitogen in question is a protein growth factor.

Having established that PDGF-A alone is not sufficient for retinal astrocyte proliferation and has no additional effect at 10% serum (data not shown), all following experiments have been carried out in 10% serum.

5.2.4 The rate of proliferation of P1 retinal astrocytes declines during the first three days in culture

In order to investigate rates of retinal astrocyte proliferation at these different time points, P1 and P7 retina were dissociated and the retinal cells plated simultaneously. A 2-hour BrdU pulse was given after 24, 48 and 72 hours in culture to monitor levels of

proliferation. Levels of retinal astrocyte proliferation in P1 cultures declined from an initial high level (approximately 30% labelling index) seen at 24 hours in culture. By 72 hours, the labelling index had declined to less than 5% (Fig 5.2A). After this time P1 retinal astrocyte proliferation remained low (data not shown). P7 retinal astrocytes showed a very different behaviour. Their proliferation rate was low in comparison (1 to 12% BrdU labelling index) and remained so after 72 hours (Fig 5.2B).

The behaviour of P1 retinal astrocytes also contrasted with another P1 retinal cell type – endothelial cells. Cells were immunostained for either GFAP or collagen IV and the BrdU labelling index was compared. The BrdU labelling index of collagen IV^+ endothelial cells remained constant at a low rate, at the time points tested (Fig 5.2C and Fig 5.2D).

It is possible that the observed decline in proliferation of retinal astrocytes could be due to changes in GFAP expression that changed the numbers of retinal astrocytes identified. To address this, another marker for astrocytes -Pax-2 – (Chu et al 2001) was used to identify retinal astrocytes. The suitability of this marker was initially tested and it was found that an antibody against Pax-2 co-expressed with GFAP approximately 98% after 24 hours and 100% after 72 hours (Fig 5.3A). This established Pax-2 as a suitable retinal astrocyte marker. The BrdU labelling index was then measured over time using Pax-2 as an astrocyte marker. Using the anti-Pax-2 antibody, a similar decline in P1 retinal astrocyte proliferation was seen as with the anti-GFAP antibody (Fig 5.3B). This confirms that changes in proliferation were not due to changes in GFAP expression.

Fig 5.2 **Retinal astrocyte proliferation steadily declines after three days in culture.** **(A)** Culture cells were pulse labelled with BrdU for 2 hours after 24, 48 and 72 hours in culture. **(B)** P1 and P7 cells were plated simultaneously and the labelling index compared after 24, 48 and 72 hours, as in (A). Each point represents the mean +/- s.d number of retinal astrocytes in triplicate samples at each time point. **(C)** P1 cultures were immunostained for both GFAP and collagen IV to compare the BrdU labelling index between retinal astrocytes and endothelial cells. $GFAP^+$ retinal astrocyte proliferation declines from an initially high level (>30% labelling index) whereas, collagen IV^+ endothelial cell proliferation remains at a constant low level (<10% labelling index). **(D)** shows a collagen IV^+ endothelial cell after 24 hours and a collagen IV^+ $BrdU^+$ cell after 72 hours in culture. **(E)** shows a cumulative BrdU label performed on P1 and P7 cells. Cells were incubated in BrdU at the time of plating and labelling was analysed at 24, 48 and 72 hours afterwards. After plotting this data on a graph, the S-phase time of P1 cells was calculated using the equations shown.

A

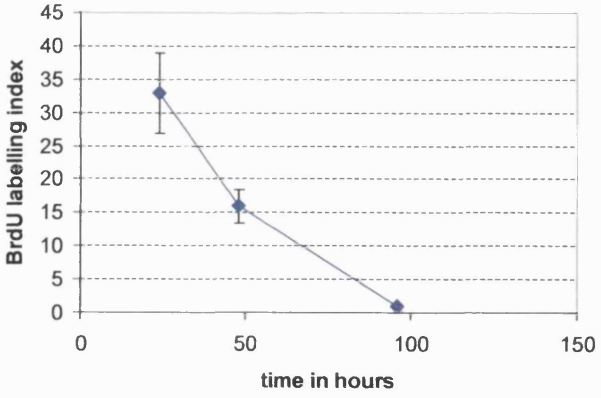
BrdU labelling index
45
40
35
30
25
20
15
10
5
0
0
50
100
150
time in hours

B

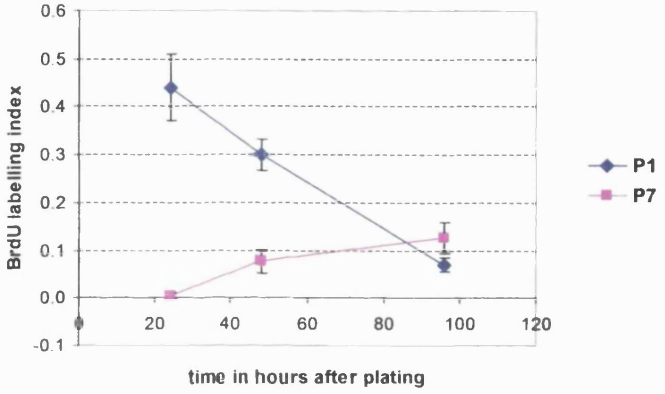
BrdU labelling index
0.6
0.5
0.4
0.3
0.2
0.1
0.0
-0.1
0
20
40
60
80
100
120
time in hours after plating
P1
P7

C

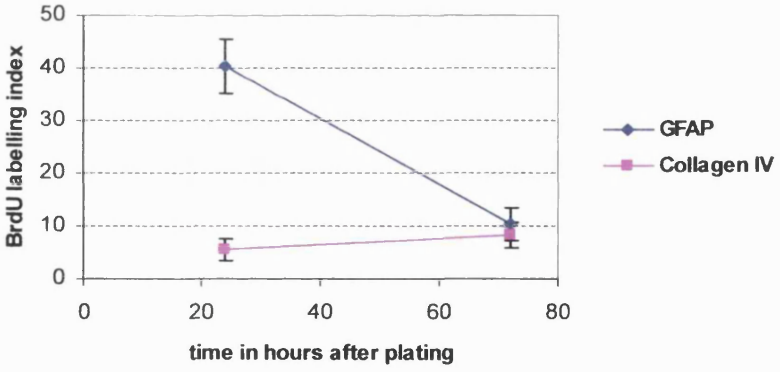
BrdU labelling index
50
40
30
20
10
0
0
20
40
60
80
time in hours after plating
GFAP
Collagen IV

D

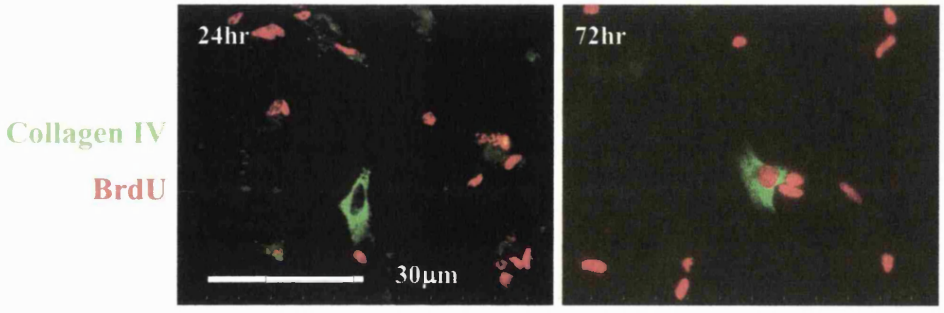
Collagen IV
BrdU
24hr
30µm
72hr

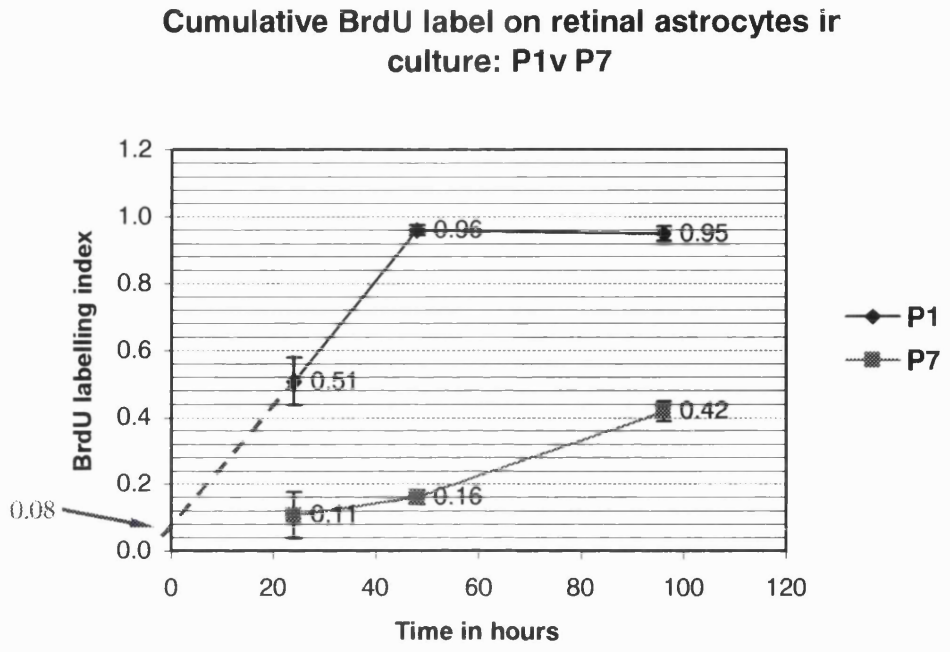

Figure 5.2E. The above graph shows labelling index plotted against time (t), for a cumulative BrdU label on P1 and P7 retinal astrocytes in culture. This gives a straight line that plateaus when all cells are labelled (Labelling index, Ll = 1). The S phase time can be calculated from this graph, as shown below.

If m=gradient and i=intercept then:-

Ll = mt + I

When t=0, Ll= Ts/Tc (where Ts=S phase time and Tc=cell cycle time):-

Ll = i = Ts/Tc

When Ll=1, t=Tc-Ts:-

1 = m(Tc-Ts) + Ts/Tc

m = (1-Ts/Tc)/(Tc-Ts)
= 1/Tc

Hence, after a cumulative label, cell cycle time can be calculated by **Tc=1/m** and S phase time by **Ts=i/m**. Estimating from the graph above for P1 data, i= Ts/Tc= 0.08 at time= 0, and m= 0.45/24= 0.01875. Therefore Ts=i/m=0.08/0.01875= **4.3 hours**.
Tc=1/m=1/0.01875= **53 hours.**

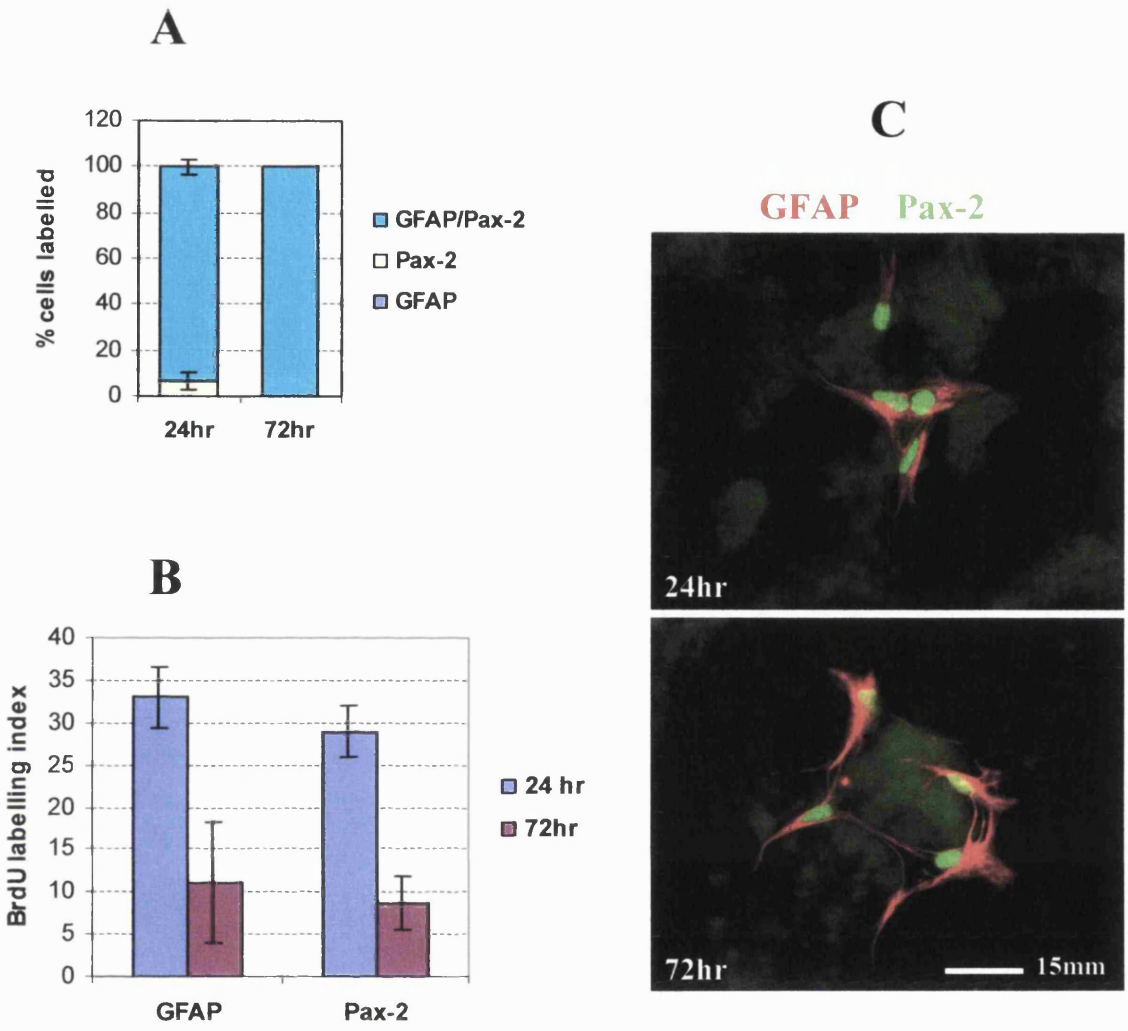

Fig 5.3 **Comparison of two markers for astrocytes: GFAP and Pax-2.** Cells were pulsed with BrdU after 24 hr and 72 hr in culture and then immunostained for GFAP, Pax-2 and BrdU. **(A)** most GFAP$^+$ labelled cells were Pax-2$^+$ and visa versa after 24 hr and 72 hours in culture. **(B)** proliferation of Pax-2 and GFAP labelled cells was compared, yielding similar results. **(C)** Antibodies against Pax-2 (green) and GFAP (red) labelled the same cells in this high power image. Pax-2 is found in the nucleus whereas GFAP is cytoplasmic.

5.2.5 P1 retinal astrocytes proliferate at a higher rate than P7 retinal astrocytes in vitro

To test if secreted factors from other retinal cells, could play a role in determining the proliferative rates of P7 or P1 cells, P1/P7 co-cultures were performed. The two cell populations were separated by membrane inserts in the culture dish. After 24 and 48 hours, the BrdU labelling index was analysed (Fig 5.4). This demonstrated that neither cell population appeared to affect the proliferation rate of the other. The presence of P1 cells didn't accelerate the proliferation rate of P7 cells and P7 cells didn't slow the proliferation of P1 cells.

This suggests that at least no long-range paracrine factor is acting to influence proliferation of retinal astrocytes. It does not discount the possibility that another short-range secreted or membrane bound factor could be involved. Therefore, P1 and P7 retinal astrocytes could either be intrinsically different in their proliferation rates, or could be responding to a short-range factor released by another cell type in the culture.

5.2.6 Co-culture of P1 retinal astrocytes with HUVECs show no effect of HUVECs on astrocyte proliferation

In Chapter 3, I described how retinal astrocyte proliferation correlated with those areas not yet vascularised. What properties of the vasculature could therefore affect the rate of

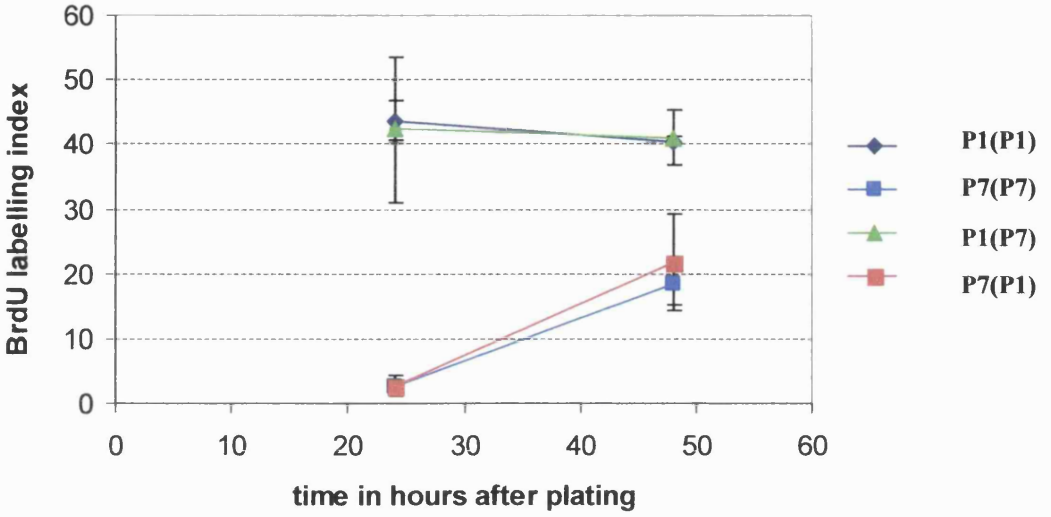

Fig 5.4 **P1 and P7 proliferate at different rates in culture: testing if these different aged cells can affect the proliferation rates of each other.** P1 and P7 cells were co-cultured in 24 well plates, separated by a 0.4μm pore size membrane. P1 cells were plated at the bottom of the well with P7 cells placed on the membrane insert above (and visa versa). Cells on the bottom of the plate were then analysed for BrdU incorporation after 24 and 48 hours. Neither age cell population appeared to affect the proliferation rate of the other cell population.

retinal astrocyte proliferation? In this section I test out two possibilities in the culture system: that the presence of endothelial cells has some anti-proliferative effect on astrocytes, or that lower levels of oxygen in the absence of vasculature, affect proliferation.

Could these factors explain the decline of P1 retinal astrocyte proliferation in culture? It is possible that P1 cells taken from an avascular, hypoxic retina stop proliferating in response to higher oxygen levels encountered in culture conditions. It is also possible that P1 cells taken from an avascular retina, decline in response to the presence of a growing number of endothelial cells.

In this section, I address the latter possibility that enodothelial cells may inhibit retinal astrocyte proliferation. P1 retinae contain some endothelial cells around the optic nerve disc but they are not in contact with most astrocytes already in the retina. In culture however, these endothelial cells are present in the P1 cultures, as seen by collagen IV staining. These cells proliferate in culture so could increasing numbers of endothelial cells affect the proliferation rate of astrocytes? At P7, endothelial cells are more numerous. If endothelial cells are affecting astrocyte proliferation, could this quantitative difference account for the decline in astrocyte proliferation?

To address whether endothelial cells are directly affecting astrocyte proliferation, co-cultures were performed between human umbilical vein endothelial cells (HUVEC) and P1 retinal cultures to see if they could enhance or reduce the decline seen in astrocyte

proliferation. Co-cultures were given a pulse of BrdU for two hours after 24 and 48 hours in culture. In these co-cultures, HUVECs can be seen quite clearly next to BrdU labelled astrocytes in the culture dish (Fig 5.5C/D), and do not seem to exert an effect on astrocyte proliferation when analysed quantitatively (Fig 5.5E).

5.2.7 Culture in 1.5% oxygen prevents a decline in astrocyte proliferation

As mentioned, P1 cells are taken from an avascular retina in which they experience relatively low levels of oxygen. The 20% oxygen levels in atmospheric air and in tissue culture incubators are unphysiologically high. Oxygen concentrations in vivo have been averaged at levels as low as 3% oxygen (Guyton and Hall 1996). Before an adequate vascular supply has developed, levels of oxygen may well be lower than this during development. It may be possible that 20% oxygen levels mimics arrival of the vasculature when retinal astrocytes are exposed to such levels.

To test directly if low levels of oxygen could effect the proliferation of astrocytes, P1 cells were cultured in an incubator maintained at 1.5% oxygen. A 2-hour BrdU pulse was given at 24-hour intervals to monitor astrocyte proliferation. In contrast to the decline seen at 20% oxygen, at 1.5% oxygen the decline in astrocyte proliferation was largely prevented. After 72 hours in 20% oxygen, the BrdU labelling index has declined to approximately 10%, whereas under 1.5% oxygen, levels persist at approximately 30% (Fig 5.6A).

Fig 5.5 **Co-culturing P1 retinal cells with a human endothelial cell line (HUVECs), did not affect the proliferation rate of retinal astrocytes.**

Dissociated P1 retinal cells were mixed with HUVEC cells before plating and then plated together in 10% FCS. Control cultures of either P1 cells or HUVECs alone were plated simultaneously. Cells were given a 2 hour BrdU pulse after 24 and 48 hours in culture and then fixed and immunostained for GFAP and BrdU. **(A)** shows a co-culture visualised after 24 hours under the light microscope. **(B)** shows HUVEC cells grown in 10% fetal calf serum after 24 hours in culture, viewed under the light microscope. HUVECs were identified by their granular nucleus. **(C)** show cultures visualised under the light microscope after 48 hours. **(D)** shows the same field of view as (C) but under a fluorescence microscope. A HUVEC (arrow) can be seen next to a proliferating retinal astrocyte (arrow head). **(E)** the BrdU labelling index was similar for retinal astrocytes grown in co-culture with or without HUVECs.

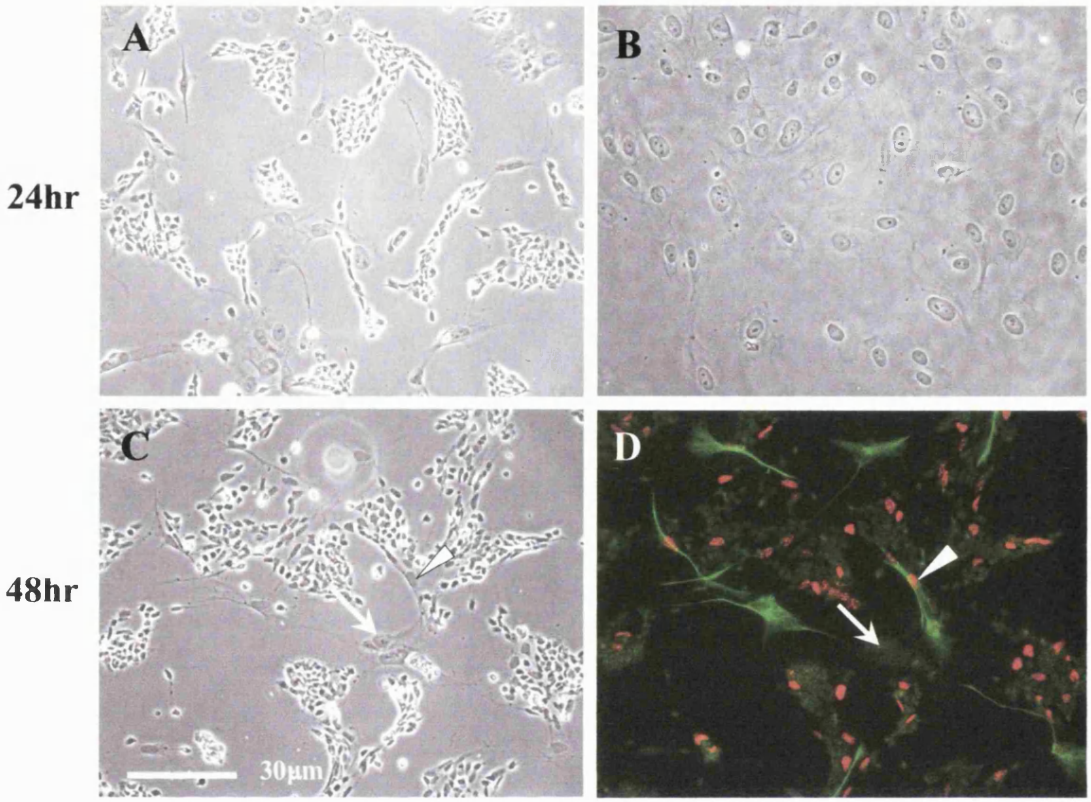
24hr
48hr
A
B
C
D
30µm

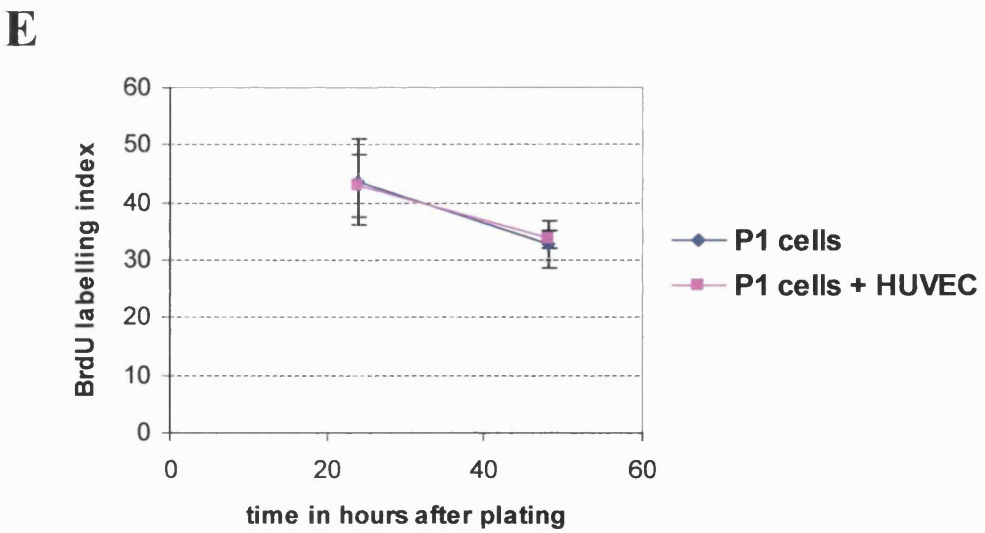
E
BrdU labelling index
60
50
40
30
20
10
0
0
20
40
60
time in hours after plating
P1 cells
P1 cells + HUVEC

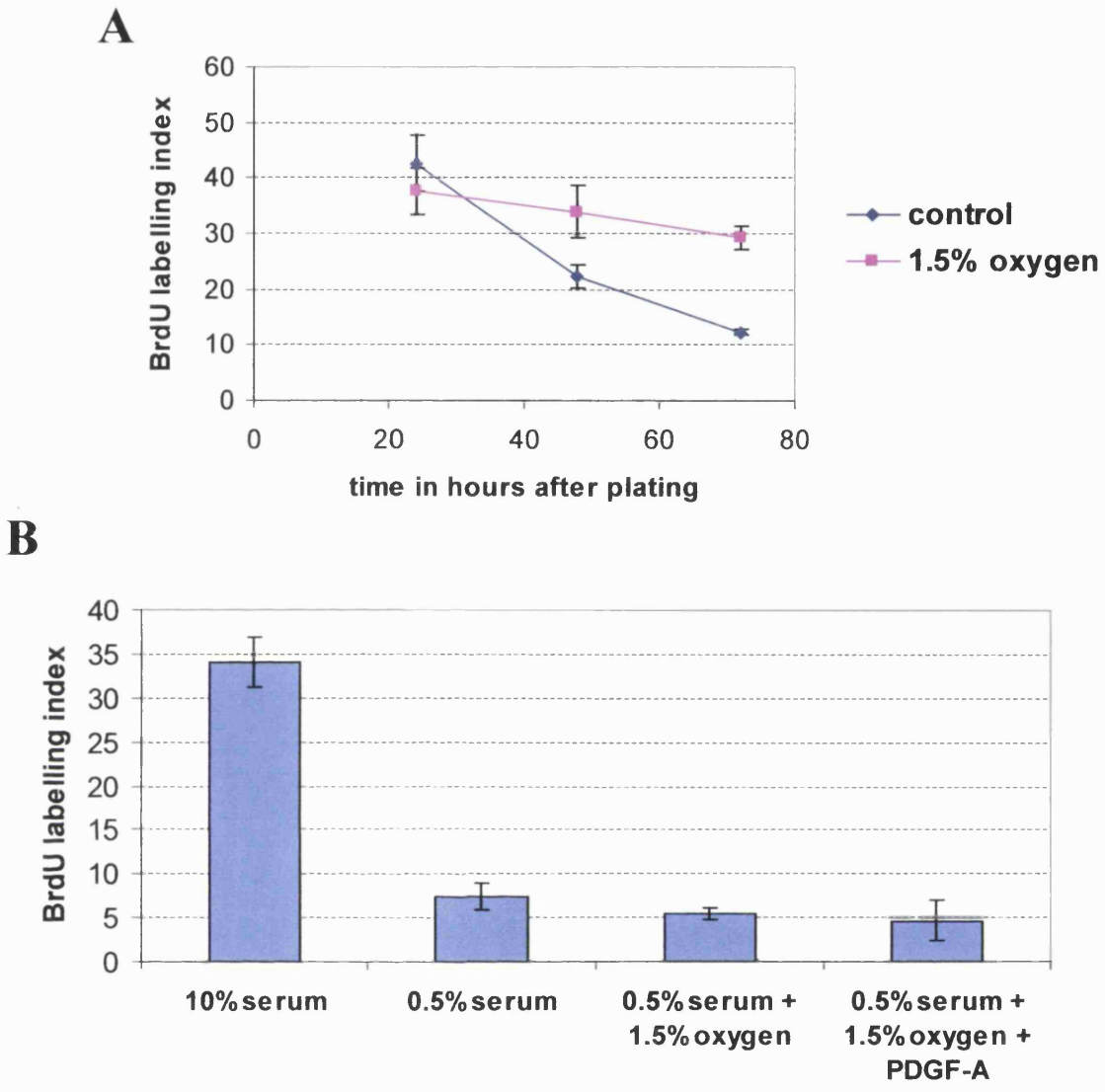

Fig 5.6 **A drop in the rate of retinal astrocyte proliferation is prevented if cells are grown at lower levels of oxygen.** P1 cells were dissociated, plated in 10% serum and kept at 20% oxygen or at 1.5% oxygen. The BrdU labelling index was calculated at 24 and 72 hours after plating. **(A)** shows that the drop in the labelling index seen at 20% oxygen is prevented to some extent in the culture grown at 1.5% oxygen **(B)** cultures were grown at low levels of oxygen (1.5%) in the presence of low serum (0.5%) and PDGF-A. Low oxygen was not sufficient to stimulate retinal astrocyte proliferation under these conditions.

Low levels of oxygen alone are not however sufficient for proliferation, serum factors are required too. For example, in low levels of serum (0.5%) proliferation is the same at 20% or at 1.5% oxygen. If 10ng/ml of PDGF-A is added on top of the low serum, low levels of oxygen can still not increase the proliferation level (Fig 5.6B). It appears therefore that low oxygen is permissive for high levels of proliferation but can't stimulate proliferation by itself.

When P7 cells were cultured in 1.5% oxygen, no increase in levels of proliferation were observed compared to controls at 20% oxygen. It appears therefore, that the response to oxygen is specific to P1 cells (data not shown).

How does oxygen affect retinal astrocyte proliferation? Could oxygen affect retinal astrocyte proliferation directly or are there other cells that sense oxygen concentrations and then secrete factors to promote retinal astrocyte proliferation? To test this, medium transfer experiments were performed. Medium was taken from cells grown 72 hours in 1.5% oxygen and transferred onto freshly isolated P1 cells to see if it could increase the rate of retinal astrocyte proliferation. The medium had no effect on proliferation of P1 cells, suggesting that hypoxia is either having a direct effect on astrocytes themselves or is leading to a short range paracrine interaction involving another retinal cell (Fig 5.7).

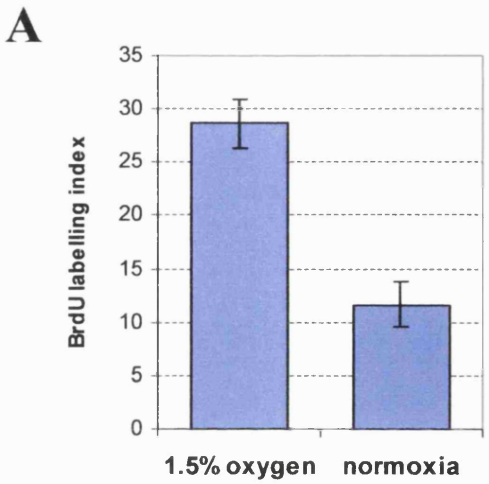

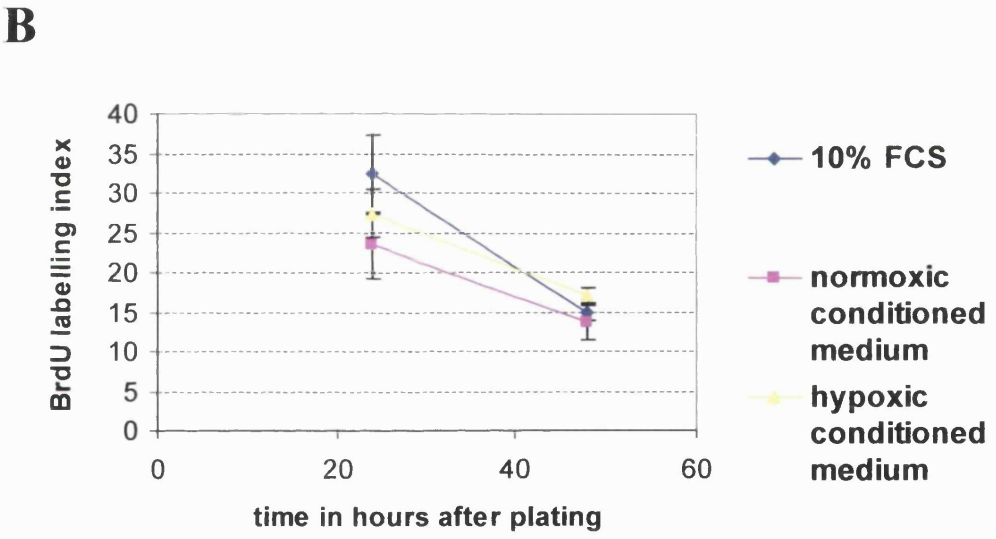

Fig 5.7 **The influence of low oxygen on astrocyte proliferation is not transferable via conditioned medium.** Cells were grown at 1.5% and 20% oxygen. The labelling index for these cells was calculated after 72 hours in culture **(A).** The medium from both cultures was then collected and transferred onto fresh P1 cells. There appeared to be no difference in the labelling index of cells grown in hypoxia or normoxia conditioned medium **(B).**

5.2.8 Does hypoxia prevent differentiation of astrocytes in culture?

The model proposed in Chapter 4 suggests that oxygen may lead to differentiation of astrocytes. This is based on results showing that retinal astrocyte proliferation is virtually zero in vascularised regions. The culture work above is consistent with this in terms of proliferation but are other processes affected also? In Chapter 3, I suggest that in vivo, retinal astrocytes in the peripheral areas of the retina, appear to be least m ature. This is indicated by their low-level *GFAP* expression, high proliferation and location in the least differentiated part of the developing retina. Since low oxygen can sustain high levels of retinal astrocyte proliferation in this in vitro system, c an it also affect *GFAP* levels directly, as suggested in vivo?

To detect differences of *GFAP* expression in culture, an in situ hybridisation was performed on culture cells to see if astrocytes that stopped proliferating, upregulated *GFAP* mRNA. Indeed, cells proliferating in low oxygen showed low-level expression of *GFAP* mRNA, whereas same-aged cultures grown in 20% oxygen showed very strong expression of *GFAP* mRNA (Fig 5.8).

VEGF mRNA expression was also analysed by in situ hybridisation in these cultures. Under 20% oxygen, no *VEGF* mRNA expression was detected, whereas under 1.5% oxygen, strong *VEGF* mRNA expression was detected in many cells in the culture dish

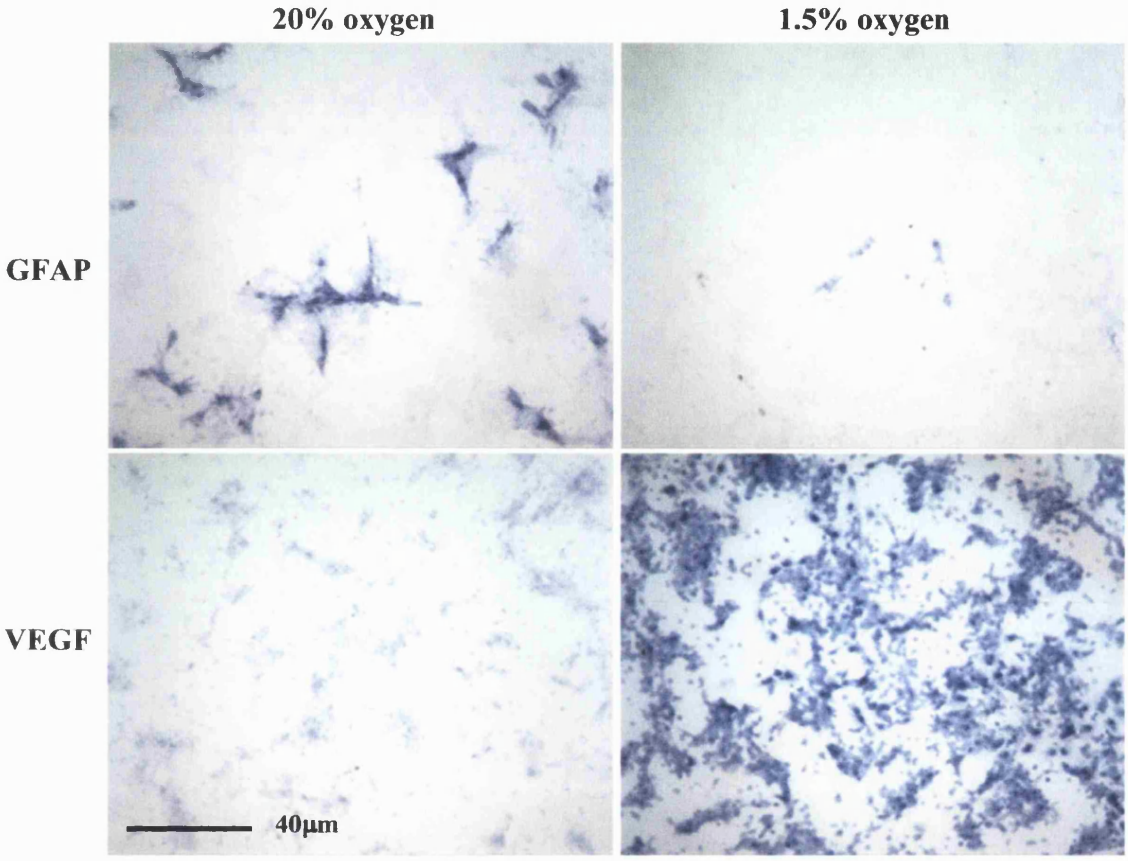

Fig 5.8 **Cells in cultures grown under 1.5% oxygen up-regulate VEGF but down-regulate GFAP.** Cells were plated at both 20% and 1.5% oxygen. After 72 hours, cells were fixed and stained by in situ hybridisation with a probe aginst GFAP mRNA or VEGF mRNA. Strong expression of GFAP mRNA is seen in cells grown at 20% oxygen but weak expression is seen in cells grown at 1.5% oxygen (top panels). VEGF mRNA normally up-regulated under hypoxia, is up-regulated in cells grown at 1.5% oxygen but is poorly expressed in cells grown at 20% oxygen.

(Fig 5.8). This demonstrates that cells in the retinal culture system respond to changes in oxygen concentration in a similar way to that observed in vivo.

5.2.9 Cobalt chloride does not mimic hypoxia in sustaining retinal astrocyte proliferation

Cobalt chloride has been found to up-regulate HIF-1α in culture cells and for this reason has been used to mimic the effect of hypoxia on HIF-1α stabilisation (see introduction). Does cobalt chloride mimic the effect of hypoxia on retinal astrocyte proliferation in this culture system? Cobalt chloride was added to P1 cultures at a range of concentrat ions. At 100μM a slightly lower than usual BrdU labelling index is apparent after 24 hours, suggesting a possible toxic effect at this concentration (Fig 5.9B). At lower concentrations however, cobalt chloride does not seem to have any affect on retinal astrocyte proliferation.

Despite this, an in situ hybridisation on P1 cells after 72 hours, reveals that as in hypoxia, *GFAP* mRNA is down regulated in 100μM cobalt chloride (Fig 5.9A). *VEGF* mRNA is also upregulated in these cultures, as it is under 1.5% oxygen.

Fig 5.9 **Cells in the presence of cobalt chloride down-regulate *GFAP* and up-regulate *VEGF*.** P1 retinal cultures were grown in 20% oxygen in the presence of 100μM cobalt chloride. Control cultures were grown in the absence of cobalt chloride and plated s imultaneously. **(A)** after 72 hours cells were stained by in situ hybridisation with probes against *GFAP* mRNA or *VEGF* mRNA. In the presence of cobalt chloride, *GFAP* mRNA levels were down regulated and *VEGF* mRNA was up-regulated in some cells. **(B)** the labelling index was calculated in the presence or absence of cobalt chloride. The drop in proliferation after 72 hours was not prevented at either 25, 50 or 100μM cobalt chloride. At 100 μM cobalt chloride a slight decrease in proliferation rate was observed after 24 hours.

A

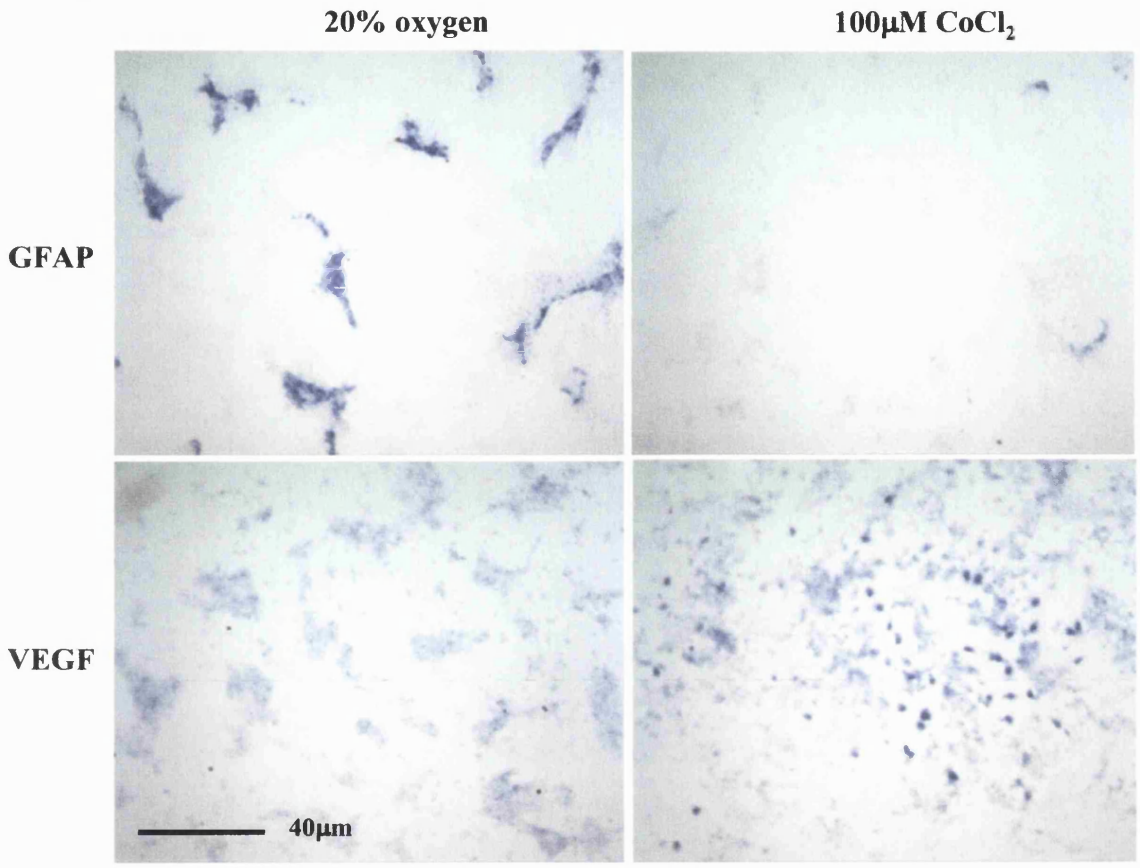
20% oxygen
100μM $CoCl_2$
GFAP
VEGF
40μm

B

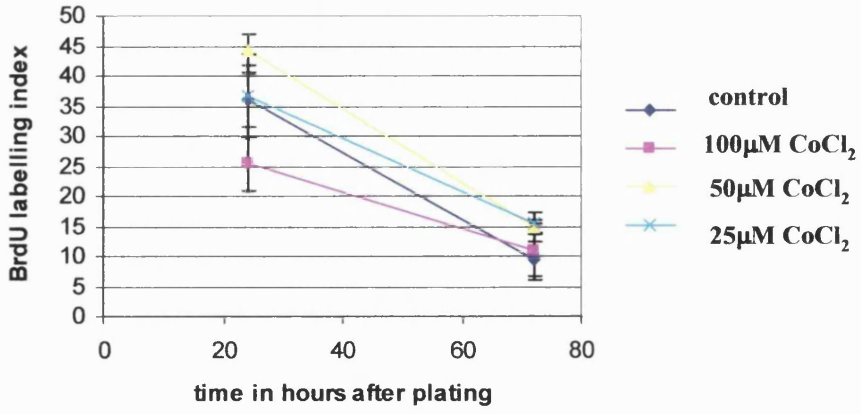
BrdU labelling index
50
45
40
35
30
25
20
15
10
5
0
0
20
40
60
80
time in hours after plating
control
100μM $CoCl_2$
50μM $CoCl_2$
25μM $CoCl_2$

5.3.0 N-acetyl cysteine, an oxygen free radical scavenger, cannot mimic the effect of low oxygen on retinal astrocyte proliferation

A level of 20% oxygen is commonly used for cell culture incubations, however cells are rarely exposed to such high levels in vivo. Oxygen may become damaging when cells are unable to defend themselves against excessively high concentrations of free oxygen radicals (Sochman, 2002). So-called oxidative stress may result in a temporary or permanent change in the properties of proteins and possibly, a change in nuclei acids. Could these high levels of oxygen prevent proliferation of retinal astrocytes? Do astrocytes proliferate more in low levels of oxygen simply because the toxic effect of free oxygen radicals is reduced?

To test this, an oxygen free radical scavenger – N-acetyl cysteine was added to P1 cultures. At various concentrations this drug had no effect on astrocyte proliferation, except at the highest concentrations used in which astrocytes survived poorly (Fig 5.10). This suggests that by simply lowering the free radicals that astrocytes are exposed to, this cannot stimulate proliferation.

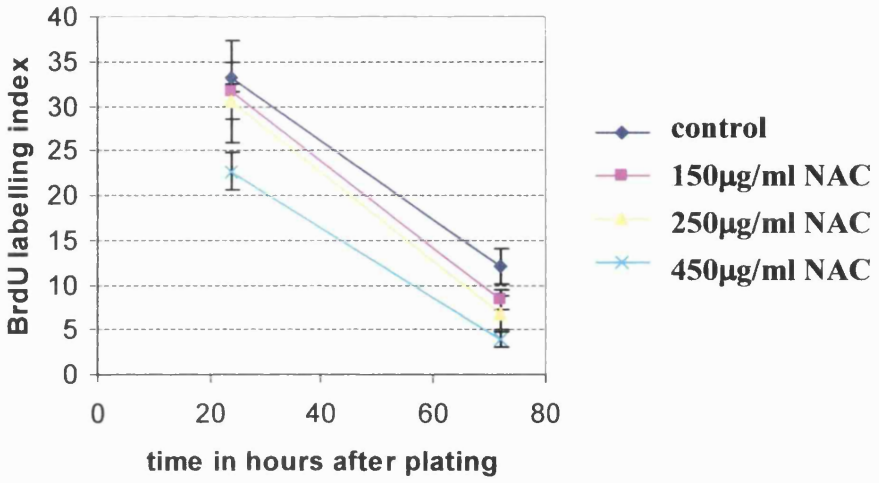

Fig 5.10 **N-acetyl cysteine cannot mimic the effect of low oxygen on retinal astrocyte proliferation.** P1 cells were plated in medium containing 150, 250 or 450 µg/ml N-acetyl cysteine, an oxygen free radical scavenger. The BrdU labelling index was calculated as before, after 24 and 72 hours in culture. A slight decrease in proliferation at 24 hours is apparent at the highest concentration used. N-aectyl cysteine may be toxic at this concentration. At lower concentrations, no effect on retinal astrocyte proliferation was seen.

5.3 Discussion

In this chapter I introduced a culture system for retinal astrocytes. I showed that P1 astrocytes proliferate at a maximum rate in medium containing 10% serum. PDGF-A was able to stimulate retinal astrocyte but only in the presence of sufficient quantities of serum. The rate of proliferation declined however after 48 and 72 hours in culture. This decline could be prevented by culturing astrocytes in low (1.5%) oxygen levels. In these hypoxic conditions, *GFAP* was down-regulated and *VEGF*, a marker of hypoxia, was up-regulated.

5.3.1 PDGF–A requires another serum factor(s) in order to stimulate astrocyte proliferation

I have shown that astrocyte proliferation is saturated in 10% serum, since at 20% serum, proliferation did not increase any further. Furthermore, the addition of PDGF-A was unable to stimulate proliferation above the rate seen at 10% serum. It may be that cell proliferation was unable to operate any faster in the cell or that the action of PDGF-A and another mitogen/mitogens were saturated at this point.

PDGF-A is a component of serum but is not the only factor necessary in serum for astrocyte proliferation. At 0.5% serum and at 5,10 or 20ng/ml PDGF-A, a range over which in most culture systems PDGF-A has biological activity, there is no effect of the mitogen (data not shown for 5 and 20 ng/ml). Only at intermediate levels of serum (2

and 5%), PDGF-A has a potent effect on proliferation. It appears therefore that for PDGF-A to have any action at all, another mitogen is required in sufficient amounts. 0.5% serum may contain insufficient quantities of unknown factor, therefore retinal astrocyte are unable to proliferate even in the presence of PDGF-A. At 10% serum, PDGF-A is unable to stimulate retinal astrocyte proliferation perhaps because it is already present in saturating concentrations, or because cells are already proliferating at maximum speed.

This behaviour contrasts with the situation for cultured O2 -A progenitors (originating from rat optic nerve), which respond with increased proliferation to increasing amounts of PDGF-A, when grown in 0.5% serum. For another glial cell, the Schwann cell, Glial Growth Factor (GGF) is known to stimulate their proliferation, but only has an effect in the presence of enough serum (Raff et al., 1978) . This appears similar to the situation for retinal astrocytes described here. Cheng et al (Cheng et al., 1998) have investigated this further, and shown that GGF can stimulate proliferation of Schwann cells in the absence of serum, but only in high density cultures. These authors suggest that this is due to the higher concentrations of an autocrine factor.

In the case of retinal astrocytes, the identity of this serum factor required for proliferation remains to be established. It is known however that it is heat labile and cannot be dialysed out of serum. It remains to be seen whether this factor/factors are important in vivo during development.

5.3.2 Astrocyte proliferation is not affected by long-range secreted factors from endothelial cells or older retinal cells

In co-culture experiments, P7 retinal cells had no effect on the proliferation of P1 astrocytes. Similarly, P1 retinal astrocytes did not affect P7 retinal astrocytes. This suggests the absence of a long-range secreted factor released by P7 retinal cells that may act upon P1 cells to decrease their proliferation. It also suggests the absence of a long-range factor released by P1 cells that stimulates proliferation of older P7 cells. The co-culture experiments performed here, do not rule out the possibility that a cell bound or short-range paracrine factor may be operating, that is not at sufficient concentration. Alternatively, P1 and P7 cells could be intrinsically different somehow, in their ability to proliferate. This data is consistent with the results suggesting that oxygen may act directly on astrocytes, or via a short-range paracrine factor to stimulate retinal astrocyte proliferation. For example, if low oxygen directly stimulates P1 retinal astro cyte proliferation then co-culturing these cells with P7 cells would not affect the proliferation rate of P7 retinal astrocytes.

Previous co-culture experiments have revealed the presence of a long-range factor determining retinal ganglion cell production during development. Older retinal ganglion cells were found to release an active factor that inhibited the production of retinal ganglion cells in younger cell cultures (Waid and McLoon, 1998). Retinal ganglion cells are amongst the first cells to develop in the retina and few are produced late in development. This example illustrates how long-range paracrine factors can be involved

in limiting cell number during development. In this case, the factor appears to act by controlling cell fate determination in retinal ganglion cells.

Despite the correlation between presence of blood vessels and astrocyte proliferation, it does not appear that endothelial cells themselves secrete paracrine factors acting on astrocytes. It is possible that human endothelial cells are unable to affect retinal astrocytes when mouse endothelial cells would. However, not only does co-culture with HUVEC fail to reduce P1 retinal astrocyte proliferation but also co-culture with P7 cells. As shown in Fig 5.1A, numerous collagen IV^+ endothelial cells are present in dissociated P7 cultures, but do not appear to affect proliferation in P1 cells across a permeable membrane.

Barres and collegues (Mi et al., 2001) show that rat optic nerve astrocytes are induced to differentiate by purified endothelial cells, via the secreted factor LIF. In these experiments, GFAP expression was induced in E17 and P1 optic nerve astrocyte precursor cells upon exposure to purified endothelial cells. Rates of proliferation were not addressed however in this study. It remains possible that endothelial cell derived LIF is involved in some stage of retinal astrocyte differentiation but this has not yet been studied.

5.3.3 Oxygen levels control astrocyte proliferation

There is evidence that astrocytes are well adapted to cope with changing oxygen conditions. They are thought to protect neurons from oxidative stress accumulated with age (Ramirez et al., 2001) but also they store large quantities of glycogen to supply them in conditions of poor anaerobic metabolism during hypoxia. It is know that in the adult, astrocytes are more resilient to hypoxia than neurons for example. Their mitochondria are especially resistant to free radical exposure. They also remain viable in stressful situations in which neurons die (Almeida et al., 2002). Based on in vitro studies, it is often assumed that neurones have a higher oxidative capacity, while astrocytes depend more on glycolysis (Erecinska and Silver, 2001). Astrocytes are thought to be especially resistant to oxidative stress because of their relatively high antioxidant content and their capacity to regenerate glutathione and ascorbate which can act as oxygen free radical scavengers (Ramirez et al., 2001; Kettenmann, 1999). So perhaps astrocytes are specialized in their adaptation to low levels of oxygen.

Brain cell regions or individual cells exhibit differential sensitivities to the same level of oxygen deprivation and/or time of duration. Differences in blood supply, rates of glycolysis, greater number of K^+ ATP channels per cell etc can be reasons for different vulnerability. Turtles for instance are resistant to life under low oxygen tension (Buck and Hochachka, 1993). One adaptation these animals use is 'channel arrest' which reduces expenditure of energy for ion movements (Erecinska and Silver, 2001). The

mechanism may occur by decreasing the activity of K^+ and Ca^{2+} channels on exposure to low oxygen (Haddad and Jiang, 1997).

In diseased states such as ischemia, glial cells are the cells that often become activated, in keeping with their role in protecting neurons and encouraging new vessel growth (Sharp et al., 2002). Reactive gliosis associates with up-regulation of enzymatic and non-enzymatic antioxidant defenses that may help astrocytes to protect neurons from free radicals (Ramirez et al., 2001; Ridet et al., 1997).

As mentioned in the introduction there are other examples such as during placental cytotrophoblast development where lower levels of oxygen can stimulate proliferation of precursor cells. Human dermal fibroblasts have also been reported to be stimulated under low oxygen concentrations (Falanga and Kirsner, 1993). In a study looking at the response of CNS precursor cells to reduced oxygen concentrations, it was found that E14 nestin-positive cells demonstrated increased rates of proliferation and increased cell numbers. Another study in neural cells showed that neural crest derived carotid body chromaffin cells responded with increased proliferation to lowered oxygen (Nurse and Vollmer, 1997). These cells are expected to be responsive to lowered oxygen because they are functionally specialized oxygen sensing chemoreceptors in the carotid artery. These examples suggest that regulation of cell proliferation by oxygen levels is not an isolated phenomenon restricted to retinal astrocytes.

Many studies in vitro have suggested a correlation between intensity of GFAP expression and astrocyte maturity (Brenner, 1994; Gomes et al., 1999) leading to its use as a marker of mature astrocytes. In the developing rat hippocampus, up -regulation of GFAP expression has been reported at the onset of astrocyte maturation (Catalani et al., 2002). In the retina, (Fruttiger unpublished observations) *GFAP* levels are down-regulated towards the periphery as previously mentioned. Hence, in the culture system, the proliferation and absence of *GFAP* immunoreactivity/low levels of expression, are consistent with a less mature state. As discussed in the introduction, hypoxia is known to affect proliferation and prevent differentiation in other cell types such as neural crest derived neuroblastoma cells and cytotrophoblasts of the placenta.

Interestingly, interactions of subventricular zone (SVZ) progenitors (including astrocyte progenitors) with blood vessels, occur at the same time as up-regulation of intermediate filament proteins (Zerlin and Goldman, 1997). These authors suggest that interactions with the endothelial cells or matrix at the pial surface may cause the different iation of SVZ cells into astrocytes. These results are also consistent with the idea that oxygen levels brought by the blood vessels are able to control astrocyte differentiation.

Astrocytes have long been known to respond to hypoxia during development – they detect hypoxia and up-regulate *VEGF* to stimulate growth of the vasculature in the retina. Hence, hypoxia is already established as a developmental control signal for astrocyte behaviour as well as for angiogenesis (Zhang et al., 1999).

Why is 1.5% oxygen critical to astrocyte proliferation in vitro? In the developing and adult brain, oxygen levels are an order of magnitude lower than the standard 20% oxygen used in tissue culture (Studer et al., 2000). Such levels are non-physiologically high. Because the solubility of dissolved oxygen in interstitial fluid and culture medium is the same, a gas phase oxygen concentration of 1-5% oxygen in culture should give rise to oxygen concentrations in the culture medium that approach average physiological levels (Morrison et al., 2000).

However, the precise relationship between the oxygen concentration I have used in culture and oxygen concentrations in vivo is difficult to determine because oxygen levels vary widely in vivo (Erecinska and Silver, 2001). Also the kinetics of oxygen diffusion may vary in important ways between the in vitro cultures and in vivo tissues. Thus it is difficult to precisely compare oxygen levels in vitro and in vivo. In the mammalian brain, interstitial tissue oxygen levels range from approximately 1-5% (Erecinska and Silver, 2001). What are normal oxygen levels in the retina during development? This is not known exactly. Measurements by microelectrode have been made in larger structures of the brain usually in adult animals. In the adult rat, mean brain oxygen levels have been calculated at 1.6% oxygen based on extensive sampling. It comes with little surprise therefore that retinal astrocyte behaviour at this oxygen concentration in vitro is similar to the behaviour seen in vivo.

So does the response of retinal astrocytes to low oxygen, operate through the HIF pathway, the global transcriptional activator that mediates changes in gene expression in responses to changes in oxygen concentration?

VEGF and HIF-1α certainly show temporal correlations in a wide variety of situations, as previously described (see introduction). In the retina, HIF has been co-localised with *VEGF* expression during normal development (Ozaki et al., 1999). As this association reflects, HIF often leads to up-regulation of *VEGF*, one of its target genes. Given that *VEGF* is upregulated in cultures maintained at 1.5% oxygen, could HIF be involved in upregulation of *VEGF* here? One attempt to answer this question was to use cobalt chloride, a chemical known to stabilise HIF in cells. In media containing cobalt chloride, *VEGF* mRNA is up-regulated but it is not clear in what cell type this occurs. *GFAP* is also down-regulated in cobalt chloride as it is under hypoxic conditions, but proliferation is unaffected. The meaning of these results is unclear. It could indicate that HIF is not involved in the response of astrocytes to hypoxia. However, on closer inspection of the effect of cobalt chloride in other systems, a different interpretation is possible.

Originally, cobalt was identified as a chemical mimic for hypoxia because it triggered erythropoietin expression with no obvious additional effects. It was suggested that the iron centres of the oxygen sensors were replaced by non-oxygen-binding cations generated by cobalt chloride. According to the model, this locks the oxygen sensor in the deoxy conformation.

Iron chelators like desferrioxamine (DFF) can also mimic hypoxia. However, it was found that blockers of hypoxia or cobalt chloride have different effects, suggesting that hypoxia, cobalt and DFF interact with different steps along the oxygen signal transduction pathway, or that they each affect additional pathways that cross -talk with the oxygen pathway. For instance mitochondrial inhibitors have been shown to block hypoxic but not cobalt chloride-dependent induction of *erythropoietin* mRNA (Chandel et al., 1998). Also, another mitochondrial inhibitor blocked hypoxia, cobalt and DFF dependent induction of *erythropoeitin* but induced HIF-1α and *VEGF* (Agani and Semenza, 1998; Wenger, 2000). For a long time, cobalt chloride has been labelled a mimic of hypoxia. Perhaps this chemical is not quite the perfect mimic of hypoxia after all. This may explain why it was able to up-regulate *VEGF* mRNA and down-regulate *GFAP* mRNA but not stimulate proliferation in retinal astrocyte cultures. If cobalt chloride does up-regulate HIF however, what does this imply for HIF involvement in the proliferation response? Either HIF is not involved, or some other modification of HIF, or a different pathway, is triggered by hypoxia but not by cobalt chloride.

Another possibility as mentioned is that oxidative stress has some role to play in the decline of astrocyte proliferation in 20% oxygen. Could culturing in low oxygen levels relieve the oxidative stress on astrocytes thereby permitting higher levels of proliferation (Sochman, 2002) Use of N-acetyl cysteine in cultures does not support this theory. Despite its reported role as a free radical scavenger, it fails to maintain astrocyte proliferation in P1 cultures. In these experiments however, oxygen free radicals have not been measured directly to test the efficacy of the drug.

An alternative theory advocated by Schmacker and colleagues is that conversely cells actually release reactive oxygen species (ROS) on exposure to hypoxia, as part of an adaptive response (Chandel and Schumacker, 2000; Abele, 2002). These authors suggest that ROS activate expression of the hypoxia-stimulated genes *VEGF* and *erythropoietin.* It remains to be studied whether this could be a mechanism for hypoxia induced gene expression and proliferation amongst retinal astrocytes.

In vivo, HIF has been seen to promote tumour progression and is expressed in the majority of common human cancers (Semenza, 2001). However tumour cells in culture undergo apoptosis when cultured in hypoxia, as other cells have been reported to do under hypoxia. Hypoxia stimulates HIF binding to p53, which MDM then targets for ubiquitination. Although controversial, one theory is that HIF, by stabilising p53, is creating a powerful selection pressure for loss of p53, in order to stimulate tumour growth (Carmeliet et al., 1998). Embryonic stem cells from *HIF*-/- mice grow better than *HIF*+/+ ones, with increased proliferation. Tumours induced in nude mice, proliferate more and are much bigger if initiated from *HIF*-/- cells, although they are less vascularised and more hypoxic.

The evidence from this paper (Carmeliet et al., 1998) supports a role for a HIF independent pathway that stimulates proliferation in hypoxic conditions. Perhaps a similar pathway is acting during development, to stimulate retinal astrocyte proliferation in low oxygen conditions. Another alternative however is that these experiments are just

reflecting the apoptotic effects that HIF has in tumour cells. The increased proliferation may reflect a lack of apoptosis in the HIF null tumours rather than a stimulus to proliferation directly.

It remains to be seen whether proliferation in astrocytes is stimulated via HIF or another pathway. To test the role of HIF, expression of stabilised HIF-1α in astrocytes perhaps by transfection of culture cells or by making a transgenic mouse, may clarify this issue. Does for instance, stabilisation of HIF-1α, induce proliferation in retinal astrocytes?

Chapter 6. Role of *Ink4a/Arf* locus in controlling cell number during retinal development

6.1 Introduction

What other mechanism could have led to the cessation of retinal astrocyte proliferation? One possibility is an involvement of cyclin dependent kinase inhibitors. As discussed in the introduction, such proteins have demonstrated anti-proliferative behaviour in vitro and in vivo during development. The potential role of the *Ink4a/Arf* locus, encoding two growth arrest proteins – Ink4a/p16 and p19/ARF – is investigated in this chapter.

Ink4a/Arf null mice were crossed with *GFAP-hPDGF-A* mice to see if the growth arrest observed could be prevented in an Ink4a null background. However, in the absence of the *Ink4a/Arf* locus, astrocyte proliferation stopped as normal. On investigating retinal development in *Ink4a/Arf* null mice though, a phenotype was noticed that has not been previously described. This included excess cells in the vitreous humour and tissue disorganisation in the retina. On further investigation, the excess cells in the vitreous humour, appeared to be an abnormal growth of the hyaloid vasculature. During this study, similar findings were published by McKeller et al (McKeller et al., 2002) who furthermore identified Arf in particular as being responsible for the developmental phenotype. The study here, was terminated after this publication, but the results found up to this point are presented in this thesis.

The *INK4a/ARF* tumour suppressor locus encodes two proteins, p16INK4a and p19ARF (p14ARF in humans), which modulate the activity of the RB and p53 pathways respectively (Quelle et al., 1995). Deletion of this locus is one of the most frequen t mutations found in human gliomas at a rate of 60% (Uhrbom et al., 2002). Gliomas are incurable primary brain tumours of the CNS thought to arise from either a CNS progenitor or an astrocyte. Genetic alterations described in human gliomas include disruption of the cell cycle arrest pathways and abnormal receptor tyrosine kinase signalling that results in activation of Ras, Akt and other downstream proteins (Uhrbom et al., 2002). In fact, in those gliomas that retain an intact *Ink4a/Arf* locus, mutations in other component of the p53 and Rb pathways seem to be obligatory.

The exact role that proteins of this locus perform is still unknown. However it has been suggested from in vitro experiments that p16Ink4a may function to render cells immortal by disrupting their ability to enter G1 growth arrest and senescence. Cultured primar y mouse astrocytes deficient for the *Ink4a/Arf* locus are immortal and acquire characteristics of undifferentiated glia including progenitor-like morphology and expression of nestin and loss of GFAP expression (Holland et al., 1998).

The role of *Ink4a/Arf* in tumour suppression in mice, has been extensively studied. *Ink4a/Arf* null mice develop a variety of spontaneous tumours within their first year of life (Stone et al., 1996). This phenotype could however, be to a large extent due to loss of *Arf* alone as the *Arf* null mice showed most of the same traits as the *Ink4a/Arf* null mice (Kamijo et al., 1997). *Ink4a* null mice do show additionally however, spontaneous

melanoma formation in some mice, a tumour type not yet found in *Ink4a/ARF* or *Arf*null mice. Intriquingly, when *Ink4a* null mice are crossed with *Ink4a/Arf*null mice, the *Ink4a* null *Arf* +/- show a high susceptibility to develop carcinogen induced melanomas, while retaining the WT *Arf* allele. This indicates that there may be a complex and subtle interplay between the *Ink4a* and *Arf* loci depending on cellular context. It has been suggested that one function of *Ink4a/Arf* loss in gliomas is to make differentiated astrocytes susceptible to oncogenic stimuli by promoting an undifferentiated phenotype of astrocytes (Uhrbom et al., 2002).

In mice *Ink4a/Arf* loss has been shown to be either essential to the formation of a number of experimentally induced tumour types in co -operation with activation of certain signal transduction pathways or to enhance tumour initiation and tumour progression in others , depending on cell of origin and oncogenic stimulation. Urhbom et al. (Uhrbom et al., 2002) show that Ras infection in neural progenitors or differentiated astrocytes that are *Ink4a/Arf* null, leads to dedifferentiation of astrocytes and formation of CNS gliomas. Bachoo et al. (Bachoo et al., 2002) also show that in *Ink4a/Arf* null astrocytes that EGF receptor activation can govern terminal differentiation and transformation along the neural stem cell to astrocyte pathway.

So does the *Ink4a/Arf* locus play any role during development? As described in the introduction, other members of the Ink family are known to act during development in the eye and retina, but so far, the role of *Ink4a/Arf* has not been analysed. Here I report the phenotype observed during development of the retina in *Ink4a/Arf* null mice.

6.2 Results

6.2.1 Mice lacking the *Ink4a/Arf* locus show a developmental abnormality in the eye

Litter mates from a *Ink4a/Arf*-/+ and *Ink4a/Arf*-/+ breeding pair were analysed. Tail tips were taken from each pup to genotype. The eyes were removed, fixed and then embedded for wax sectioning. Cross sections of the eye were analysed under a light microscope. This work was done in collaboration with Peter Hitchcock at the University of Michigan, who performed the wax sectioning.

At P0 in the retina of *Ink4a/Arf*-/- mice, a noticeable accumulation of cells or tissue appeared in the vitreous (Fig 6.1). At P2, a more striking phenotype with variable penetrance was visible (Fig 6.1A arrow). In severe cases, an abnormal pigmented tissue had accumulated between the lens and the inner retina. At P5, this tissue could be seen clearly, attatched to the lens. By 4 weeks severe disorganisation of retinal tissue is apparent, with the retina developing into folds and the lens degenerating. By this time the abnormal vitreous tissue had physically attatched to the lens and neuroretina. The vitreous tissue persisted in adult mice.

6.2.2 Abnormality of the hyaloid in *Ink4a/Arf*-/- mice

One tissue that resides between the lens and the retina is the hyaloid vasculature, which normally regresses shortly after birth. To determine if this is the tissue affected in the Ink null mice, the hyaloid vasculature was isolated. P3 animals were chosen given that the phenotype develops between P0 and P5. BrdU was injected into these pups and two hours later the pups were killed. The hyaloid vasculature was dissected away from the lens and retina and flat mounted on microscope slides. The hyaloid vessels were then visualised under the light microscope. Indeed, an abnormal growth (sometimes pigmented) was apparent in some *Ink4a/Arf* null mice (Fig 6.2B/C) but not in the heterozygote animals (Fig 6.2A). After immunostaining for BrdU, proliferating cells were revealed in the abnormal growth, suggesting that the Ink4a locus may have some role in preventing such proliferation (Fig 6.2D).

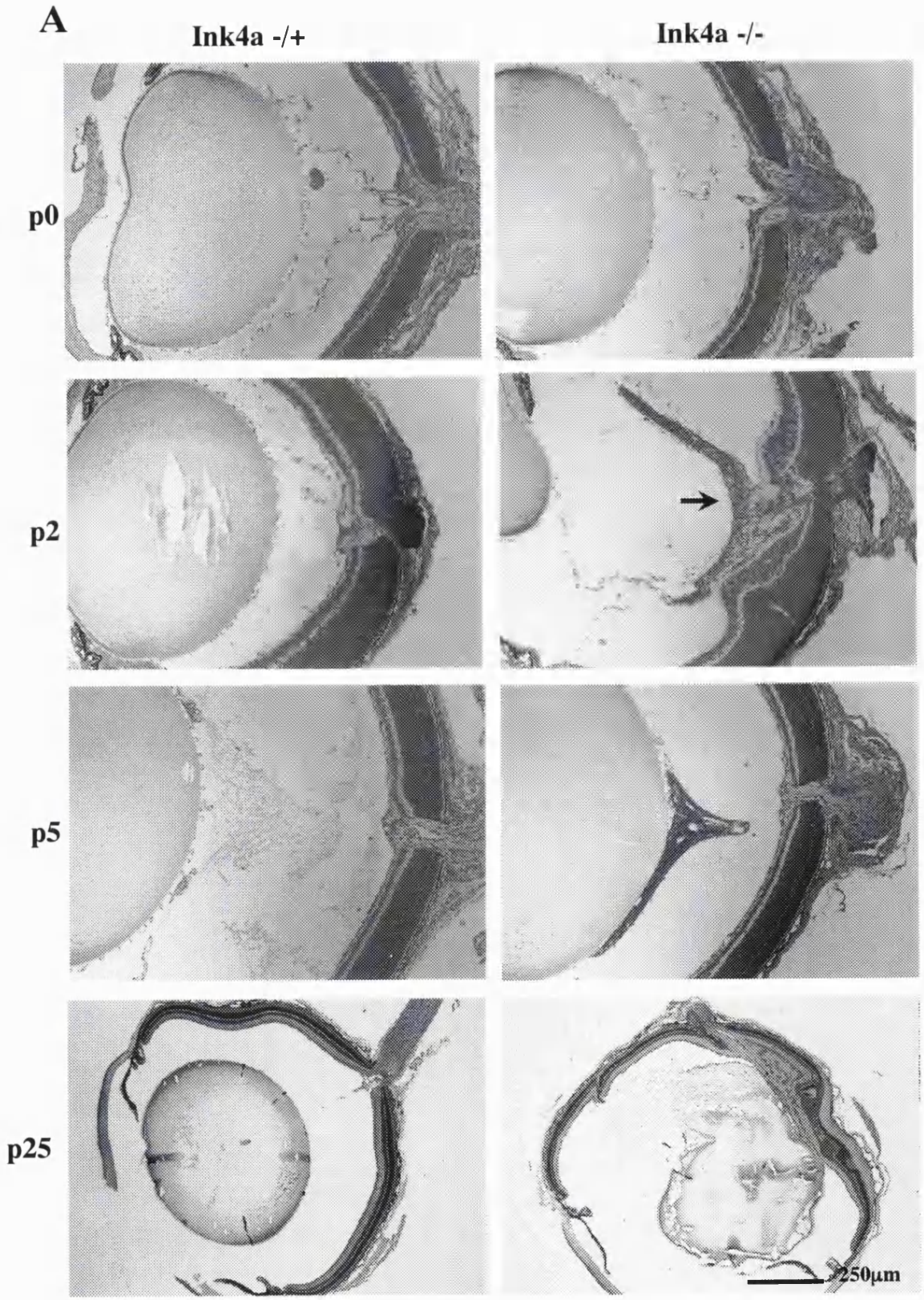
A
Ink4a -/+
Ink4a -/-
p0
p2
p5
p25
250μm

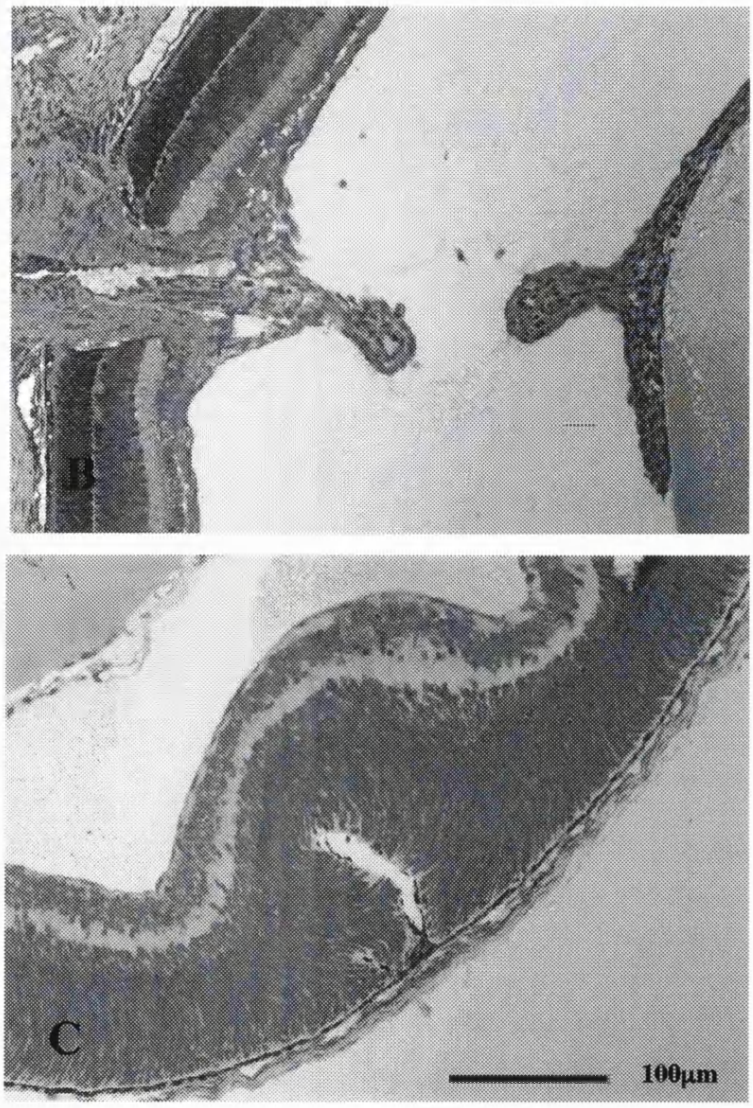

Fig 6.1 **A developmental abnormality occurs in *Ink4a/Arf* null mice.** Tissue sections of *Ink4a/Arf* null mice were prepared by Peter Hitchcock; University of Michigan. Eyes were dissected, dehydrated and then embedded in glycomethacrylate. 5µM sections were cut using a rotary microtome and then stained with toluidine blue. **(A)** By P2, an abnormal accumulation of tissue is apparent in the vitreous of *Ink4a/Arf* null mice. This tissue is seen attatched to the retina or lens in some individuals. By 4 weeks after birth, severe disorganisation of the retina and degeneration of the lens occurs. **(B)** shows a high power image of the abnormal vitreous tissue attached to the retina and lens. **(C)** shows an abnormal folding of the retina seen at P5.

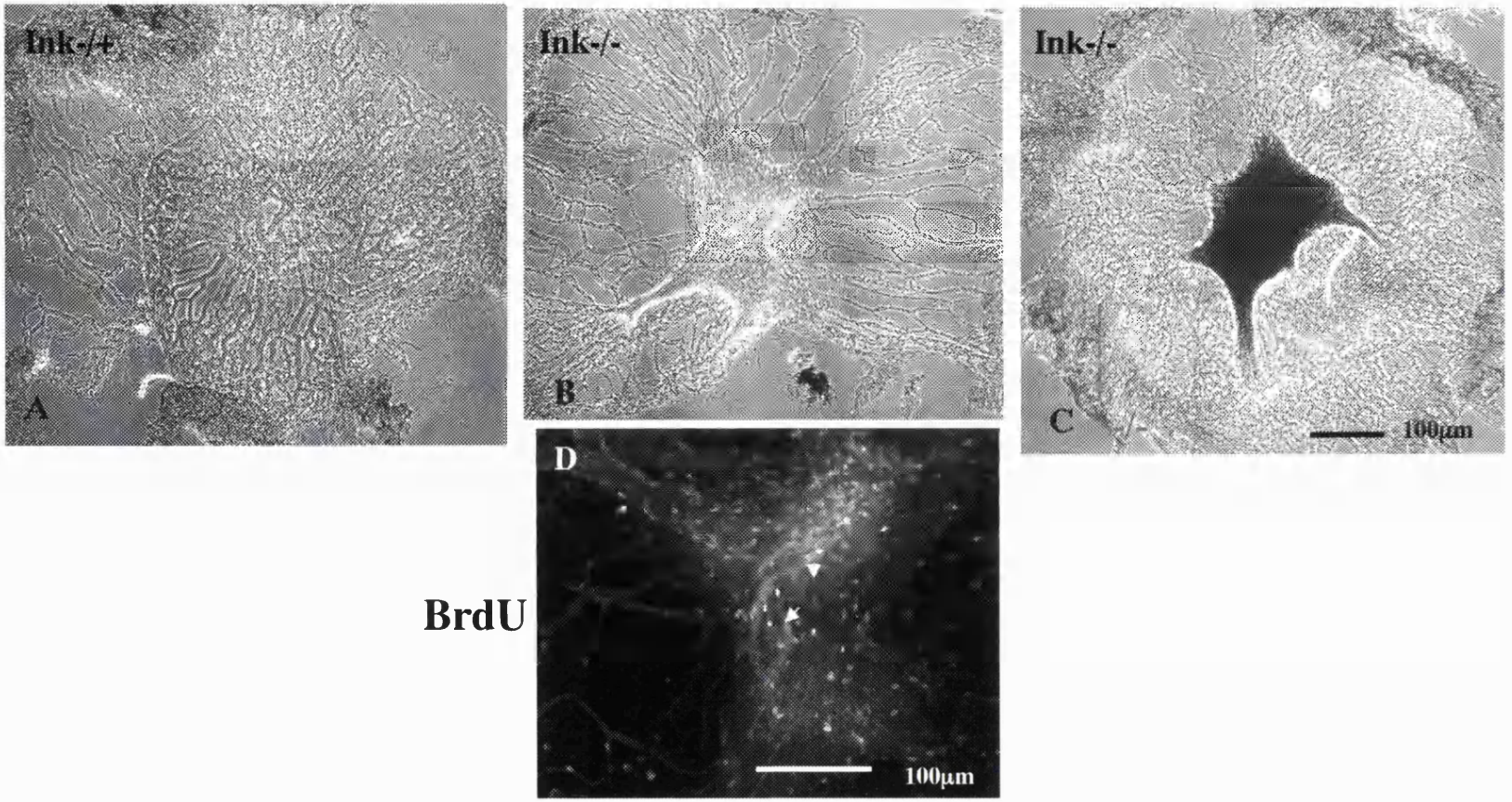

Fig 6.2 **An abnormal 'growth' develops in the hyaloid tissue of *Ink4a/Arf* null mice.** P3 mice pups were given an intra peritoneal injection of BrdU and left two hours before sacrificing. The hyaloid tissue was dissected out and mounted. Compared to the normal appearance of the hyaloid from heterozygous animals **(A)**, an abnormal growth is apparent in the hyaloid tissue in some *Ink4a/Arf* null animals **(B)** and **(C)**. Many $BrdU^+$ cells are found in this abnormal 'growth' **(D)**.

6.3 Discussion

Just after birth, an excess of cells in the vitreous appears in *Ink*4a/Arf null compared to *Ink4a/Arf*-/+ mice. This initial phenotype is followed by attatchment of this abnormal vitreous tissue to the neural retina and lens, tissue disorganisation and lens degeneration. This sequence of events suggests that perhaps the primary defect is an excess of vitreous cells. This is consistent with the results presented by (McKeller et al., 2002). These authors find a similar phenotype in *Arf* null mice including 'retrolental' tissue as the primary defect, with later abnormal retinal folds, dysplastic photoreceptor cells, and physical attachment of the retrolental mass to the neuroretina. After P14, these authors report degneration of the lens with attatchment of the retrolental t issue to the posteior lens. This phenotype is very similar to that of the human disease PHPV (persistent hyperplastic primary vitreous) which progresses with a similar sequence of similar events (Goldberg, 1997).

McKellar et al identify the retrolental tissue as part of the hyaloid vasculature. This is based on the presence of hyaloid like vessels, the presence of smooth muscle actin cells that could be pericytes, and endothelial cells. By dissecting out the hyaloid vasculature, the results presented here suggest this tissue is involved in the phenotype. The unusual growth seen in these wholemounts appeared to be an extension of this tissue.

The mouse hyaloid system normally regresses in the first two weeks after birth (Ito and Yoshioka, 1999). The vasa hyaloidea propria however that surrounds the lens normally regresses earlier between P6 and P10 in the mouse (Ito and Yoshioka 1999). For this reason, McKeller et al suggest this part of the hyaloid to be affected in the Arf null.

Given the similar phenotype found here to that presented by McKeller et al, it appears that *Arf* and not the other gene product -p16/Ink4a –of the *Ink4a* locus is responsible for the observed phenotype. Indeed, these authors find expression of Arf in the vitreous from P1 to P5. So how does Arf normally trigger regression of the hyaloid vasculature during development?

As discussed in the introduction, hyaloid regression is mediated by apopto sis in the hyaloid vasculature. What role does Arf play in this cell process? *Arf* is expressed from P1 to P5, however apoptosis in the hyaloid peaks between P7 and P8 in the mouse. McKeller et al propose that this time delay suggests Arf is unlikely to trigger apoptosis directly. Arf has been shown in many systems to act in the p53 pathway that is able to trigger apoptosis. However, McKeller et al show that in *p53* null/*Arf* null mice the phenotype still persists. They conclude that Arf is acting in a p53 independent pathway in promoting hyaloid regression during development. p53 is probably involved partially in the apoptosis necessary for hyaloid regression because in *p53* null mice, regression is slowed or imcomplete (Ikeda et al., 1999). McKeller et al suggest that although some symptoms are seen in *p53* null mice, in the *Arf* null mice the phenotype is fully penetrant.

They conclude from this that the mechanisms allowing the phenotype to develop are probably regulated by p19/Arf.

Further investigations are necessary to work out the exact role of Arf in promoting regression of the hyaloid vasculature during development. However, results shown here and from McKeller et al show the presence of proliferating cells in the excess hyaloid that persists. Arf is known in cultured fibroblasts to arrest the proliferation of cells (Quelle et al., 1995). Conversely, in cultured *Arf* null mouse embryo fibroblasts, cells proliferate continuously (Kamijo et al., 1997). Although Arf could be involved in cellular differentiation, migration or apoptosis, a simple explanation based on these observations suggest that Arf may act to prevent over-proliferation of cells in the hyaloid during development.

Chapter 7. Discussion

In this Thesis, I have looked at the development of retinal astrocytes, associated with the retinal vasculature. My work follows on from observations by Fruttiger et al (1996) that demonstrated a large overgrowth of these cells when the mitogen PDGF-AA is overexpressed in transgenic mice. In Chapter 3, I showed that, despite the continued presence of this mitogen and its receptor, the number of astrocytes and vascular cells does not increase indefinitely. Although the rate of proliferation of astrocytes is initially higher in transgenic mice, levels of proliferation decline and then cease during the first week after birth, as they do in wild type mice.

These results demonstrated that although PDGF-A is important in controlling astrocyte numbers, it is not the only limiting factor. Multiple controls might operate not only as a fail-safe mechanism but also, perhaps, in co-ordinating development of different cell types. For example, the control of astrocyte proliferation by both PDG F-A and hypoxia, links their development to both neurons, which are the major source of PDGF-A, and the vasculature, which provides oxygen.

In Chapter 3, I show that the presence of the vasculature correlates negatively with astrocyte proliferation. In Chapter 4, I describe experiments in which I manipulate the vasculature, creating areas of hypoxia and normoxia within the same retina. Areas of hypoxia correlate with areas of astrocyte proliferation suggesting that in vivo, oxygen levels rather than vascular cells per se might be a key influence on proliferation. In

Chapter 5, I show that cultured astrocytes proliferate at a higher rate in low levels of oxygen, which is consistent with the in vivo results. I argue that the decrease in retinal astrocyte proliferation during development is triggered by changing oxygen levels rather than the ingrowth of the vasculature or decreasing PDGF-A levels.

The existence of oxygen sensing to control astrocyte proliferation prompts the question, are astrocytes responding directly to oxygen and, if so, what are the intracellular pathways and signalling molecules involved? For instance, is HIF-1α involved in the astrocytes' response to hypoxia? One way to test this would be to observe the effect on astrocyte proliferation in a mouse expressing stabilised HIF-1α. It is possible to make point mutations in the *HIF-1α* gene that prevent modification by prolyl hydroxylase and subsequent degradation via the VHL protein. Would this constitutively stable form of HIF-1α trigger continuous astrocyte proliferation during development? Would astrocytes continue to proliferate beyond the time when they would normally have stopped?

In this study I have used *VEGF* as a marker of areas of hypoxia in the retina. But what is the actual oxygen concentration in the retina during development and what concentration triggers astrocyte proliferation? The in vitro work suggests that astrocytes respond by proliferating at 1.5% not 20% oxygen and similar studies on placental cells (cytotrophoblasts) suggest that these cells are responsive to oxygen over the range 2-12% oxygen. So do these values match up to those occurring during normal physiology? One way to look at this is via molecules that react directly with oxygen such as EF -5 (2-

nitoimidazole). This compound, when exposed to tissue or cells, forms hypoxia-dependent adducts with cellular macromolecules, that are detected by fluorescent monoclonal antibodies. Levels of this marker could be analysed at different stages of development in the retina, and compared directly with expression of *VEGF*.

My analysis concerned only developing retinal astrocytes. Would oxygen have similar effects on astrocytes in the brain? Much of the embryo develops in an hypoxic environment before an extensive blood supply has formed. Could the expansion of glial or other cells be a general phenomenon in response to low oxygen during development, to attract in the growing vasculature to rapidly metabolising oxygen-depleting areas? In the peripheral nervous system, for example, it seems likely that Schwann cells act as the go-between connecting peripheral nerves and the arterial vasculature that follows them. Are there equivalent oxygen-sensing cells throughout the body?

In the process of reactive gliosis, mature astrocytes are thought to be able to proliferate and undergo some sort of activation in response to injury. Glial cell activation is a hallmark of CNS injury characterized by an increase in size and number of glial cells and upregulation of *GFAP* with additional cellular changes that might cause or relieve neuronal impairment (Wang et al., 2002). In this study, I have not addressed the effect of oxygen on more mature retinal astrocytes to see if they respond at all stages of their development. Could hypoxia be a trigger throughout life, in response to conditions such as ischamia, where blood supply is cut off and oxygen levels are depleted? The HIF-1α oxygen-sensing pathway is upregulated in retinal or myocardial ischemia and promotes

neovasculatization by activating transcription of *VEGF*. Hence, the same oxygen sensing signalling pathway appears to be involved not only in development but also in diseases where hypoxia occurs (Semenza, 2001). HIF-1α mediated *VEGF* expression may play a major role in the development of retinopathy of prematurity and other ischemic retinal disorders such as diabetic retinopathy. Retinal neovascularization can be prevented by blocking VEGF suggesting that inhibition of HIF-1α activity might be of therapeutic use in these conditions (Aiello et al., 1995). Also, in the human disease where sufferers inherit a mutated *pVHL* gene that suppresses HIF-1α activity, about half of patients suffer from hemangioblastomas. pVHL targets HIF-1α for degradation and in its absence downstream genes such as *VEGF* are overexpressed leading to a high degree of vascularisation (Dollfus et al., 2002). Could this reflect an increase in proliferation and numbers of astrocytes or other cells expressing *VEGF*? In human glaucoma, a progressive loss of retinal ganglion cells occurs and this triggers deterioration in vision. The underlying pathophysiologic mechanism is still unclear, but activation of glial cells has been observed in glaucomatous optic nerve and retina, and in experimental models. Recent hypotheses suggests that the retinal glial cells might be involved in ganglion cell dysfunction (Wang et al., 2002).

Gliomas are the most common brain tumours and are thought to be derived from glial precursor cells of the brain. Tumours have long been known to develop areas of hypoxia at their core before the angiogenic switch (induction of tumor vascularization by VEGF) has occurred. *HIF-1α* and *VEGF* are often upregulated in many different types of tumours. The metabolic adaptation to hypoxia via increased glucose transporters and

glycolytic enzyme activity (Warburg effect) are thought to be mediated by HIF-1α. Cancer cells have adapted these pathways, allowing tumours to survive and even grow under hypoxic conditions. Tumour hypoxia is associated with poor prognosis and resistance to radiation therapy. They are thought to become hypoxic because new blood vessels that develop are aberrant and have poor blood flow. Hence, elements of the hypoxia response pathway are good candidates for therapeutic targeting (Harris, 2002), although it is still uncertain whether hypoxia generates an aggressive tumour phenotype or whether an aggressive tumour phenotype generates hypoxia. Based on the data presented here, the hypoxic triggering of proliferation might actually support tumour growth.

As I mentioned in Chapter 4, levels of 20% oxygen used in tissue culture are non physiological, based on measurements made of oxygen levels in the brai n by various methods. Perhaps other cells of the central nervous system proliferate better at lower levels of oxygen. Several studies have reported increased stimulation of proliferation at lower, more physiological levels of oxygen including neural cres t stem cells, thymocytes and cytotrophoblasts of the placenta. A major effort is now being devoted to research on embryonic stem cells. The vast benefit they could potentially contribute to treatment of neurodegenerative disease amongst others, has fuelled this effort. Keeping these cells alive in culture has been a challenge so far; could they too respond to low oxygen levels more similar to those they might experience in the embryo? For instance, Morrison et al have shown that neural crest stem cells in culture are stimulated to survive and proliferate more in 5% as opposed to 20% oxygen (Morrison et al 2000).

Further studies will certainly be undertaken on the role of lowered oxygen on the growth of the CNS and other cell types, given its importance in a growing number of cell types and systems. My PhD work has opened up the possibility that lowered oxygen is an important developmental control on astrocyte number. Further studies are needed to identify the signalling pathways and molecules involved in this response, and to determine whether oxygen is important in growth regulation of other cell types in the retina and brain.

Bibliography

Abbott,N.J. (2002). Astrocyte-endothelial interactions and blood-brain barrier permeability. J. Anat. *200*, 629-638.

Abele,D. (2002). Toxic oxygen: the radical life-giver. Nature *420*, 27.

Agani,F. and Semenza,G.L. (1998). Mersalyl is a novel inducer of vascular endothelial growth factor gene expression and hypoxia-inducible factor 1 activity. Mol. Pharmacol. *54*, 749-754.

Aiello,L.P., Northrup,J.M., Keyt,B.A., Takagi,H., and Iwamoto,M.A. (1995). Hypoxic regulation of vascular endothelial growth factor in retinal cells. Arch. Ophthalmol. *113*, 1538-1544.

Almeida,A., Delgado-Esteban,M., Bolanos,J.P., and Medina,J.M. (2002). Oxygen and glucose deprivation induces mitochondrial dysfunction and oxidative stress in neurones but not in astrocytes in primary culture. J. Neurochem. *81*, 207-217.

Araque,A., Parpura,V., Sanzgiri,R.P., and Haydon,P.G. (1999). Tripartite synapses: glia, the unacknowledged partner. Trends Neurosci. *22*, 208-215.

Bachoo,R.M., Maher,E.A., Ligon,K.L., Sharpless,N.E., Chan,S.S., You,M.J., Tang,Y.,DeFrances,J., Stover,E., Weissleder,R., Rowitch,D.H., Louis,D.N., and DePinho,R.A. (2002). Epidermal growth factor receptor and Ink4a/Arf: convergent mechanisms governing terminal differentiation and transformation along the neural stem cell to astrocyte axis. Cancer Cell *1*, 269-277.

Barres,B.A. (1991). New roles for glia. J. Neurosci. *11*, 3685-3694.

Barres,B.A., Hart,I.K., Coles,H.S., Burne,J.F., Voyvodic,J.T., Richardson,W.D., and Raff,M.C. (1992). Cell death and control of cell survival in the oligodendrocyte lineage. Cell *70*, 31-46.

Barres,B.A. and Raff,M.C. (1994). Control of oligodendrocyte number in the developing rat optic nerve. Neuron *12*, 935-942.

Barres,B.A. and Barde,Y. (2000). Neuronal and glial cell biology. Curr. Opin. Neurobiol. *10*, 642-648.

Bergsten,E., Uutela,M., Li,X., Pietras,K., Ostman,A., Heldin,C.H., Alitalo,K., and Eriksson,U. (2001). PDGF-D is a specific, protease-activated ligand for the PDGF beta-receptor. Nat. Cell Biol. *3*, 512-516.

Bernaudin,M., Marti,H.H., Roussel,S., Divoux,D., Nouvelot,A., MacKenzie,E.T., and Petit,E. (1999). A potential role for erythropoietin in focal permanent cerebral ischemia in mice. J. Cereb. Blood Flow Metab *19*, 643-651.

Bernaudin,M., Bellail,A., Marti,H.H., Yvon,A., Vivien,D., Duchatelle,I., MacKenzie,ET., and Petit,E. (2000). Neurons and astrocytes express EPO mRNA: oxygen-sensing mechanisms that involve the redox-state of the brain. Glia *30*, 271-278.

Betsholtz,C., Karlsson,L., and Lindahl,P. (2001). Developmental roles of platelet-derived growth factors. Bioessays *23*, 494-507.

Bignami,A., Asher,R., and Perides,G. (1991). Brain extracellular matrix and nerve regeneration. Adv. Exp. Med. Biol. *296*, 197-206.

Bloom,G.D. and Balazs,E.A. (1965). An electron microscopic study of hyalocytes. Exp. Eye Res. *4*, 249-255.

Bonfanti,L., Strettoi,E., Chierzi,S., Cenni,M.C., Liu,X.H., Martinou,J.-C., Maffei,L., and Rabacchi,S.A. (1996). Protection of retinal ganglion cells from natural and axotomy-induced cell death in neonatal transgenic mice overexpressing bcl-2. J. Neurosci. *16*, 4186-4194.

Brenner,M. (1994). Structure and transcriptional regulation of the GFAP gene. Brain Pathol. *4*, 245-257.

Brockes,J.P., Fryxell,K.J., and Lemke,G.E. (1981). Studies on cultured Schwann cells: the induction of myelin synthesis, and the control of their proliferation by a new growth factor. J. Exp. Biol. *95*, 215-230.

Buck,L.T. and Hochachka,P.W. (1993). Anoxic suppression of Na(+)-K(+)-ATPase and constant membrane potential in hepatocytes: support for channel arrest. Am. J. Physiol *265*, R1020-R1025.

Burne,J.F., Staple,J.K., and Raff,M.C. (1996). Glial cells are increased proportionally in transgenic optic nerves with increased numbers of axons. J. Neurosci. *16*, 2064-2073.

Calver,A.R., Hall,A.C., Yu,W.P., Walsh,F.S., Heath,J.K., Betsholtz,C., and Richardson,W.D. (1998). Oligodendrocyte population dynamics and the role of PDGF in vivo. Neuron *20*, 869-882.

Carmeliet,P., Dor,Y., Herbert,J.M., Fukumura,D., Brusselmans,K., Dewerchin,M., Neeman,M., Bono,F., Abramovitch,R., Maxwell,P., Koch,C.J., Ratcliffe,P., Moons,L., Jain,R.K., Collen,D., Keshert,E., and Keshet,E. (1998). Role of HIF-1alpha in hypoxia-mediated apoptosis, cell proliferation and tumour angiogenesis. Nature *394*, 485-490.

Casaccia-Bonnefil,P., Hardy,R.J., Teng,K.K., Levine,J.M., Koff,A., and Chao,M.V. (1999). Loss of p27Kip1 function results in increased proliferative capacity of oligodendrocyte progenitors but unaltered timing of differentiation. Development *126*, 4027-4037.

Catalani,A., Sabbatini,M., Consoli,C., Cinque,C., Tomassoni,D., Azmitia,E., Angelucci,L., and Amenta,F. (2002). Glial fibrillary acidic protein immunoreactive astrocytes in developing rat hippocampus. Mech. Ageing Dev. *123*, 481-490.

Cepko,C.L., Austin,C.P., Yang,X., Alexiades,M., and Ezzeddine,D. (1996). Cell fate determination in the vertebrate retina. Proc. Natl. Acad. Sci. U. S. A *93*, 589-595.

Chan-Ling,T., Tout,S., Hollander,H., and Stone,J. (1992). Vascular changes and their mechanisms in the feline model of retinopathy of prematurity. Invest Ophthalmol. Vis. Sci. *33*, 2128-2147.

Chan-Ling,T., Gock,B., and Stone,J. (1995). The effect of oxygen on vasoformative cell division. Evidence that 'physiological hypoxia' is the stimulus for normal retinal vasculogenesis. Invest Ophthalmol. Vis. Sci. *36*, 1201-1214.

Chan-Ling,T. (1997). Glial, vascular, and neuronal cytogenesis in whole-mounted cat retina. Microsc. Res. Tech. *36*, 1-16.

Chan-Ling,T.L., Halasz,P., and Stone,J. (1990). Development of retinal vasculature in the cat: processes and mechanisms. Curr. Eye Res. *9*, 459-478.

Chandel,N.S., Maltepe,E., Goldwasser,E., Mathieu,C.E., Simon,M.C., and Schumacker,P.T. (1998). Mitochondrial reactive oxygen species trigger hypoxia-induced transcription. Proc. Natl. Acad. Sci. U. S. A *95*, 11715-11720.

Chandel,N.S. and Schumacker,P.T. (2000). Cellular oxygen sensing by mitochondria: old questions, new insight. J. Appl. Physiol *88*, 1880-1889.

Cheng,L., Esch,F.S., Marchionni,M.A., and Mudge,A.W. (1998). Control of Schwann cell survival and proliferation: autocrine factors and neuregulins. Mol. Cell Neurosci. *12*, 141-156.

Chilov,D., Camenisch,G., Kvietikova,I., Ziegler,U., Gassmann,M., and Wenger,R.H. (1999). Induction and nuclear translocation of hypoxia-inducible factor-1 (HIF-1): heterodimerization with ARNT is not necessary for nuclear accumulation of HIF-1alpha. J. Cell Sci. *112 (Pt 8)*, 1203-1212.

Chu,Y., Hughes,S., and Chan-Ling,T. (2001). Differentiation and migration of astrocyte precursor cells and astrocytes in human fetal retina: relevance to optic nerve coloboma. FASEB J. *15*, 2013-2015.

Cunningham,J.J. and Roussel,M.F. (2001). Cyclin-dependent kinase inhibitors in the development of the central nervous system. Cell Growth Differ. *12*, 387-396.

DiCiommo,D., Gallie,B.L., and Bremner,R. (2000). Retinoblastoma: the disease, gene and protein provide critical leads to understand cancer. Semin. Cancer Biol. *10*, 255-269.

Doetsch,F., Caille,I., Lim,D.A., Garcia-Verdugo,J.M., and Alvarez-Buylla,A. (1999). Subventricular zone astrocytes are neural stem cells in the adult mammalian brain. Cell *97*, 703-716.

Dollfus,H., Massin,P., Taupin,P., Nemeth,C., Amara,S., Giraud,S., Beroud,C., Dureau,P., GaudricA., Landais,P., and Richard,S. (2002). Retinal hemangioblastoma in von Hippel-Lindau disease: a clinical and molecular study. Invest Ophthalmol. Vis. Sci. *43*, 3067-3074.

Durand,B. and Raff,M. (2000). A cell-intrinsic timer that operates during oligodendrocyte development. Bioessays *22*, 64-71.

Dyer,M.A. and Cepko,C.L. (2001). Regulating proliferation during retinal development. Nat. Rev. Neurosci. *2*, 333-342.

Dyer,M.A. and Cepko,C.L. (2001). p27Kip1 and p57Kip2 regulate proliferation in distinct retinal progenitor cell populations. J. Neurosci. *21*, 4259-4271.

Erecinska,M. and Silver,I.A. (2001). Tissue oxygen tension and brain sensitivity to hypoxia. Respir. Physiol *128*, 263-276.

Falanga,V. and Kirsner,R.S. (1993). Low oxygen stimulates proliferation of fibroblasts seeded as single cells. J. Cell Physiol *154*, 506-510.

Fruttiger,M., Calver,A.R., Kruger,W.H., Mudhar,H.S., Michalovich,D., Takakura,N., Nishikawa,S., and Richardson,W.D. (1996). PDGF mediates a neuron-astrocyte interaction in the developing retina. Neuron *17*, 1117-1131.

Fruttiger,M., Karlsson,L., Hall,A.C., Abramsson,A., Calver,A.R., Bostrom,H., Willetts,K., Bertold,C.H., Heath,J.K., Betsholtz,C., and Richardson,W.D. (1999). Defective oligodendrocyte development and severe hypomyelination in PDGF-A knockout mice. Development *126*, 457-467.

Fruttiger,M., Calver,A.R., and Richardson,W.D. (2000). Platelet-derived growth factor is constitutively secreted from neuronal cell bodies but not from axons. Curr. Biol. *10*, 1283-1286.

Fruttiger,M. (2002). Development of the mouse retinal vasculature: angiogenesis versus vasculogenesis. Invest Ophthalmol. Vis. Sci. *43*, 522-527.

Furukawa,T., Mukherjee,S., Bao,Z.Z., Morrow,E.M., and Cepko,C.L. (2000). rax, Hes1, and notch1 promote the formation of Muller glia by postnatal retinal progenitor cells. Neuron *26*, 383-394.

Gao,F.B. and Raff,M. (1997). Cell size control and a cell-intrinsic maturation program in proliferating oligodendrocyte precursor cells. J. Cell Biol. *138*, 1367-1377.

Gassmann,M., Kvietikova,I., Rolfs,A., and Wenger,R.H. (1997). Oxygen- and dioxin-regulated gene expression in mouse hepatoma cells. Kidney Int. *51*, 567-574.

Genbacev,O., Zhou,Y., Ludlow,J.W., and Fisher,S.J. (1997). Regulation of human placental development by oxygen tension. Science *277*, 1669-1672.

Goldberg,M.A., Dunning,S.P., and Bunn,H.F. (1988). Regulation of the erythropoietin gene: evidence that the oxygen sensor is a heme protein. Science *242*, 1412-1415.

Goldberg,M.F. (1997). Persistent fetal vasculature (PFV): an integrated interpretation of signs and symptoms associated with persistent hyperplastic primary vitreous (PHPV). LIV Edward Jackson Memorial Lecture. Am. J. Ophthalmol. *124*, 587-626.

Goldman,J.E. (1995). Lineage, migration, and fate determination of postnatal subventricular zone cells in the mammalian CNS. J. Neurooncol. *24*, 61-64.

Gomer,R.H. (2001). Not being the wrong size. Nat. Rev. Mol. Cell Biol. *2*, 48-54.

Gomes,F.C., Paulin,D., and Moura,N., V (1999). Glial fibrillary acidic protein (GFAP): modulation by growth factors and its implication in astrocyte differentiation. Braz. J. Med. Biol. Res. *32*, 619-631.

Gonzalez-Hoyuela,M., Barbas,J.A., and Rodriguez-Tebar,A. (2001). The autoregulation of retinal ganglion cell number. Development *128*, 117-124.

Gratzner,H.G. (1982). Monoclonal antibody to 5-bromo- and 5-iododeoxyuridine: A new reagent for detection of DNA replication. Science *218*, 474-475.

Grimm,C., Wenzel,A., Groszer,M., Mayser,H., Seeliger,M., Samardzija,M., Bauer,C., Gassmann,M., and Reme,C.E. (2002). HIF-1-induced erythropoietin in the hypoxic retina protects against light-induced retinal degeneration. Nat. Med. *8*, 718-724.

Haddad,G.G. and Jiang,C. (1997). O2-sensing mechanisms in excitable cells: role of plasma membrane K+ channels. Annu. Rev. Physiol *59*, 23-42.

Harris,A.L. (2002). Hypoxia--a key regulatory factor in tumour growth. Nat. Rev. Cancer *2*, 38-47.

Heldin,C.H., Ostman,A., and Ronnstrand,L. (1998). Signal transduction via platelet-derived growth factor receptors. Biochim. Biophys. Acta *1378*, F79-113.

Heldin,C.H. and Westermark,B. (1999). Mechanism of action and in vivo role of platelet-derived growth factor. Physiol Rev. *79*, 1283-1316.

Holland,E.C., Hively,W.P., DePinho,R.A., and Varmus,H.E. (1998). A constitutively active epidermal growth factor receptor cooperates with disruption of G1 cell-cycle arrest pathways to induce glioma-like lesions in mice. Genes Dev. *12*, 3675-3685.

Ikeda,S., Hawes,N.L., Chang,B., Avery,C.S., Smith,R.S., and Nishina,P.M. (1999). Severe ocular abnormalities in C57BL/6 but not in 129/Sv p53-deficient mice. Invest Ophthalmol. Vis. Sci. *40*, 1874-1878.

Ito,M. and Yoshioka,M. (1999). Regression of the hyaloid vessels and pupillary membrane of the mouse. Anat. Embryol. (Berl) *200*, 403-411.

Jaakkola,P., Mole,D.R., Tian,Y.M., Wilson,M.I., Gielbert,J., Gaskell,S.J., Kriegsheim,A., Hebestreit,H.F., Mukherji,M., Schofield,C.J., Maxwell,P.H., Pugh,C.W., and Ratcliffe,P.J. (2001). Targeting of HIF-alpha to the von Hippel-Lindau ubiquitylation complex by O2-regulated prolyl hydroxylation. Science *292*, 468-472.

Jacks,T., Fazeli,A., Schmitt,E.M., Bronson,R.T., Goodell,M.A., and Weinberg,R.A. (1992). Effects of an Rb mutation in the mouse. Nature *359*, 295-300.

Jiang,B.H., Semenza,G.L., Bauer,C., and Marti,H.H. (1996). Hypoxia-inducible factor 1 levels vary exponentially over a physiologically relevant range of O2 tension. Am. J. Physiol *271*, C1172-C1180.

Johansson,C.B., Momma,S., Clarke,D.L., Risling,M., Lendahl,U., and Frisen,J. (1999). Identification of a neural stem cell in the adult mammalian central nervous system. Cell *96*, 25-34.

Kakinuma,Y., Hama,H., Sugiyama,F., Yagami,K., Goto,K., Murakami,K., and Fukamizu,A. (1998). Impaired blood-brain barrier function in angiotensinogen-deficient mice. Nat. Med. *4*, 1078-1080.

Kamb,A. (1994). Role of a cell cycle regulator in hereditary and sporadic cancer. Cold Spring Harb. Symp. Quant. Biol. *59*, 39-47.

Kamijo,T., Zindy,F., Roussel,M.F., Quelle,D.E., Downing,J.R., Ashmun,R.A., Grosveld,G., and Sherr,C.J. (1997). Tumor suppression at the mouse INK4a locus mediated by the alternative reading frame product p19ARF. Cell *91*, 649-659.

Kettenmann,H. (1999). Physiology of glial cells. Adv. Neurol. *79*, 565-571.

Kiyokawa,H., Kineman,R.D., Manova-Todorova,K.O., Soares,V.C., Hoffman,E.S., Ono,M., Khanam,D., Hayday,A.C., Frohman,L.A., and Koff,A. (1996). Enhanced growth of mice lacking the cyclin-dependent kinase inhibitor function of p27(Kip1). Cell *85*, 721-732.

Kliche,S. and Waltenberger,J. (2001). VEGF receptor signaling and endothelial function. IUBMB. Life*52*, 61-66.

Klinghoffer,R.A., Mueting-Nelsen,P.F., Faerman,A., Shani,M., and Soriano,P. (2001). The two PDGF receptors maintain conserved signaling in vivo despite divergent embryological functions. Mol. Cell*7*, 343-354.

Lang,R., Lustig,M., Francois,F., Sellinger,M., and Plesken,H. (1994). Apoptosis during macrophage-dependent ocular tissue remodelling. Development *120*, 3395-3403.

Lee,S.J. and McPherron,A.C. (1999). Myostatin and the control of skeletal muscle mass. Curr. Opin. Genet. Dev. *9*, 604-607.

Levine,E.M., Close,J., Fero,M., Ostrovsky,A., and Reh,T.A. (2000). p27(Kip1) regulates cell cycle withdrawal of late multipotent progenitor cells in the mammalian retina. Dev. Biol.*219*, 299-314.

Li,X., Ponten,A., Aase,K., Karlsson,L., Abramsson,A., Uutela,M., Backstrom,G., Hellstrom,M., Bostrom,H., Li,H., Soriano,P., Betsholtz,C., Heldin,C.H., Alitalo,K., Ostman,A., and Eriksson,U. (2000). PDGF-C is a new protease-activated ligand for the PDGF alpha-receptor. Nat. Cell Biol. *2*, 302-309.

Lindahl,P., Johansson,B.R., Leveen,P., and Betsholtz,C. (1997). Pericyte loss and microaneurysm formation in PDGF-B-deficient mice. Science *277*, 242-245.

Ling,T.L. and Stone,J. (1988). The development of astrocytes in the cat retina: evidence of migration from the optic nerve. Brain Res. Dev. Brain Res. *44*, 73-85.

Ling,T.L., Mitrofanis,J., and Stone,J. (1989). Origin of retinal astrocytes in the rat: evidence of migration from the optic nerve. J. Comp Neurol. *286*, 345-352.

Macdonald,R., Scholes,J., Strahle,U., Brennan,C., Holder,N., Brand,M., and Wilson,S.W. (1997). The Pax protein Noi is required for commissural axon pathway formation in the rostral forebrain. Development *124*, 2397-2408.

Marti,H.H. and Risau,W. (1998). Systemic hypoxia changes the organ-specific distribution of vascular endothelial growth factor and its receptors. Proc. Natl. Acad. Sci. U. S. A *95*, 15809-15814.

Martinou,J.C., Dubois-Dauphin,M., Staple,J.K., Rodriguez,I., Frankowski,H., Missotten,M., Albertini,P., Talabot,D., Catsicas,S., Pietra,C., and . (1994). Overexpressionof BCL-2 in transgenic mice protects neurons from naturally occurring cell death and experimental ischemia. Neuron *13*, 1017-1030.

Maxwell,P.H., Wiesener,M.S., Chang,G.W., Clifford,S.C., Vaux,E.C., Cockman,M.E., Wykoff,C.C., Pugh,C.W., Maher,E.R., and Ratcliffe,P.J. (1999). The tumour suppressor protein VHL targets hypoxia-inducible factors for oxygen-dependent proteolysis. Nature *399*, 271-275.

Maxwell,P.H., Pugh,C.W., and Ratcliffe,P.J. (2001). Activation of the HIF pathway in cancer. Curr. Opin. Genet. Dev. *11*, 293-299.

McKeller,R.N., Fowler,J.L., Cunningham,J.J., Warner,N., Smeyne,R.J., Zindy,F., and Skapek,S.X. (2002). The Arf tumor suppressor gene promotes hyaloid vascular regression during mouse eye development. Proc. Natl. Acad. Sci. U. S. A *99*, 3848-3853.

Mi,H., Haeberle,H., and Barres,B.A. (2001). Induction of astrocyte differentiation by endothelial cells. J. Neurosci. *21*, 1538-1547.

Moreno,S., Hayles,J., and Nurse,P. (1989). Regulation of the cell cycle timing of mitosis. J. Cell Sci. Suppl *12*, 1-8.

Morgan,D.O. (1995). Principles of CDK regulation. Nature *374*, 131-134.

Morishita,E., Masuda,S., Nagao,M., Yasuda,Y., and Sasaki,R. (1997). Erythropoietin receptor is expressed in rat hippocampal and cerebral cortical neurons, and erythropoietin prevents in vitro glutamate-induced neuronal death. Neuroscience *76*, 105-116.

Morrison,S.J., Csete,M., Groves,A.K., Melega,W., Wold,B., and Anderson,D.J. (2000). Culture in reduced levels of oxygen promotes clonogenic sympathoadrenal differentiation by isolated neural crest stem cells. J. Neurosci. *20*, 7370-7376.

Mudhar,H.S., Pollock,R.A., Wang,C., Stiles,C.D., and Richardson,W.D. (1993). PDGF and its receptors in the developing rodent retina and optic nerve. Development *118*, 539-552.

Mukouyama,Y.S., Shin,D., Britsch,S., Taniguchi,M., and Anderson,D.J. (2002). Sensory nerves determine the pattern of arterial differentiation and blood vessel branching in the skin. Cell *109*, 693-705.

Nakae,J., Kido,Y., and Accili,D. (2001). Distinct and overlapping functions of insulin and IGF-I receptors. Endocr. Rev. *22*, 818-835.

Nakayama,K., Ishida,N., Shirane,M., Inomata,A., Inoue,T., Shishido,N., Horii,I., Loh,D.Y., and Nakayama,K. (1996). Mice lacking p27(Kip1) display increased body size, multiple organ hyperplasia, retinal dysplasia, and pituitary tumors. Cell *85*, 707-720.

Neuhaus,J., Risau,W., and Wolburg,H. (1991). Induction of blood-brain barrier characteristics in bovine brain endothelial cells by rat astroglial cells in transfilter coculture. Ann. N. Y. Acad. Sci.*633*, 578-580.

Nigg,E.A. (1995). Cyclin-dependent protein kinases: key regulators of the eukaryotic cell cycle. Bioessays *17*, 471-480.

Nurse,C.A. and Vollmer,C. (1997). Role of basic FGF and oxygen in control of proliferation, survival, and neuronal differentiation in carotid body chromaffin cells. Dev. Biol. *184*, 197-206.

Nurse,P. (1994). Ordering S phase and M phase in the cell cycle. Cell*79*, 547-550.

Orr-Urtreger,A. and Lonai,P. (1992). Platelet-derived growth factor-A and its receptor are expressed in separate, but adjacent cell layers of the mouse embryo. Development*115*, 1045-1058.

Orr-Urtreger,A., Bedford,M.T., Do,M.S., Eisenbach,L., and Lonai,P. (1992). Developmental expression of the alpha receptor for platelet-derived growth factor, which is deleted in the embryonic lethal Patch mutation. Development *115*, 289-303.

Otani,A., Kinder,K., Ewalt,K., Otero,F.J., Schimmel,P., and Friedlander,M. (2002). Bone marrow-derived stem cells target retinal astrocytes and can promote or inhibit retinal angiogenesis. Nat. Med.*8*, 1004-1010.

Otteson,D.C., Shelden,E., Jones,J.M., Kameoka,J., and Hitchcock,P.F. (1998). Pax2 expression and retinal morphogenesis in the normal and Krd mouse. Dev. Biol. *193*, 209-224.

Ozaki,H., Yu,A.Y., Della,N., Ozaki,K., Luna,J.D., Yamada,H., Hackett,S.F., Okamoto,N., Zack,D.J., Semenza,G.L., and Campochiaro,P.A. (1999). Hypoxia inducible factor-1alpha is increased in ischemic retina: temporal and spatial correlation with VEGF expression. Invest Ophthalmol. Vis. Sci.*40*, 182-189.

Palmieri,S.L., Payne,J., Stiles,C.D., Biggers,J.D., and Mercola,M. (1992). Expression of mouse PDGF-A and PDGF alpha-receptor genes during pre- and post-implantation development: evidence for a developmental shift from an autocrine to a paracrine mode of action. Mech. Dev.*39*, 181-191.

Pardee,A.B. (1989). G1 events and regulation of cell proliferation. Science*246*, 603-608.

Pellerin,L., Sibson,N.R., Hadjikhani,N., and Hyder,F. (2001). What you see is what you think--or is it? Trends Neurosci. *24*, 71-72.

Perego,C., Vanoni,C., Bossi,M., Massari,S., Basudev,H., Longhi,R., and Pietrini,G. (2000). The GLT-1 and GLAST glutamate transporters are expressed on morphologically distinct astrocytes and regulated by neuronal activity in primary hippocampal cocultures. J. Neurochem. *75*, 1076-1084.

Perron,M. and Harris,W.A. (2000). Determination of vertebrate retinal progenitor cell fate by the Notch pathway and basic helix-loop-helix transcription factors. Cell Mol. Life Sci. *57*, 215-223.

Pfrieger,F.W. and Barres,B.A. (1996). New views on synapse-glia interactions. Curr. Opin. Neurobiol. *6*, 615-621.

Pierce,E.A., Avery,R.L., Foley,E.D., Aiello,L.P., and Smith,L.E. (1995). Vascular endothelial growth factor/vascular permeability factor expression in a mouse model of retinal neovascularization. Proc. Natl. Acad. Sci. U. S. A *92*, 905-909.

Pimentel,B., Rodriguez-Borlado,L., Hernandez,C., and Carrera,A.C. (2002). A Role for phosphoinositide 3-kinase in the control of cell division and survival during retinal development. Dev. Biol.*247*, 295-306.

Pomerantz,J., Schreiber-Agus,N., Liegeois,N.J., Silverman,A., Alland,L., Chin,L., Potes,J., Chen,K., Orlow,I., Lee,H.W., Cordon-Cardo,C., and DePinho,R.A. (1998). The Ink4a tumor suppressor gene product, p19Arf, interacts with MDM2 and neutralizes MDM2's inhibition of p53. Cell*92*, 713-723.

Potter,C.J. and Xu,T. (2001). Mechanisms of size control. Curr. Opin. Genet. Dev.*11*, 279-286.

Prat,A., Biernacki,K., Wosik,K., and Antel,J.P. (2001). Glial cell influence on the human blood-brain barrier. Glia *36*, 145-155.

Provis,J.M., van Driel,D., Billson,F.A., and Russell,P. (1985). Development of the human retina: patterns of cell distribution and redistribution in the ganglion cell layer. J. Comp Neurol. *233*, 429-451.

Provis,J.M. (1987). Patterns of cell death in the ganglion cell layer of the human fetal retina. J. Comp Neurol. *259*, 237-246.

Provis,J.M., Leech,J., Diaz,C.M., Penfold,P.L., Stone,J., and Keshet,E. (1997). Development of the human retinal vasculature: cellular relations and VEGF expression. Exp. Eye Res.*65*, 555-568.

Provis,J.M. (2001). Development of the primate retinal vasculature. Prog. Retin. Eye Res.*20*, 799-821.

Quelle,D.E., Zindy,F., Ashmun,R.A., and Sherr,C.J. (1995). Alternative reading frames of the INK4a tumor suppressor gene encode two unrelated proteins capable of inducing cell cycle arrest. Cell*83*, 993-1000.

Raff,M.C., Abney,E., Brockes,J.P., and Hornby-Smith,A. (1978). Schwann cell growth factors. Cell *15*, 813-822.

Raff,M.C. (1996). Size control: the regulation of cell numbers in animal development. Cell*86*, 173-175.

Raff,M.C., Durand,B., and Gao,F.B. (1998). Cell number control and timing in animal development: the oligodendrocyte cell lineage. Int. J. Dev. Biol. *42*, 263-267.

Ramirez,J.M., Ramirez,A.I., Salazar,J.J., de Hoz,R., and Trivino,A. (2001). Changes of astrocytes in retinal ageing and age-related macular degeneration. Exp. Eye Res. *73*, 601-615.

Rapaport,D.H. and Stone,J. (1982). The site of commencement of maturation in mammalian retina: observations in the cat. Brain Res. *281*, 273-279.

Reichel,M.B., Ali,R.R., D'Esposito,F., Clarke,A.R., Luthert,P.J., Bhattacharya,S.S., and Hunt,D.M. (1998). High frequency of persistent hyperplastic primary vitreous and cataracts in p53-deficient mice. Cell Death. Differ. *5*, 156-162.

Ridet,J.L., Malhotra,S.K., Privat,A., and Gage,F.H. (1997). Reactive astrocytes: cellular and molecular cues to biological function. Trends Neurosci.*20*, 570-577.

Roussel,M.F. (1998). Key effectors of signal transduction and G1 progression. Adv. Cancer Res.*74*, 1-24.

Ruas,M. and Peters,G. (1998). The p16INK4a/CDKN2A tumor suppressor and its relatives. Biochim. Biophys. Acta *1378*, F115-F177.

Sandercoe,T.M., Madigan,M.C., Billson,F.A., Penfold,P.L., and Provis,J.M. (1999). Astrocyte proliferation during development of the human retinal vasculature. Exp. Eye Res.*69*, 511-523.

Schatteman,G.C., Morrison-Graham,K., van Koppen,A., Weston,J.A., and Bowen-Pope,D.F. (1992). Regulation and role of PDGF receptor alpha-subunit expression during embryogenesis. Development *115*, 123-131.

Semenza,G.L. (2001). Hypoxia-inducible factor 1: control of oxygen homeostasis in health and disease. Pediatr. Res. *49*, 614-617.

Semo,M., Bryce,J., and Jeffery,G. (2001). Oxygen modulates cell death in the proliferating retina. Eur. J. Neurosci. *13*, 1257-1260.

Serrano,M., Lee,H., Chin,L., Cordon-Cardo,C., Beach,D., and DePinho,R.A. (1996). Role of the INK4a locus in tumor suppression and cell mortality. Cell *85*, 27-37.

Sharp,F.R., Liu,J., and Bernabeu,R. (2002). Neurogenesis following brain ischemia. Brain Res. Dev. Brain Res. *134*, 23-30.

Sherr,C.J. (2001). Parsing Ink4a/Arf: "pure" p16-null mice. Cell *106*, 531-534.

Shioi,T., Kang,P.M., Douglas,P.S., Hampe,J., Yballe,C.M., Lawitts,J., Cantley,L.C., and Izumo,S. (2000). The conserved phosphoinositide 3-kinase pathway determines heart size in mice. EMBO J. *19*, 2537-2548.

Shweiki,D., Itin,A., Soffer,D., and Keshet,E. (1992). Vascular endothelial growth factor induced by hypoxia may mediate hypoxia-initiated angiogenesis. Nature *359*, 843-845.

Siren,A.L., Fratelli,M., Brines,M., Goemans,C., Casagrande,S., Lewczuk,P., Keenan,S., Gleiter,C., Pasquali,C., Capobianco,A., Mennini,T., Heumann,R., Cerami,A., Ehrenreich,H., and Ghezzi,P. (2001). Erythropoietin prevents neuronal apoptosis after cerebral ischemia and metabolic stress. Proc. Natl. Acad. Sci. U. S. A *98*, 4044-4049.

Sochman,J. (2002). N-acetylcysteine in acute cardiology: 10 years later: what do we know and what would we like to know?! J. Am. Coll. Cardiol. *39*, 1422-1428.

Soriano,P. (1997). The PDGF alpha receptor is required for neural crest cell development and for normal patterning of the somites. Development *124*, 2691-2700.

Steinberg,R.H. (1987). Monitoring communications between photoreceptors and pigment epithelial cells: effects of "mild" systemic hypoxia. Friedenwald lecture. Invest Ophthalmol. Vis. Sci. *28*, 1888-1904.

Steinhauser,C., Berger,T., Frotscher,M., and Kettenmann,H. (1992). Heterogeneity in the Membrane Current Pattern of Identified Glial Cells in the Hippocampal Slice. Eur. J. Neurosci. *4*, 472-484.

Stone,J. and Dreher,Z. (1987). Relationship between astrocytes, ganglion cells and vasculature of the retina. J. Comp Neurol. *255*, 35-49.

Stone,J., Itin,A., Alon,T., Pe'er,J., Gnessin,H., Chan-Ling,T., and Keshet,E. (1995). Development of retinal vasculature is mediated by hypoxia-induced vascular endothelial growth factor (VEGF) expression by neuroglia. J. Neurosci. *15*, 4738-4747.

Stone,J., Chan-Ling,T., Pe'er,J., Itin,A., Gnessin,H., and Keshet,E. (1996). Roles of vascular endothelial growth factor and astrocyte degeneration in the genesis of retinopathy of prematurity. Invest Ophthalmol. Vis. Sci. *37*, 290-299.

Strom,R.C. and Williams,R.W. (1998). Cell production and cell death in the generation of variation in neuron number. J. Neurosci. *18*, 9948-9953.

Studer,L., Csete,M., Lee,S.H., Kabbani,N., Walikonis,J., Wold,B., and McKay,R. (2000). Enhanced proliferation, survival, and dopaminergic differentiation of CNS precursors in lowered oxygen. J. Neurosci. *20*, 7377-7383.

Su,T.T. and O'Farrell,P.H. (1998). Size control: cell proliferation does not equal growth.Curr. Biol. *8*, R687-R689.

Tanigaki,K., Nogaki,F., Takahashi,J., Tashiro,K., Kurooka,H., and Honjo,T. (2001). Notch1 and Notch3 instructively restrict bFGF-responsive multipotent neural progenitor cells to an astroglial fate. Neuron *29*, 45-55.

Temple,S. and Raff,M.C. (1986). Clonal analysis of oligodendrocyte development in culture: evidence for a developmental clock that counts cell divisions. Cell *44*, 773-779.

Turner,D.L. and Cepko,C.L. (1987). A common progenitor for neurons and glia persists in rat retina late in development. Nature *328*, 131-136.

Uhrbom,L., Hesselager,G., Ostman,A., Nister,M., and Westermark,B. (2000). Dependence of autocrine growth factor stimulation in platelet-derived growth factor-B-induced mouse brain tumor cells. Int. J. Cancer *85*, 398-406.

Uhrbom,L., Dai,C., Celestino,J.C., Rosenblum,M.K., Fuller,G.N., and Holland,E.C. (2002). Ink4aArf loss cooperates with KRas activation in astrocytes and neural progenitors to generate glioblastomas of various morphologies depending on activated Akt. Cancer Res. *62*, 5551-5558.

van Heyningen,P., Calver,A.R., and Richardson,W.D. (2001). Control of progenitor cell number by mitogen supply and demand. Curr. Biol. *11*, 232-241.

van Lookeren,C.M. and Gill,R. (1998). Tumor-suppressor p53 is expressed in proliferating and newly formed neurons of the embryonic and postnatal rat brain: comparison with expression of the cell cycle regulators p21Waf1/Cip1, p27Kip1, p57Kip2, p16Ink4a, cyclin G1, and the proto-oncogene Bax. J. Comp Neurol. *397*, 181-198.

Vetter,M.L. and Brown,N.L. (2001). The role of basic helix-loop-helix genes in vertebrate retinogenesis. Semin. Cell Dev. Biol. *12*, 491-498.

Vidal,A. and Koff,A. (2000). Cell-cycle inhibitors: three families united by a common cause. Gene *247*, 1-15.

Waid,D.K. and McLoon,S.C. (1998). Ganglion cells influence the fate of dividing retinal cells in culture. Development *125*, 1059-1066.

Walz,W. (2000). Controversy surrounding the existence of discrete functional classes of astrocytes in adult gray matter. Glia *31*, 95-103.

Walz,W. (2000). Role of astrocytes in the clearance of excess extracellular potassium. Neurochem. Int.*36*, 291-300.

Wang,G.L. and Semenza,G.L. (1993). Desferrioxamine induces erythropoietin gene expression and hypoxia-inducible factor 1 DNA-binding activity: implications for models of hypoxia signal transduction. Blood *82*, 3610-3615.

Wang,G.L. and Semenza,G.L. (1995). Purification and characterization of hypoxia-inducible factor 1. J. Biol. Chem. *270*, 1230-1237.

Wang,L., Cioffi,G.A., Cull,G., Dong,J., and Fortune,B. (2002). Immunohistologic evidence for retinal glial cell changes in human glaucoma. Invest Ophthalmol. Vis. Sci.*43*, 1088-1094.

Watanabe,G., Pena,P., Shambaugh,G.E., III, Haines,G.K., III, and Pestell,R.G. (1998). Regulation of cyclin dependent kinase inhibitor proteins during neonatal cerebella development. Brain Res. Dev. Brain Res. *108*, 77-87.

Watanabe,T. and Raff,M.C. (1988). Retinal astrocytes are immigrants from the optic nerve. Nature*332*, 834-837.

Weinberg,R.A. (1995). The retinoblastoma protein and cell cycle control. Cell*81*, 323-330.

Wenger,R.H. (2000). Mammalian oxygen sensing, signalling and gene regulation. J. Exp. Biol.*203 Pt 8*, 1253-1263.

Yu,A.Y., Shimoda,L.A., Iyer,N.V., Huso,D.L., Sun,X., McWilliams,R., Beaty,T., Sham,J.S., Wiener,C.M., Sylvester,J.T., and Semenza,G.L. (1999). Impaired physiological responses to chronic hypoxia in mice partially deficient for hypoxia-inducible factor 1alpha. J. Clin. Invest*103*, 691-696.

Zaman,K., Ryu,H., Hall,D., O'Donovan,K., Lin,K.I., Miller,M.P., Marquis,J.C., Baraban,J.M., Semenza,G.L., and Ratan,R.R. (1999). Protection from oxidative stress-induced apoptosis in cortical neuronal cultures by iron chelators is associated with enhanced DNA binding of hypoxia-inducible factor-1 and ATF-1/CREB and increased expression of glycolytic enzymes, p21(waf1/cip1), and erythropoietin. J. Neurosci. *19*, 9821-9830.

Zerlin,M. and Goldman,J.E. (1997). Interactions between glial progenitors and blood vessels during early postnatal corticogenesis: blood vessel contact represents an early stage of astrocyte differentiation. J. Comp Neurol. *387*, 537-546.

Zhang,P., Liegeois,N.J., Wong,C., Finegold,M., Hou,H., Thompson,J.C., Silverman,A., Harper,J.W., DePinho,R.A., and Elledge,S.J. (1997). Altered cell differentiation and proliferation in mice lacking p57KIP2 indicates a role in Beckwith-Wiedemann syndrome. Nature *387*, 151-158.

Zhang,Y. and Stone,J. (1997). Role of astrocytes in the control of developing retinal vessels. Invest Ophthalmol. Vis. Sci. *38*, 1653-1666.

Zhang,Y., Porat,R.M., Alon,T., Keshet,E., and Stone,J. (1999). Tissue oxygen levels control astrocyte movement and differentiation in developing retina. Brain Res. Dev. Brain Res.*118*, 135-145.

Zhu,L. and Skoultchi,A.I. (2001). Coordinating cell proliferation and differentiation. Curr. Opin. Genet. Dev. *11*, 91-97.

Zhu,M., Provis,J.M., and Penfold,P.L. (1999). The human hyaloid system: cellular phenotypes and inter-relationships. Exp. Eye Res. *68*, 553-563.

Zindy,F., Cunningham,J.J., Sherr,C.J., Jogal,S., Smeyne,R.J., and Roussel,M.F. (1999). Postnatal neuronal proliferation in mice lacking Ink4d and Kip1 inhibitors of cyclin-dependent kinases. Proc. Natl. Acad. Sci. U. S. A *96*, 13462-13467.